SELECTIVE CANCELLATION OF INTERFERENCE FOR CDMA

by

Parag Agashe

Thesis submitted to the Faculty of the
Virginia Polytechnic Institute and State University
in partial fulfillment of the requirements for the degree of

MASTER OF SCIENCE
in
Electrical Engineering

Approved:

Dr. Brian D. Woerner
(Chairman)

Dr. Theodore S. Rappaport

Dr. Ira Jacobs

January 1996
Blacksburg, Virginia

Selective Cancellation of Interference for CDMA

by

Parag Agashe

Committee Chairman: Dr. Brian D. Woerner

Electrical Engineering

Abstract

Recently, it has been shown that Multiple Access Interference (MAI) cancellation is a promising technique for improving the performance and capacity of the reverse link in a Code Division Multiple Access (CDMA) cellular system. However, it has been observed that indiscriminate cancellation of all received signals can degrade performance. This thesis explores the use of selective cancellation to improve the performance of practical CDMA systems. First, this thesis considers the performance of adaptive interference cancellation applied to a CDMA microcellular environment. This thesis employs a circular geometry and a closed form expression for the Bit Error Rate of a CDMA system with interference cancellation to analyze the effect of out-of-cell interference. Results are presented which indicate that out-of-cell interference will severely limit the benefits of interference cancellation in a multicellular system. Attempts to cancel all out-of-cell interference will further degrade performance. However, the use of selective interference cancellation in which only the strongest out-of-cell interferers are cancelled may result in significant performance enhancement. These results are shown to agree closely with those obtained using a hexagonal geometry. The MAI is modeled using both the simple and an improved Gaussian approximation.

This thesis also investigates the use of selective cancellation with bit averaging. Amplitude estimates over several consecutive symbols can be averaged

to improve the accuracy of the estimate. An expression for the BER of the interference cancellation receiver with hard decisions is developed. Results show that averaging power estimates leads to considerable improvement in capacity. Results are also presented for the case of perfect power estimates.

Acknowledgments

I would like to express my sincere gratitude to Dr. Brian Woerner for being an excellent advisor and professor. He was a source of constant encouragement and guidance throughout my academic years at Virginia Tech. The confidence he placed in me by giving me the opportunity to work on this extremely interesting and challenging project cannot be reciprocated with mere words. Without his whole-hearted involvement, this thesis would not have been successfully completed. I am thankful to my committee members Dr. Theodore Rappaport and Dr. Ira Jacobs for their valuable comments and suggestions.

I would like to thank the Advanced Research Projects Agency (ARPA) and the Mobile and Portable Radio Research Group (MPRG) Industrial Affiliates for supporting this project.

I am grateful to every member of the Mobile and Portable Radio Research Group (MPRG) who assisted me through this work. I am especially thankful to Mike Beuhrer, Ashish Kaul, Nitin Mangalvedhe, Prabhakar Koushik, Kevin Saldanha, Francis Dominique and Ning Yang for their help from time to time. I appreciate the help extended to me by the MPRG staff members.

Finally, I dedicate this work to my parents for their love and encouragement.

Contents

Acknowledgments iv

1 Introduction 1

1.1 Spread Spectrum 3

1.2 Spread Spectrum Techniques 4

1.3 Direct Sequence Spread Spectrum 5

1.4 Code Division Multiple Access 10

1.4.1 Advantages of CDMA for Cellular Radio 11

1.4.2 Disadvantages of CDMA for Cellular Radio 13

1.5 Generation and Characteristics of PN Sequences 13

1.6 Direct Sequence Spread Spectrum CDMA Model 16

1.7 Outline of Thesis 18

2 Receiver Structures for CDMA Systems 20

2.1 Correlation Receiver 20

2.2 RAKE Receiver 21

2.3 The Near-Far Problem 23

2.4 Multiuser Receivers 26

3 Multistage Interference Cancellation 30

3.1 Adaptive Multistage Interference Cancellation Model 30

3.1.1 The Interference Cancellation Model 30

3.1.2 Assumptions 32

3.2 Analysis of Receiver Performance 33

3.3 BER Analysis for Interference Cancellation 34

3.4 Extensions 37
3.5 Improved Gaussian Approximation 40
3.6 Conclusion 42

4 Cancellation of Multicell Interference **43**
4.1 Motivation 43
4.2 Cell Layout 44
4.2.1 Hexagonal Layout 44
4.2.2 Circular Layout 46
4.3 Multicell Analysis of Interference Cancellation 49
4.3.1 Interference Cancellation on In-Cell Users Only 50
4.3.2 Complete Interference Cancellation 51
4.3.3 Selective Interference Cancellation 52
4.4 Numerical Results 53
4.4.1 Circular Layout 53
4.4.2 Hexagonal Layout 62
4.4.3 The Improved Gaussian Approximation 66

5 Cancellation with Bit Averaging **71**
5.1 Motivation 71
5.2 Hard Decisions 73
5.3 Perfect Power Estimates 75
5.3.1 Analysis 75
5.3.2 Results 76
5.4 Imperfect Power Estimates 80
5.4.1 Analysis 80
5.4.2 Results 82
5.5 Summary 94

6 Conclusions **95**
6.1 Conclusions 95
6.2 Future work 96

Bibliography **98**

List of Figures

1.1 Direct Sequence Spread Spectrum system 6
1.2 Spreading Procedure for $N = 7$ 7
1.3 **a.** Power Spectral Density of a rectangular pulse of duration T_b, **b.** Power Spectral Density of a BPSK modulated signal, **c.** Power Spectral Density of the spread signal. 9
1.4 Autocorrelation function for maximal-length PN sequences 14
1.5 A Pseudo-Random Sequence Generator 15
1.6 Gold Code Sequence Generator 16
1.7 DSSS CDMA Model 17

2.1 Correlation Receiver 21
2.2 RAKE Receiver 22
2.3 Performance of a Conventional Receiver under the Near-Far effect (N=31, K=3) 25
2.4 Optimum Multiuser Receiver 27
2.5 Multistage Receiver (A sub-optimum multiuser receiver) 29

3.1 Block Diagram of a two stage interference cancellation receiver for three users 31
3.2 Performance of Interference Cancellation in a Single Cell, ($N = 31$, $\frac{E_b}{N_0} =$ 15 dB) 36
3.3 BER vs. Eb/N0 for Interference Cancellation in a Single Cell, ($N = 31, K = 20$) 38

4.1 Hexagonal Model for Cell Layout 45
4.2 Circular Model for Cell Layout 47

4.3 Interference Cancellation for a Single Cell Environment ($N = 128$, $\frac{E_b}{N_0} =$ 15 dB, Perfect Power Control). 54
4.4 Performance of Interference Cancellation for Multicellular Environment, No Interference Cancellation on Out-of-Cell Interferers ($N =$ 128, $\frac{E_b}{N_0} = 15$dB, $d = 1000$ m, $n = 4$) 55
4.5 Performance of Interference Cancellation for Multicellular Environment, Complete Interference Cancellation ($N = 128$, $\frac{E_b}{N_0} = 15$dB, $d = 1000$ m, $n = 4$) 56
4.6 Performance of Interference Cancellation for Multicellular Environment, Selective Interference Cancellation ($N = 128$, $\frac{E_b}{N_0} = 15$dB, $d = 1000$ m, $n = 4$) 57
4.7 Performance of Interference Cancellation for Multicellular Environment, Selective Interference Cancellation ($N = 128$, $\frac{E_b}{N_0} = 15$dB, $d = 1000$ m, $n = 2$) 58
4.8 Performance of Interference Cancellation for Multicellular Environment, Selective Interference Cancellation ($N = 128$, $\frac{E_b}{N_0} = 10$dB, $d = 1000$ m, $n = 4$) 59
4.9 Performance of Interference Cancellation for Multicellular Environment, Selective Interference Cancellation ($N = 128$, $\frac{E_b}{N_0} = 15$dB, $d = 5000$ m, $n = 4$) 60
4.10 Performance of Interference Cancellation for Multicellular Environment using Hexagonal Geometry, No Interference Cancellation on Out-of-Cell Interferers ($N = 128$, $\frac{E_b}{N_0} = 15$ dB, $r = 1000$ m, $n = 4$) 63
4.11 Performance of Interference Cancellation for Multicellular Environment using Hexagonal Geometry, Complete Interference Cancellation ($N = 128$, $\frac{E_b}{N_0} = 15$ dB, $r = 1000$ m, $n = 4$) 64
4.12 Performance of Interference Cancellation for Multicellular Environment using Hexagonal Geometry, Selective Interference Cancellation ($N = 128$, $\frac{E_b}{N_0} = 15$ dB, $r = 1000$ m, $n = 4$) 65

4.13 Performance of Interference Cancellation for Multicellular Environment using Hexagonal Geometry and the Improved Gaussian Approximation, No Interference Cancellation on out-of-cell interferers ($N = 128$, $\frac{E_b}{N_0} = 15$ dB, $r = 1000$ m, $n = 4$) 67
4.14 Performance of Interference Cancellation for Multicellular Environment using Hexagonal Geometry and the Improved Gaussian Approximation, Complete Interference Cancellation ($N = 128$, $\frac{E_b}{N_0} = 15$ dB, $r = 1000$ m, $n = 4$) 68
4.15 Performance of Interference Cancellation for Multicellular Environment using Hexagonal Geometry and the Improved Gaussian Approximation, Selective Interference Cancellation ($N = 128$, $\frac{E_b}{N_0} = 15$ dB, $r = 1000$ m, $n = 4$) 69

5.1 Performance of Interference Cancellation with hard decisions, assuming Perfect Amplitude Estimates, No Bit Averaging ($N = 31$, $\frac{E_b}{N_0} = 15$ dB) 77
5.2 Performance of Interference Cancellation with hard decisions, assuming Perfect Amplitude Estimates, Averaging Estimates over 100 bits ($N = 31$, $\frac{E_b}{N_0} = 15$ dB) 78
5.3 BER vs. E_b/N_0 for Interference Cancellation with hard decisions, assuming Perfect Amplitude Estimates, No bit Averaging($N = 31, K = 20$) 79
5.4 Simulated and Analytical BER vs. E_b/N_0 for Interference Cancellation with hard decisions, assuming Perfect Amplitude Estimates ($N = 31, K = 20$) o : Analytical Results, * : Simulated Results 81
5.5 Performance of Interference Cancellation with hard decisions, No Bit Averaging ($N = 31$, $\frac{E_b}{N_0} = 15$ dB) 83
5.6 Performance of Interference Cancellation with soft decisions, ($N = 31$, $\frac{E_b}{N_0} = 15$ dB) 84
5.7 BER vs. E_b/N_0 for Interference Cancellation with hard decisions, No Bit Averaging, ($N = 31, K = 20$) 86
5.8 Performance of Interference Cancellation with hard decisions, Averaging Amplitude Estimates over 2 bits($N = 31$, $\frac{E_b}{N_0} = 15$ dB) 87

5.9 Performance of Interference Cancellation with hard decisions, Averaging Amplitude Estimates over 10 bits($N = 31, \frac{E_b}{N_0} = 15$ dB) 88
5.10 Performance of Interference Cancellation with hard decisions, Averaging Amplitude Estimates over 100 bits($N = 31, \frac{E_b}{N_0} = 15$ dB) 89
5.11 BER vs. E_b/N_0 for Interference Cancellation with hard decisions, Averaging Amplitude Estimates over 2 bits($N = 31, K = 20$) 91
5.12 BER vs. E_b/N_0 for Interference Cancellation with hard decisions, Averaging Amplitude Estimates over 10 bits($N = 31, K = 20$) 92
5.13 BER vs. E_b/N_0 for Interference Cancellation with hard decisions, Averaging Amplitude Estimates over 100 bits($N = 31, K = 20$) 93

Chapter 1

Introduction

In the past few years, there has been enormous growth in the field of wireless communications. The demand for wireless communications products and services is growing rapidly as their size and cost is being reduced. This reduction in size and cost has been made possible by improvements in RF circuit fabrication methods, digital signal processing, and new large scale integration circuits. In particular, the cellular telephone industry has been expanding at an amazing rate [1]. Today, there are over 13 million users of cellular phones in the US alone, and industry experts predict that this market will grow more than 25% a year for the next five years. This phenomenal growth presents the cellular service providers, equipment manufacturers, and researchers with the great challenge of being able to keep up with the insatiable demand for more and more capacity.

Early mobile radio systems used high powered transmitters with tall antennas to cover as large an area as possible. However, this resulted in inefficient use of the frequency spectrum, since reusing the same frequencies within the service area would cause interference. This limited the capacity of the system. A major concern was how to balance the conflicting demands for large coverage and huge capacity. This gave rise to the idea of reusing frequencies by dividing the region to be covered into cells. Each cell has a base station, and users in a cell communicate with the base station of that cell. A set of frequencies used in a certain cell can be used again in a far away cell, thus improving the capacity of the system. All cellular systems have the following common features [2]:

1. Multicell configuration.

2. Frequency reuse.

3. Ability to hand-off a mobile from cell to cell to keep a call up.

4. Connectivity to a fixed Public Switched Telephone Network (PSTN).

5. Ability to work in a controlled interference environment.

The world's first cellular system was implemented by the Nippon Telephone and Telegraph company (NTT) in Japan in 1979. It was called the Nordic Mobile Telephone System (NMT450). This system had a basic capacity of 4000 subscribers, and was expandable to 8000 subscribers. It operated in the 400 MHz frequency band. Later, systems like Advanced Mobile Phone System (AMPS), Extended European Total Access Communication System (ETACS) and NMT900 were introduced. These were designed to operate in the 800 and 900 MHz frequency bands. Existing urban analog systems have reached maximum capacity and are unable to meet the increasing demand for capacity. The lack of spectrum and the inability of the analog cellular systems to keep up with the demand for capacity caused the introduction of digital cellular. A number of digital cellular systems have been developed worldwide. Some of the widely used ones are the Global System for Mobile Communications (GSM), and US and Japanese Digital Cellular. These digital systems use Time Division Multiple Access (TDMA) to give access of the channel to a large number of users. The US Digital Cellular system was defined by the Telecommunications Industries Association (TIA) Interim Standard IS-54. It provides a potential threefold increase in capacity over AMPS (not counting a slight improvement in trunking efficiency). Shortly after TDMA was adopted, QUALCOMM, a San Diego based company introduced a competing Code Division Multiple Access (CDMA) standard, which has been claimed to provide a 10 to 20-fold increase in capacity over conventional analog systems [3]. Unlike the present conventional analog and other digital systems, which divide up the available spectrum into into narrow channels, CDMA is a wide-band technique that spreads multiple signals over a wide segment of the cellular broadcast spectrum. CDMA employs Spread Spectrum (SS) technology, which has been used in military satellite systems for a long time. Each telephone or data call is assigned a unique

code that permits it to be distinguished from the large number of calls transmitted over the same frequency at the same time. As long as the receiver has the right code, it can distinguish the desired signal from all others.

1.1 Spread Spectrum

The theoretical capacity of a channel to transfer information at a certain rate is a function of the signal to noise ratio and the channel bandwidth. The theoretical upper bound for the bit rate that can be achieved with arbitrarily low bit error rate in a Gaussian noise environment is given by Shannon's law for channel capacity:

$$C = W \log_2 \left(1 + \frac{S}{N}\right) \tag{1.1}$$

where C is the capacity of the channel in bits per second, W is the bandwidth in Hz, and S/N is the signal to noise ratio. An increase in the channel capacity can be obtained by either increasing the signal to noise ratio, or by increasing the bandwidth used to transfer the information. A Spread Spectrum system is one in which the transmitted signal is spread over a wide frequency band, much wider than the minimum bandwidth required to transmit the information being sent. Thus, SS relies on expanding the bandwidth of the signal to be transmitted. Spread Spectrum techniques have long been used for military applications because of their high immunity to interference and excellent security.

Spread Spectrum Systems are characterized by the following properties [4]:

1. Transmitted signal occupies a bandwidth which is many times greater than the message bandwidth.

2. Carrier signal is pseudo-random in nature. The transmitted signal is produced by modulating the output of a pseudo-random sequence generator with the message signal.

3. Message detection involves correlating the received signal with the same pseudo-random spreading signal. This operation is called despreading. Thus, the receiver has to be able to generate a time synchronized copy of the same pseudo-random sequence as in the transmitter.

Other received signals, either wide-band or narrow-band, have a low correlation with the desired signal's spreading code, and and hence will have the same effect as noise. Thereby assigning a different pseudo-random sequence for each user, many users can simultaneously share the same frequency band. CDMA makes use of spread spectrum techniques.

1.2 Spread Spectrum Techniques

There are many alternative techniques for generating spread spectrum signals. These include [5]:

1. **Direct Sequence Spread Spectrum (DSSS)**: Direct Sequence systems are the most widely used form of spread spectrum systems. In DSSS, the spectrum is spread by multiplying the data stream by a spreading sequence that has a much higher frequency. Each information bit is symbolized by a large number of coded bits called chips. DSSS may be thought of as an additional phase modulation of an already modulated signal [6]. In this thesis, we focus on DSSS signals.

2. **Frequency Hopping (FH)**: In frequency hopping, the carrier frequency of the transmitted signal is shifted in a pattern determined by a code sequence. We may therefore consider FH as analogous to Frequency Shift Keying (FSK) technique, whereas DSSS is analogous to Phase Shift Keying (PSK) technique.

3. **Chirp Modulation**: Here, the signals used are just swept frequency pulses which do not employ coding. Chirp modulation is also called Pulsed-FM. Although chirp modulation is sometimes classified as spread spectrum, it is not true spread spectrum because of the absence of a pseudo-noise (PN) generator.

4. **Time Hopping**: Time hopping systems control their time of transmission and period with a code sequence.

5. **Hybrid Formats**: These systems incorporate both DSSS and FH.

For the research conducted in this thesis, DSSS is utilized and is discussed in greater details in the next section.

1.3 Direct Sequence Spread Spectrum

Figure 1.1a presents a DSSS transmitter. DSSS signals are generated by modulating the data with a pseudo-noise code sequence which has a rate much higher than that of the original signal. The modulator can be a simple exclusive-OR gate. The PN code consists of N chips for each data bit. The transmitted signal is the data signal multiplied by the spreading sequence, so that the transmitted bandwidth is N times the data bandwidth. This higher bandwidth signal is called the spread signal. The spread signal modulates a carrier frequency and is then transmitted. The usual modulation technique for spread spectrum is phase modulation. The pseudo-random sequence is also called the chip sequence. The processing gain of the system is the number of chips per bit, which is N. For example, if the bit rate is 1 Mb/s, it requires an information bandwidth of 1 MHz. If each bit is coded by 63 chips, then the chip rate is 63 M chips/s, which needs a bandwidth of 63 MHz. The bandwidth is thus spread from 1 MHz to 63 MHz. The processing gain for this example is 63 or 18 dB. Figure 1.1 shows a simple BPSK DSSS transmitter. The data signal $b(t)$ is expressed as

$$b(t) = \sum_{i=-\infty}^{\infty} b_i p_T(t - iT), \tag{1.2}$$

where $b_i \in \{\pm 1\}$ is an independent identically distributed (iid) random variable representing the ith data bit, and $p_T(t)$ is a unit rectangular pulse given by $p_T(t) = 1$ for $0 \leq t \leq T$ and $p_T(t) = 0$ otherwise. The data bit duration is T. The data signal $b(t)$ is spread using the PN sequence $a(t)$ expressed as

$$a(t) = \sum_{j=-\infty}^{\infty} a_j p_{T_c}(t - jT_c), \tag{1.3}$$

where $a_j \in \{\pm 1\}$ is the jth chip of the periodic PN Sequence, and $p_{T_c}(T)$ is a unit rectangular pulse of duration T_c. The sequence $a(t)$ is a binary sequence like $b(t)$, but at a much higher rate. In fact, the rate of $a(t)$ is much greater than $b(t)$, such that $a(t)$ separates the data signal into chips, and the rate of $a(t)$ is the chip rate $\frac{1}{T_c}$. The PN sequence is generated in a deterministic manner, and is repetitive. However, the sequence length before repetition is usually very long, and for practical purposes, we assume that the sequence is truly random. Section 1.5 will describe in more detail how the PN sequence is generated. The spread data is modulated by the carrier at

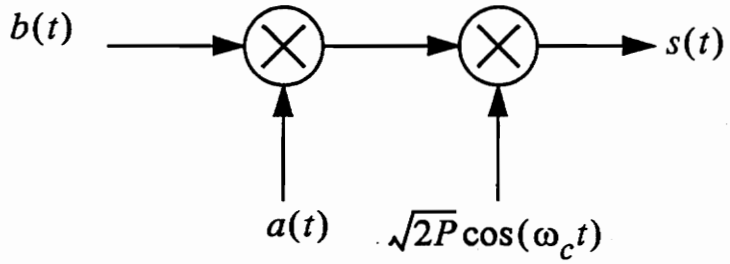

(a) DS/SS Transmitter

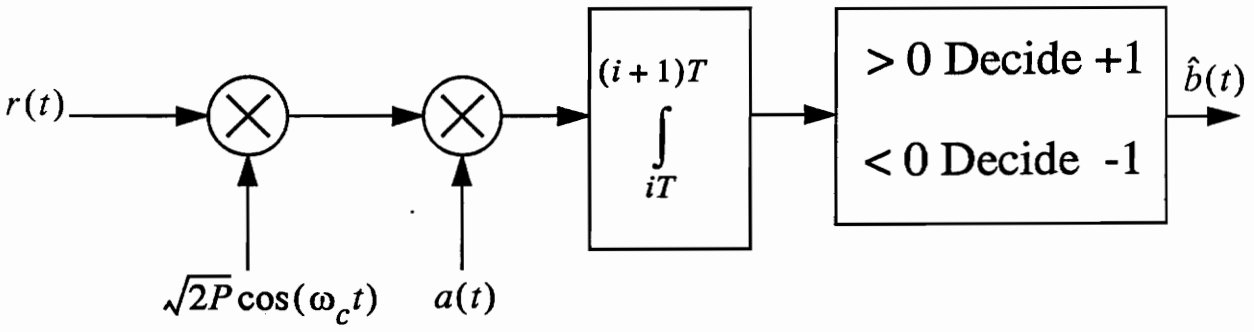

(b) Correlation Receiver

Figure 1.1: Direct Sequence Spread Spectrum System, where: $b(t)$ is the data signal, $a(t)$ is the spreading signal, $s(t)$ is the transmitted signal, $r(t)$ is the received signal, and $\hat{b(t)}$ is an estimate of the data signal.

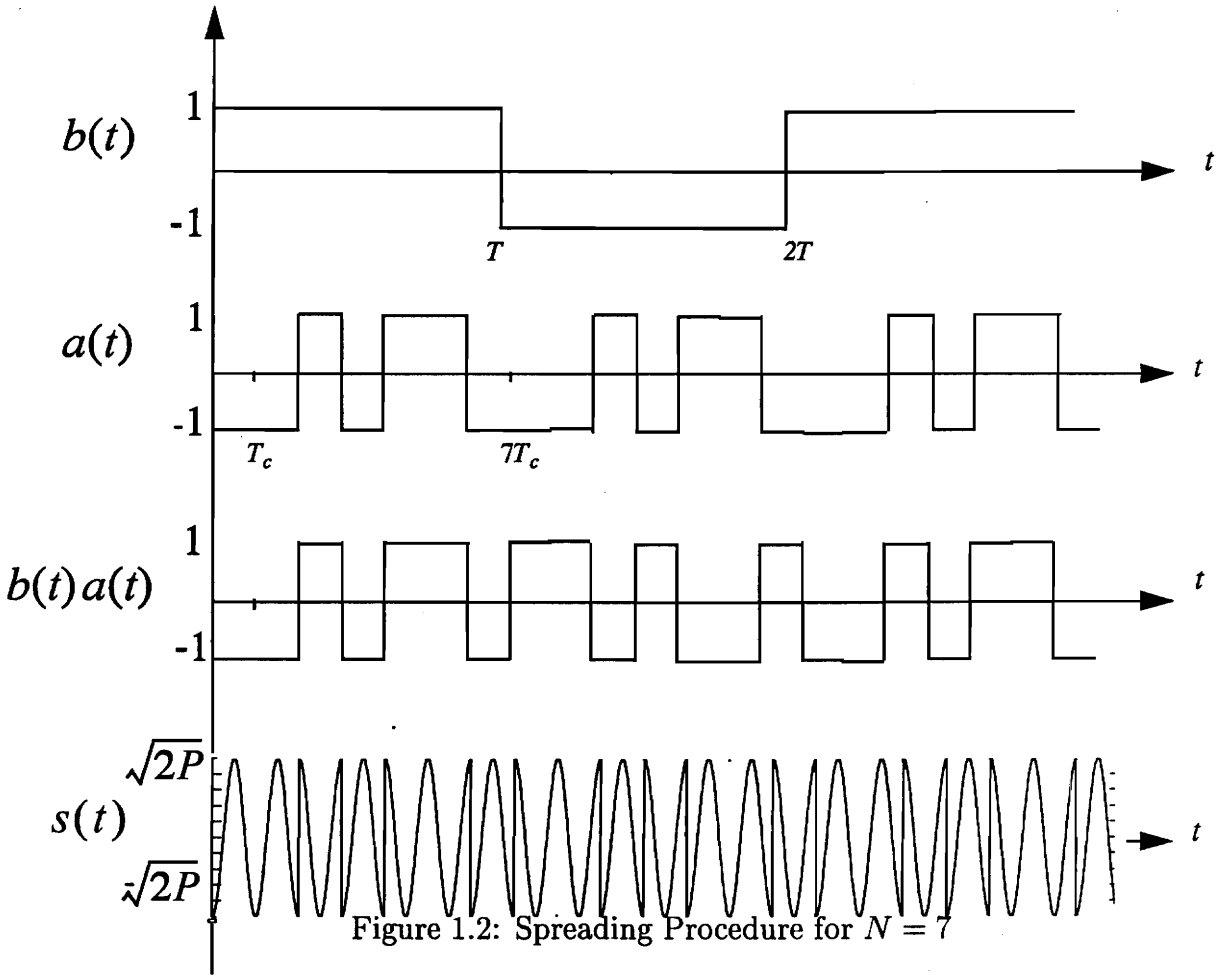

Figure 1.2: Spreading Procedure for $N = 7$

frequency ω_c radians/s, phase θ, and power P. The transmitted signal $s(t)$ is given by

$$s(t) = \sqrt{2P}a(t)b(t)\cos(\omega_c t + \theta). \tag{1.4}$$

Figure 1.2 illustrates an example of the DSSS spreading procedure. The data sequence is assumed to be $\{+1, -1, +1\}$, and the periodic PN sequence is $\{-1, -1, +1, -1, +1, +1, -1\}$. Thus, the PN sequence consists of $N = 7$ chips. The product sequence $b(t)a(t)$ is similar to $a(t)$, and if $a(t)$ were really random, $b(t)a(t)$ would be another random sequence having the same chip rate as $a(t)$. In this example, the spreading code is repeated for each data pulse. This is called code on pulse DSSS.

Note that the spreading sequence and the data stream are shown synchronous to each other in Figure 1.2. While this is not absolutely necessary, it helps in the clock recovery process at the receiver if the data and spreading waveform are synchronous. This spread data then modulates the carrier to yield a BPSK signal $s(t)$ which is transmitted. If the data rate is f_b, the bandwidth of a BPSK signal is $2f_b$, and the bandwidth of the spread spectrum signal is $\frac{2}{T_c}$. Thus, the spectrum has been spread by the ratio $\frac{1}{f_b \cdot T_c}$. However, since the power transmitted still remains the same, the power spectral density $S(f)$ of $s(t)$ is reduced by a factor of $f_b \cdot T_c$. Figure 1.3 shows the power spectral densities of the original data signal, the BPSK modulated signal, and the spread signal. Figure 1.3a plots the power spectral density of the data, assuming the pulse shape to be rectangular with duration T_b and amplitude A. Figure 1.3b is a plot of the power spectral density of the modulated signal. Now,we spread this signal in frequency by a factor of N. This will cause scaling in the amplitude by a factor of $\frac{1}{N}$, since the area under the power spectral density curve (total power) is not altered by the spreading procedure, and must remain constant. This gives the power spectral density of the transmitted signal, as shown in Figure 1.3c.

Figure 1.1 also shows a correlation receiver for the BPSK DSSS signal. The received signal, $r(t)$, is a delayed and corrupted version of the transmitted signal $s(t)$. The received signal is given by

$$r(t) = s(t - \tau) + n(t), \tag{1.5}$$

where τ is a finite propagation delay and $n(t)$ is an Additive White Gaussian Noise (AWGN) process. The function of the receiver is complementary to that of the transmitter. To recover the data, the receiver first multiplies the incoming signal $r(t)$ with the carrier $\sqrt{2P}\cos(\omega_c t)$, and then by the spreading signal $a(t)$. Thus, it is necessary to regenerate both the carrier and the spreading signal at the receiver. The resulting waveform is then integrated to the bit duration in the correlator to produce a decision statistic Z_i for the ith data bit. Thus, Z_i is given by

$$Z_i = \int_{iT}^{(i+1)T} r(t)a(t)\cos(\omega_c t)dt. \tag{1.6}$$

This decision statistic is compared with a threshold to give an estimate of the transmitted bit $\hat{b_i}$, where $\hat{b_i} = -1$ if $Z_i < 0$, and $\hat{b_i} = +1$ if $Z_i > 0$. This receiver model is

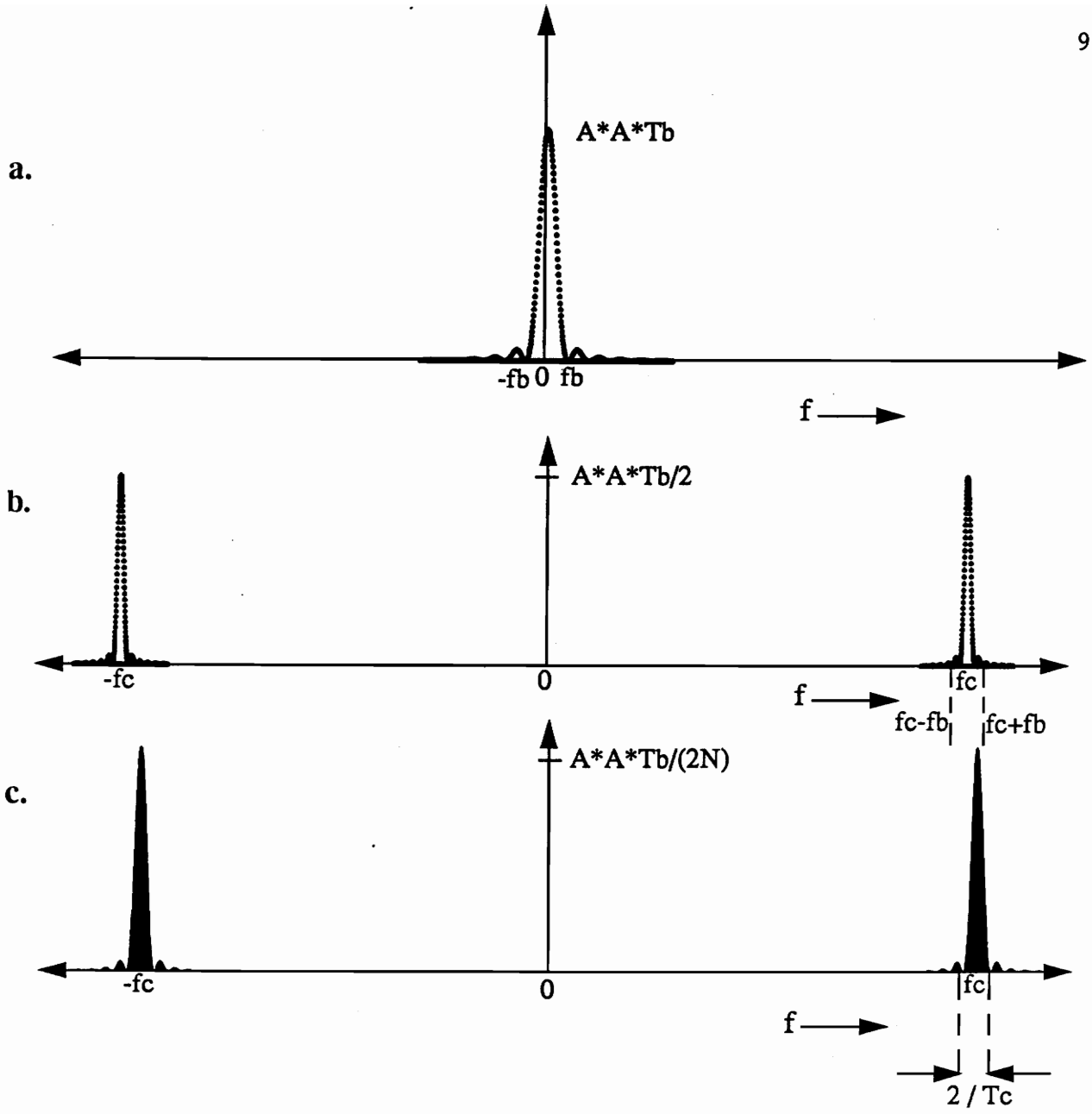

Figure 1.3: **a.** Power Spectral Density of a rectangular pulse of duration T_b, **b.** Power Spectral Density of a BPSK modulated signal, **c.** Power Spectral Density of the spread signal.

a mathematical abstraction of the physical receiver. A practical DSSS system would typically employ a super-heterodyne receiver in which the despreading is done either at an Intermediate Frequency (IF) or at baseband, and the integration operation would be performed using a matched filter.

1.4 Code Division Multiple Access

In order to permit multiple users to access a communications channel, a system employs one or more of the following multiple access techniques:

1. Frequency Division Multiple Access (FDMA)
2. Time Division Multiple Access (TDMA)
3. Code Division Multiple Access (CDMA)

FDMA As the name suggests, this technique involves dividing the available frequency spectrum into a large number of individual radio channels, each having enough bandwidth to support a single link.

TDMA In TDMA, data packets from different users are multiplexed in time. Each user is provided a time slot on the channel. For a particular user, data is transmitted only during the user's time slot. Systems such as GSM and US Digital Cellular employ a combination of TDMA and FDMA.

CDMA Spread Spectrum techniques have been used in military communications for decades, because of their anti-jamming, low probability of intercept, and multipath rejection capabilities. CDMA uses spread spectrum to provide multiple access communications. Each user in a CDMA system occupies the entire allocated spectrum, using a direct sequence spread spectrum waveform. Each user is assigned a unique pseudo-random code, also known as a signature sequence. A large number of users share the same frequency at the same time using their own signature sequences. Each signature sequence has low autocorrelation and low cross-correlation with all other signature sequences. The low correlation between the codes is used to achieve near orthogonality between signals of different users. Note that while FDMA and TDMA are perfectly orthogonal multiple access techniques, in practice, asynchronous CDMA

cannot be perfectly orthogonal, since we cannot generate a large number of signature sequences with zero cross-correlation. A correlation receiver for CDMA decodes the received signal by multiplying it by the signature sequence of the desired user. The situation is analogous to two people conversing over dinner at a crowded restaurant in a foreign country. Although surrounded by people carrying on conversations in many different languages, these people are able to tune out the other conversations and understand each other because they are speaking the same language. The code used by CDMA is similar to the language shared by the two diners. It allows many conversations to occur simultaneously, while each conversation is understood only by its intended recipients. A cellular system based on CDMA has been developed by QUALCOMM, Inc. and standardized by TIA as an Interim Standard (IS-95). The use of CDMA for cellular radio was motivated originally by capacity reasons, since AMPS is facing capacity limitations in crowded urban centers. However, there are many potential advantages for CDMA.

1.4.1 Advantages of CDMA for Cellular Radio

CDMA has the following advantages:

1. **Increased Capacity** While FDMA and TDMA must rely on path loss to provide isolation among cells (and must allocate different frequencies to adjoining cells), CDMA can reuse the same spectrum in all cells, thereby increasing capacity. Thus, CDMA increases system capacity, and reduces busy signals, dropped calls and cross-talk that result from system overcrowding.

2. **Inherent resistance to multipath fading** A multipath environment causes frequency selective fading. With a narrow-band signal, a frequency null can disrupt the whole channel. For a wide spectrum signal, however, the width of a frequency null is typically only a small part of the signal's bandwidth. This gives the signal an inherent ability to combat fading. Thus, CDMA improves call quality in congested downtown locations and areas with hilly terrain that experience interference from multipath. In fact, multipath signals can be used to advantage to provide a form of diversity. This concept is exploited in the RAKE receiver [7].

3. **Soft Capacity** There is a soft limit on capacity. The BER for all users increases gradually as the number of users increases, but the limit is not set by the number of channels. In other words, CDMA can squeeze additional users on the same radio channel at the cost of degraded voice quality. TDMA and FDMA have a hard limit on capacity.

4. **Soft Hand-off** CDMA utilizes a patented method of handing off calls between cells, known as soft hand-off. This is a make-before-break system, in which two base stations maintain a link with one mobile simultaneously. This method reduces the chances of call disruption during hand-off or of dropped calls due to failed hand-off.

5. **Overlay Capability** In the North American cellular system, there are no current plans to allocate additional spectrum for digital cellular. The analog and digital cellular systems will have to coexist in the same spectrum for the forseable future. In such situations, CDMA can be used with less interference between the two systems. This ability to coexist with existing RF systems is a major advantage for the CDMA technique.

6. **No Frequency Planning necessary** The AMPS system requires the signal to be at least 18 dB above the co-channel interference to provide acceptable call quality. CDMA systems can operate with a much smaller signal to interference ratio, allowing the use of the same set of frequencies in every cell. Thus, CDMA gets rid of the ongoing frequency planning required with other systems.

7. **Voice Activity Detection** The QUALCOMM system uses a variable rate vocoder with voice activity detection. The human voice activity cycle is about 35%. When users assigned to a channel are not talking, all other users on that channel benefit due to reduced interference. CDMA capacity is only interference limited, and any reduction in interference converts directly into an increase in capacity. Also, voice activity detection considerably reduces the effective data rate and the battery drain.

1.4.2 Disadvantages of CDMA for Cellular Radio

CDMA has the following disadvantages:

1. **Self Interference** Since it is not practically possible to achieve perfect orthogonality in asynchronous CDMA, there will always be some interference from other users sharing the channel. Moreover, multipath components of the same signal will also cause interference because of nonzero autocorrelation of the codes used.

2. **Near-Far Problem**

   If an interferer in a CDMA system is sufficiently stronger than the desired user, the interferer will dominate the performance of a conventional CDMA receiver. This problem is referred to as the near-far problem. The near far problem makes power control a basic requirement for a CDMA system. We will discuss the near-far problem in more detail in Section 2.3.

1.5 Generation and Characteristics of PN Sequences

PN codes are designed to have low autocorrelation and cross-correlation. Autocorrelation refers to the degree of correspondence between a code and a phase shifted replica of itself. We can define the autocorrelation as

$$R(\tau) = \int_{-\infty}^{\infty} f(t)f(t-\tau)dt. \tag{1.7}$$

Figure 1.4 provides a plot of the autocorrelation function of a maximal-length PN sequence. Note that the plot shows peak correlation for shifts of zero, and integer multiples of the code length. Between zero and ± 1 chip shifts, the autocorrelation decreases linearly, giving the plot a triangular shape. All other shifts result in a small autocorrelation.

The cross-correlation of two codes is a measure of the agreement between the two codes. When a large number of users have to share the same frequency spectrum, they must be assigned codes with low cross-correlation to keep the interference between them within acceptable levels. Thus, the cross-correlation between codes is an important consideration in CDMA systems. Poorly chosen codes with high cross-correlation

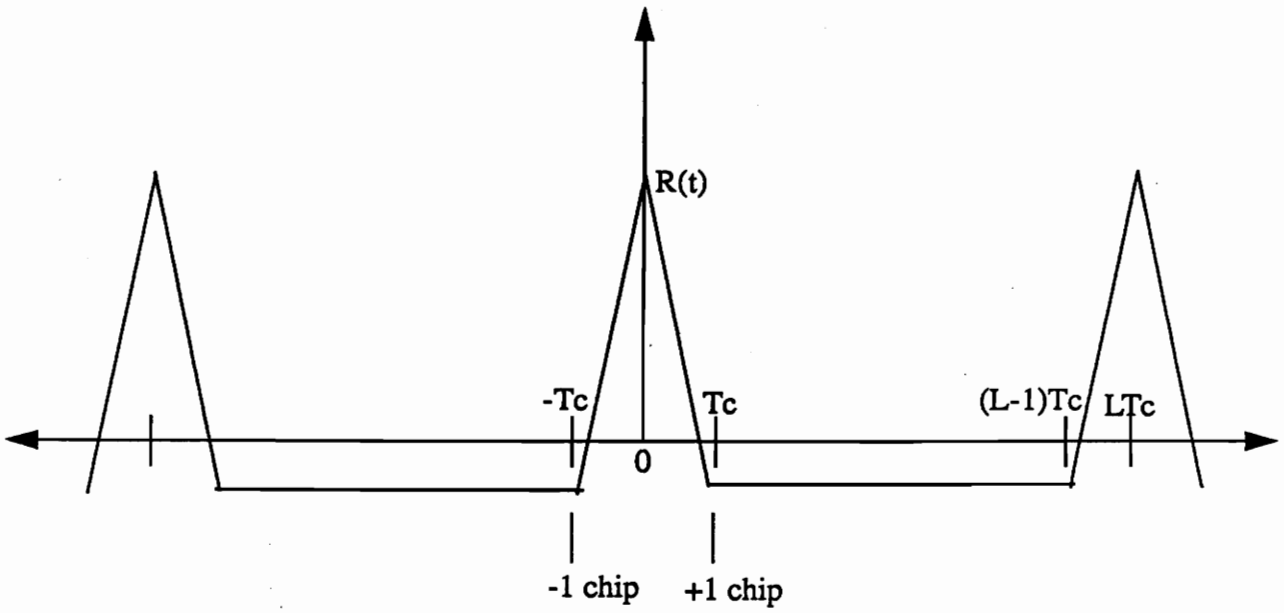

Figure 1.4: Autocorrelation function for maximal-length PN sequences

between them will increase the Multiple Access Interference (MAI) and cause false synchronization alarm in the receivers. Similar to the case of autocorrelation, the cross-correlation between two codes $f(t)$ and $g(t)$ is defined as

$$R_{cross}(\tau) = \int_{-\infty}^{\infty} f(t)g(t-\tau)dt. \tag{1.8}$$

Figure 1.5 shows a widely used PN sequence generator. It consists of digital flip flop circuits connected in series. The outputs of certain flip flops are fed to a parity generator. The parity generator output is the input of the first flip flop. The PN sequence generated is a function of the Q's which are connected to the input of the parity generator. It is not possible to generate a truly random sequence. We can, however, find the Q's which should be connected to the parity generator input to get a maximal PN sequence of length [6], $L = 2^N - 1$. Maximal codes are the longest codes that can be generated by a shift register of a given length. For example, for $N = 15$, $D_0 = Q_{13} \oplus Q_{14}$ provides the longest sequence with length 32767. Other feedback connections to the parity generator will generate non-maximal code sequences. Non-maximal code sequences often exhibit poorer correlation properties than maximal codes, and are usually avoided. Other codes (such as Gold codes) can be generated

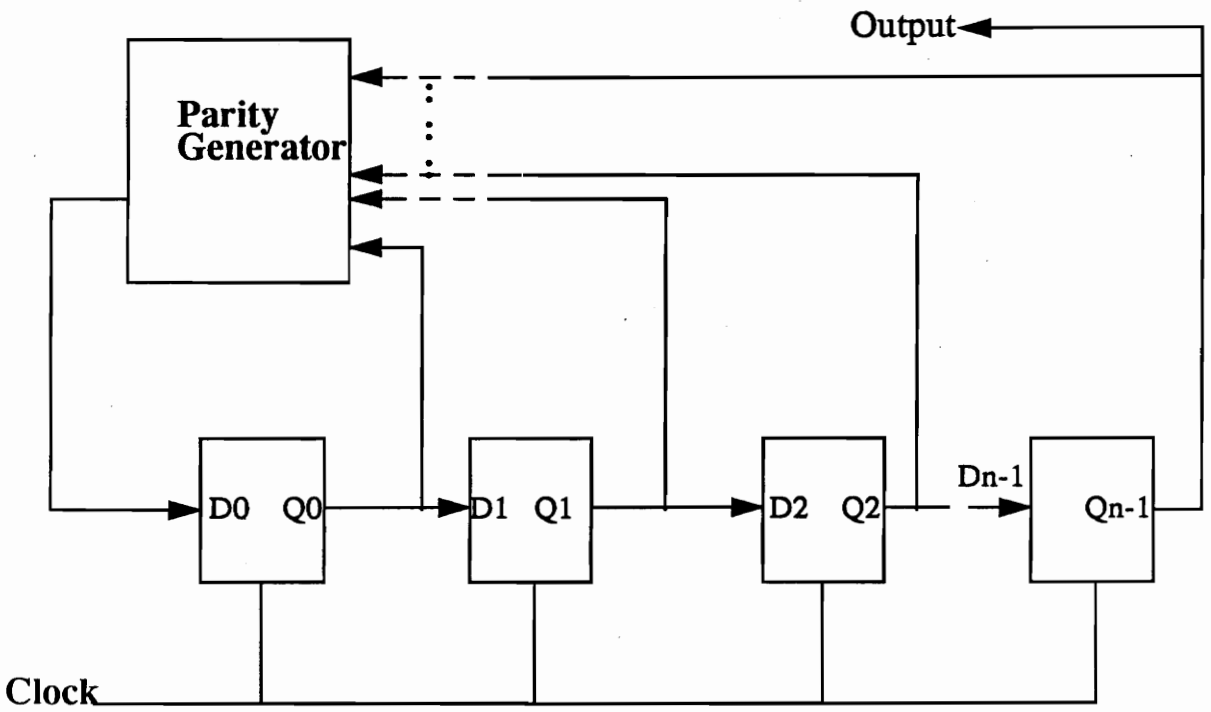

Figure 1.5: A Pseudo-Random Sequence Generator

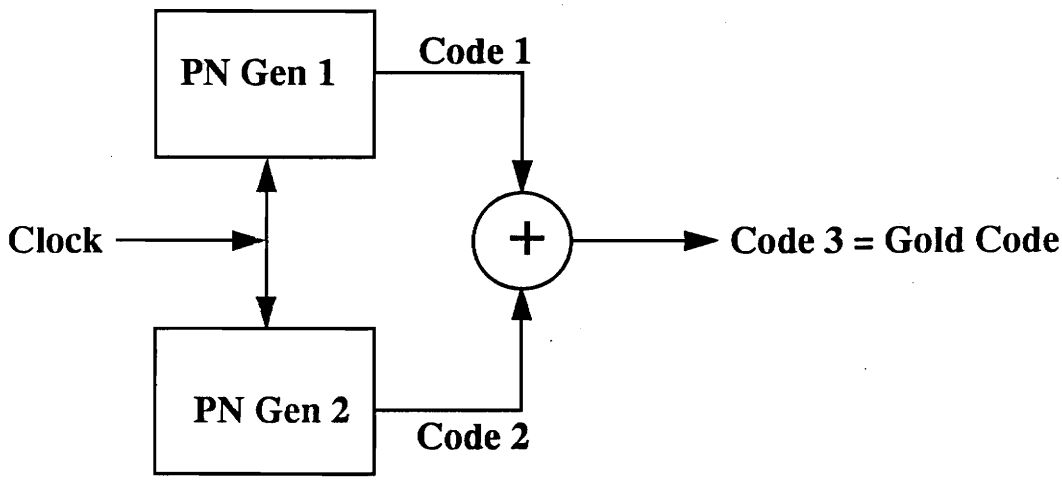

Figure 1.6: Gold Code Sequence Generator

by taking linear combinations of maximal codes. Such codes are called composite codes. Gold codes are generated by modulo-2 addition of a pair of maximal length sequences. Figure 1.6 shows a Gold code generator. The Gold codes which have the most desirable spectral characteristics are those in which the number of ones exceeds the number of zeros by one. These are called balanced codes. Gold code sequence generators are useful because they supply a large number of codes with good cross-correlation properties for use in a CDMA system.

1.6 Direct Sequence Spread Spectrum CDMA Model

In this section, a simple model for a DSSS CDMA system is presented. This model is shown in Figure 1.7. This model will be employed for the analytical studies presented in this thesis. We assume that the receiver is located at a base station of a central cell within a ring of surrounding cells, and that transmissions are along the reverse channel from mobile units to the base station. There are a total of K users per cell and the kth user transmits the binary data signal $b_k(t) = \sum_{i=-\infty}^{\infty} b_{k,i} p_T(t - iT)$, where $b_{k,i} \in \{\pm 1\}$ is the ith data bit of the kth user and $p_T(t)$ is a rectangular pulse with

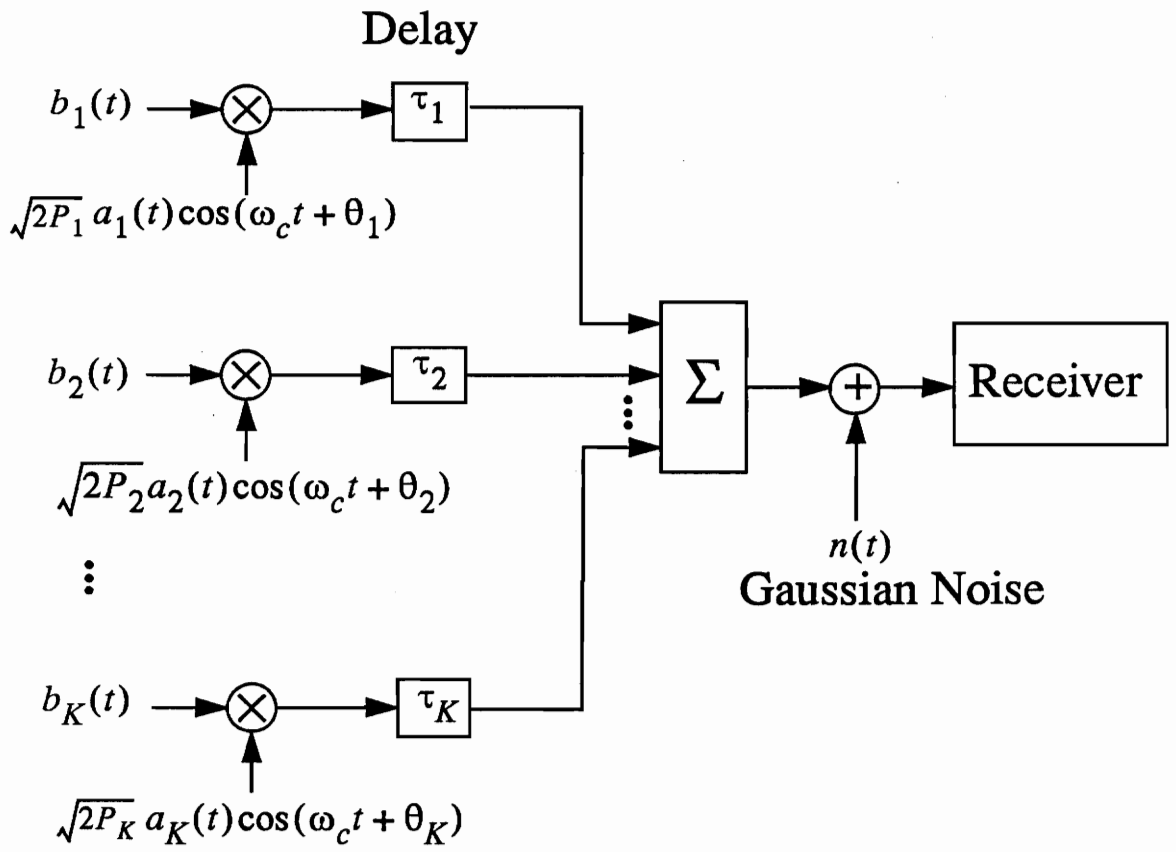

Figure 1.7: DSSS CDMA Model

amplitude 1 and duration T. The kth user's signal is spread by the signature signal $a_k(t) = \sum_{j=-\infty}^{\infty} a_{k,j} p_{T_c}(t - jT_c)$, where $a_{k,j} \in \{\pm 1\}$ is the jth chip of the kth user, and each rectangular chip pulse has duration T_c. The ratio of the bit duration T to the chip duration T_c is the processing gain $N = \frac{T}{T_c}$. The signal $s_k(t)$ transmitted by the kth user is given by

$$s_k(t) = \sqrt{2P_k} b_k(t) a_k(t) \cos(\omega_c t + \theta_k), \tag{1.9}$$

where P_k is the signal power and θ_k is the phase respectively of the kth user, and ω_c is the common carrier frequency.

The received signal $r(t)$is given by

$$r(t) = n(t) + \sum_{k=1}^{K} \sqrt{2P_k} a_k(t - \tau_k) b(t - \tau_k) \cos(\omega_c t + \phi_k), \tag{1.10}$$

where $n(t)$ is an additive white Gaussian noise (AWGN) process with two-sided power spectral density $\frac{N_0}{2}$, τ_k is the random delay associated with the kth user which is uniformly distributed on $[0, T)$, and $\phi_k = [\theta_k - \omega_c \tau_k] \mathrm{mod} 2\pi$. Although we have modeled only a single transmission path, this model can be extended to the more general case in which all resolvable multipath components are represented by the signal $s_k(t)$ and all unresolvable multipath components are contained in the noise process $n(t)$.

1.7 Outline of Thesis

Chapter 1 introduced the fundamentals of spread spectrum and CDMA, and presented a model for the DSSS CDMA system. In Chapter 2, we discuss various structures for CDMA receivers, including the correlation receiver, RAKE receiver, and multiuser receivers. Chapter 3 focuses on the analytical techniques used in this thesis. It introduces a model for the adaptive multistage interference cancellation receiver. This is the same as the model used in [8][9][10], where the performance of this receiver was analyzed to get a closed form expression for the Bit Error Rate (BER). We discuss some important extensions of this expression. An improved Gaussian approximation for modeling the interference is also presented [11]. Chapters 4 and 5 present the original contribution of this thesis. Chapter 4 introduces the idea of selective cancellation

on out-of-cell interferers, and develops a criterion for selecting out-of-cell interferers for interference cancellation. A circular geometry and the analytical techniques presented in Chapter 3 are used to analyze the performance of interference cancellation in a multi-cellular CDMA environment. Numerical results are presented for a typical micro-cellular environment. The use of averaging amplitude estimates over several bits to improve the selective cancellation criteria is investigated in Chapter 5. Chapter 6 concludes this thesis.

Chapter 2

Receiver Structures for CDMA Systems

A DSSS correlation receiver was introduced in Section 1.3. In this chapter, we present an overview of different structures that have been proposed for CDMA receivers. In Chapter 3, we will focus more specifically on the class of multiuser receivers.

2.1 Correlation Receiver

Figure 2.1 presents a correlation receiver at the base station of a CDMA cellular system. At the base station, there is a separate receiver for each user, and all receivers are presented with the same incoming signal $r(t)$, which is the sum of the signals of all users and the AWGN, as given by Eqn. 1.10. Each receiver correlates the incoming signal with a synchronized copy of the desired PN code to generate a decision statistic which is used to estimate the transmitted bit stream. Thus, conventional correlation detectors operate by enhancing the desired user, and treat the MAI which is inherent in CDMA as additive noise. This would work well if the MAI were truly uncorrelated with the desired signal. Unfortunately, some correlation between the codes cannot be avoided, and this causes significant degradation. As a result, capacities for single cell CDMA systems employing a correlation receiver can be significantly lower than those for FDMA or TDMA systems which are truly orthogonal. Moreover, if an interferer is significantly stronger than the desired user it will dominate performance due to the

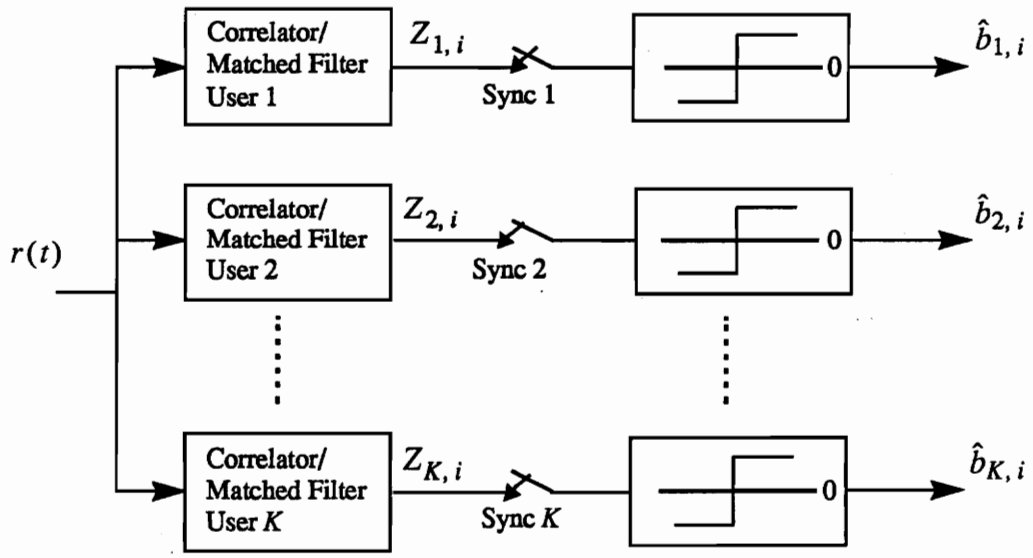

Figure 2.1: Correlation Receiver

near-far effect. This would limit the utility of the CDMA system to applications where each user's received power is approximately the same. The near-far effect is discussed in more details in Section 2.3. Performance of the conventional receiver will also be limited by multipath, since the multipath components will appear as interference because of nonzero autocorrelation of the PN code used. The conventional correlation detector can thus be severely limited by the near-far problem and multipath.

2.2 RAKE Receiver

When a signal travels through a practical channel, it undergoes reflection and scattering off objects in its path. The multipath components could interfere either constructively or destructively, depending on their relative phases. This causes inter-symbol interference which limits the data rate of unequalized narrow-band systems (because delays are much smaller than the bit period). In wide band signaling, however, the

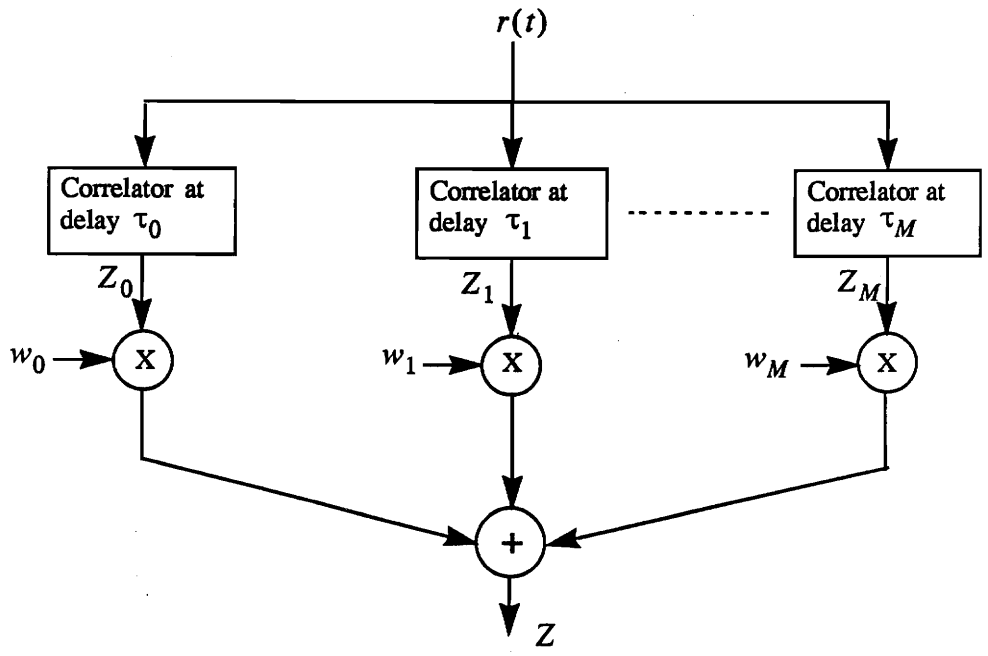

Figure 2.2: RAKE Receiver

duration of the transmitted symbols is small compared to the multipath delay introduced by the channel. This provides an inherent time diversity in case of wide band signals. Multipath can be used to advantage in CDMA by using a RAKE receiver. The RAKE receiver was first introduced by Price and Green [7]. The RAKE receiver exploits the time diversity by using information in multipath components in the decision process. As shown in Figure 2.2, a RAKE receiver consists of M correlation receivers, each attempting to track a different delayed version of the transmitted signal. Thus, at any time, the RAKE receiver would attempt to receive the M strongest multipath components. Figure 2.2 shows a RAKE receiver with M fingers. Without loss of generality, we can assume that the first component arrives with a delay $\tau_0 = 0$, and the later components arrive at τ_1 through τ_M. The first component is extracted by correlating the received signal with the signature sequence in the first

finger of the receiver. To extract the second component, the correlation receiver in the second finger to aligned with the received signal at time delay τ_1. This results in a strong correlation peak, indicating the presence of a second multipath component. This operation can be repeated for an arbitrary number of fingers in the RAKE. A decision statistic Z_m is obtained at the output of each correlator. These decision statistics must be combined in such a manner so as to extract maximum information from the multipath components. Each decision statistic Z_m is multiplied with weight W_m, where W_m is based on the confidence in the decision statistic Z_m. Then, the overall decision statistic is given by $Z = \sum_{m=1}^{M} W_m Z_m$. Different methods of combining the decision statistics include equal gain combining, maximal ratio combining, Minimum Mean Squared Error (MMSE) combining etc. In the equal gain combining method, decision statistics from all fingers of the RAKE are weighted equally. This would however place equal confidence in the weak and strong multipath components. Instead, the magnitude of the decision statistic $|Z_m|$ can be used to determine the weight W_m for each component, so as to accentuate the strong components and to suppress the weak components. In the maximal ratio combining method, signals from different fingers of the RAKE are weighted proportionately to their signal to noise power ratios and then added, so as to maximize the signal to noise ratio of the overall decision statistic. With a fairly mild set of assumptions, maximal ratio combining is equivalent to weighting the decision statistics from the RAKE fingers in proportion to their magnitude. More sophisticated adaptive methods such as MMSE combining may also be used. For all the combining methods, the weighted signals must be co-phased before combining. The overall decision statistic is used to generate an estimate of the transmitted signal.

2.3 The Near-Far Problem

The MAI in a CDMA cellular system may be modeled using the Gaussian Approximation. Assuming that signals from all users are received with equal power and modeling the MAI as a Gaussian random variable leads to the following expression

for the Bit Error Rate (BER) of a conventional receiver[12][13]:

$$P_b = Q\left\{\frac{1}{\sqrt{\frac{(K-1)}{3N} + \frac{N_0}{2E_b}}}\right\}, \tag{2.1}$$

where $Q(u)$ is the standard Q-function given by $Q(u) = \int_u^\infty \frac{1}{\sqrt{2\pi}} e^{-\lambda^2/2} d\lambda$, K is the number of equal power users in the system, N is the processing gain, and E_B is the energy per bit for each user, and $\frac{N_0}{2}$ is the two-sided power spectral density of the noise. Each user contributes a factor of $\frac{E_b}{3N}$ to the power spectral density of the noise. The factor N arises due to the fact that each user's energy is reduced by the processing gain, and the factor 3 is present because the MAI is not aligned in phase or time with the desired user. Since there are $K-1$ interferers, a factor of $(K-1)\frac{E_b}{3N}$ is added to the noise spectral density as seen in Eqn. 2.1. In a practical cellular system, the signals from all users may not be received at the same power. Equation 2.1 can be extended to account for unequal received powers as follows. If the signal powers received from the various users are unequal, then user k will contribute $\frac{E_b^{(k)}}{3N}$ to the noise level, where $E_b^{(k)}$ is the energy per bit for user k. Adding these to the noise power spectral density, we can express the BER of user 1 as

$$P_b = \left\{\frac{1}{\sqrt{\frac{\sum_{k=2}^{K} E_b^{(k)}}{3E_b^{(1)}N} + \frac{N_0}{2E_b}}}\right\}. \tag{2.2}$$

If an interferer has significantly higher power than the desired user, then the interferer will dominate performance, resulting in reducing the capacity of the CDMA system. This phenomenon is called the near-far effect. Equation 2.2 illustrates the near-far effect. If the powers of the received signals are very dissimilar, then the performance of a conventional receiver can degrade significantly, even if there is low cross-correlation between the received signals. This happens because the output of a conventional detector contains a spurious component which is linear in the amplitude of each of the interfering users, as seen in Eqn. 2.2. Figure 2.3 is a plot of the BER of a conventional receiver as a function of the signal to noise ratio for the cases of equal power users and when the power received from an interferer is 3 dB higher than that of the desired user. This figure points out the degradation in performance of a conventional receiver due

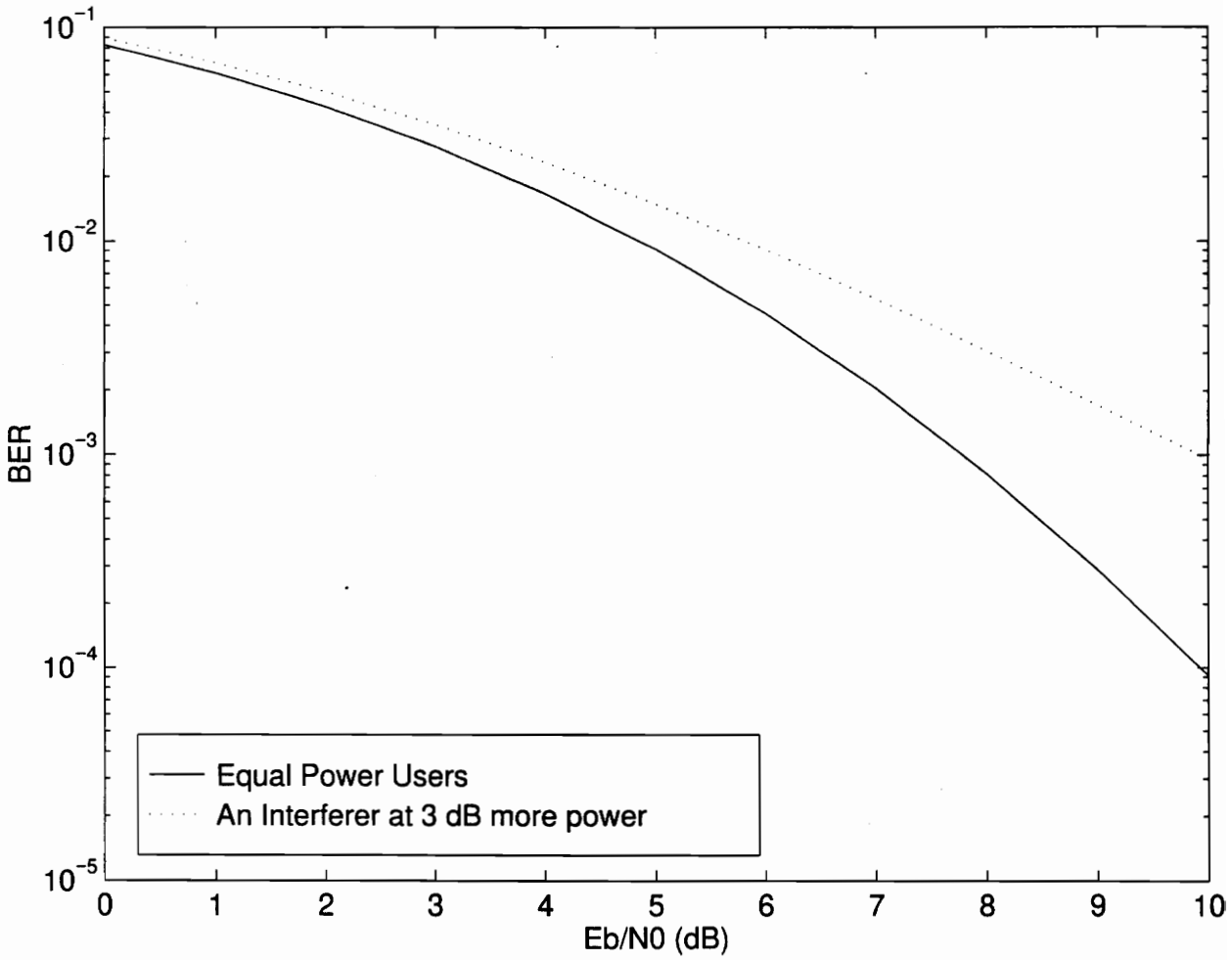

Figure 2.3: Performance of a Conventional Receiver under the Near-Far effect (N=31, K=3)

to the near-far effect. Thus, as MAI increases, the BER of the conventional receiver goes on degrading, and it is unable to detect signals transmitted by weak users. If an interferer is significantly stronger than the desired user, it will dominate performance in a conventional receiver. This could be remedied by using power control. In open loop power control, the mobile station senses the power received from the base station, and adjusts its power output accordingly. Closed loop power control can override the open loop setting by sending power control bits from the base station to the mobile. Field trials have shown that in spite of power control, the received power at the base station in an IS-95 system varies according to a log-normal distribution with a variance of $1 - 2$ dB. The effect of imperfect power control on the performance of CDMA receivers is investigated in [14], where it is shown that power level variations of $1 - 2$ dB can can result in capacity losses of the order of $15 - 30$ %. It is worth mentioning again that the near-far problem cannot be eliminated by using codes with good cross-correlation properties. CDMA performance can be greatly enhanced by using receivers designed to compensate for the MAI. Since MAI is such an important factor for determining the capacity of a cellular CDMA system [3], there has been considerable interest in various techniques to combat MAI in DSSS CDMA systems. One such technique is the use of multiuser receivers.

2.4 Multiuser Receivers

Multiuser receivers for CDMA exploit the fact that the base station receives signals from all users simultaneously and could potentially share information to make better decisions on the received data. Since such receivers work on the principle of simultaneous reception of signals from multiple users, they are suited for the base station of a cellular radio system. Other single user interference rejection techniques which do not require knowledge of the spreading codes of other users [15][16][17] must be employed to combat MAI at the mobile. The optimal multi-user detector was shown in [18][19] to significantly enhance capacity and near-far resistance. This leads us to conclude that the near-far problem is not inherent to DS-CDMA, but only to conventional single user detectors. The optimal multiuser receiver is shown in Figure 2.4. It consists of a bank of matched filters followed by a Viterbi decision algorithm for

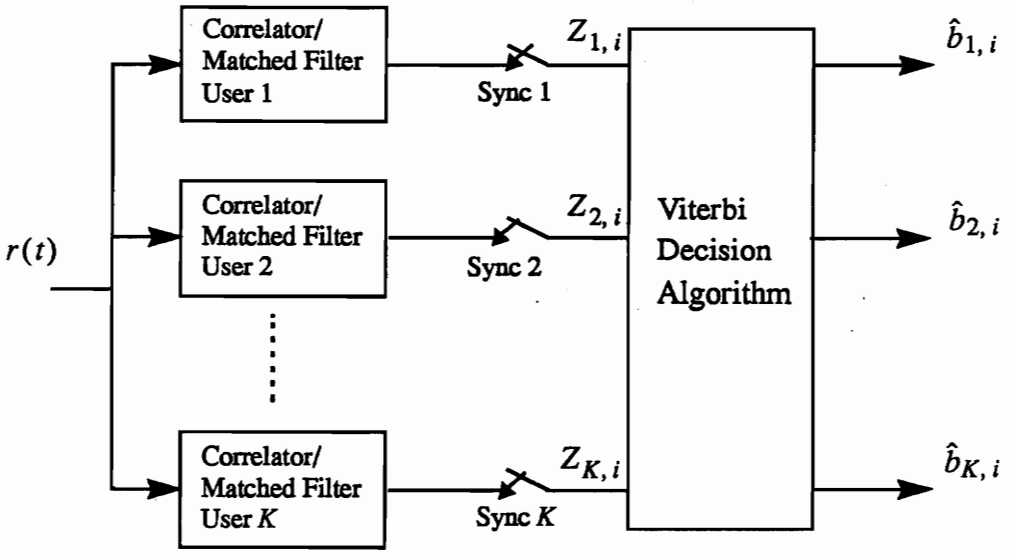

Figure 2.4: Optimum Multiuser Receiver

maximum likelihood sequence estimation. The complexity of the Viterbi algorithm is exponential in the number of users (on the order of 2^K). This makes the optimum multiuser receiver too complex to implement in practice. Moreover, when the received signals are asynchronous, it requires a priori knowledge of the power, amplitude and delay of each arriving signal [18].

As a result of the very high complexity of the optimum multiuser receiver, research has focussed on sub-optimal receivers which achieve significant performance improvement with reasonable complexity. Researchers have investigated a variety of sub-optimal approaches including reduced complexity decision algorithms [20], decorrelating receivers [21], and both successive [21] and parallel [22][23] implementations of multistage interference cancellation. A survey of various multiuser receiver techniques is presented in [24].

The structure of a multistage receiver is shown in Figure 2.5. The detector consists of a bank of K matched filters followed by a bank of K M-stage processors. The first stage is a conventional CDMA detector and provides a decision statistic for each user from the received signal. Then, M stages of processing is performed on the decision statistic, where each stage processes the decision statistic obtained from the previous stage. The basic idea in the multistage interference cancellation receiver proposed in [22] and [23] is to use the decision statistic to estimate the data transmitted by each user, reconstruct the interfering signal, and subtract this estimated interference from the received signal to obtain a cleaner version of the desired signal. This operation may be repeated iteratively to get multiple stages of data estimation, signal reconstruction and interference cancellation in the hope of getting successively better estimates of the desired signal. Such a receiver exhibits significant performance improvement over the conventional receiver, and approaches the performance and near far resistance of an optimum receiver. The complexity is linear in the number of users K, which is considerably less complex than that of the optimum multiuser receiver. The popular suboptimal receiver proposed in [22] assumed perfect knowledge of the arriving signal amplitudes and delays. Subsequently, researchers have investigated the performance of a large number of variations on this approach [25][26][27]. The condition for a priori knowledge of signal amplitudes has been relaxed in [28]. Recent work has demonstrated that cancellation of strong interferers is significantly more

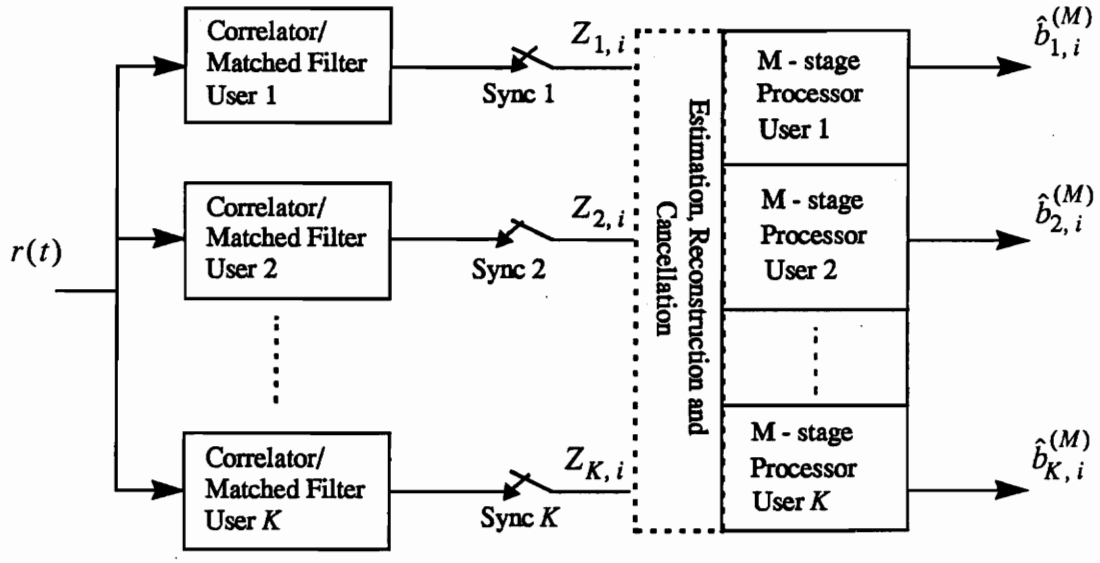

Figure 2.5: Multistage Receiver (A sub-optimum multiuser receiver)

important than cancellation of weak interferers, leading to the idea of successive cancellation [27] and soft cancellation [26]. In this thesis, we focus on the multistage approach which has been extended to adapt to variable received power levels [25][29]. In the next chapter, we consider a more detailed mathematical model for multistage interference cancellation.

Chapter 3

Adaptive Multistage Interference Cancellation

3.1 Adaptive Multistage Interference Cancellation Model

3.1.1 The Interference Cancellation Model

We employ a simple model for the adaptive multistage interference cancellation receiver which was used in [8][9][10]. Figure 3.1 presents this model. We assume that the receiver is located at a base station of a central cell within a ring of surrounding cells, and that transmissions are along the reverse channel from mobile units to the base station. As represented in the model developed in Section 1.6, the signal $s_k(t)$ transmitted by the kth user is given by

$$s_k(t) = \sqrt{2P_k} b_k(t) a_k(t) \cos(\omega_c t + \theta_k), \tag{3.1}$$

and the received signal $r(t)$is given by

$$r(t) = n(t) + \sum_{k=1}^{K} \sqrt{2P_k} a_k(t - \tau_k) b(t - \tau_k) \cos(\omega_c t + \phi_k), \tag{3.2}$$

The first stage of the receiver is a conventional CDMA receiver in which $r(t)$ is correlated with a synchronous copy of the spreading signal. Let $Z_{k,i}^{(s)}$ be the decision

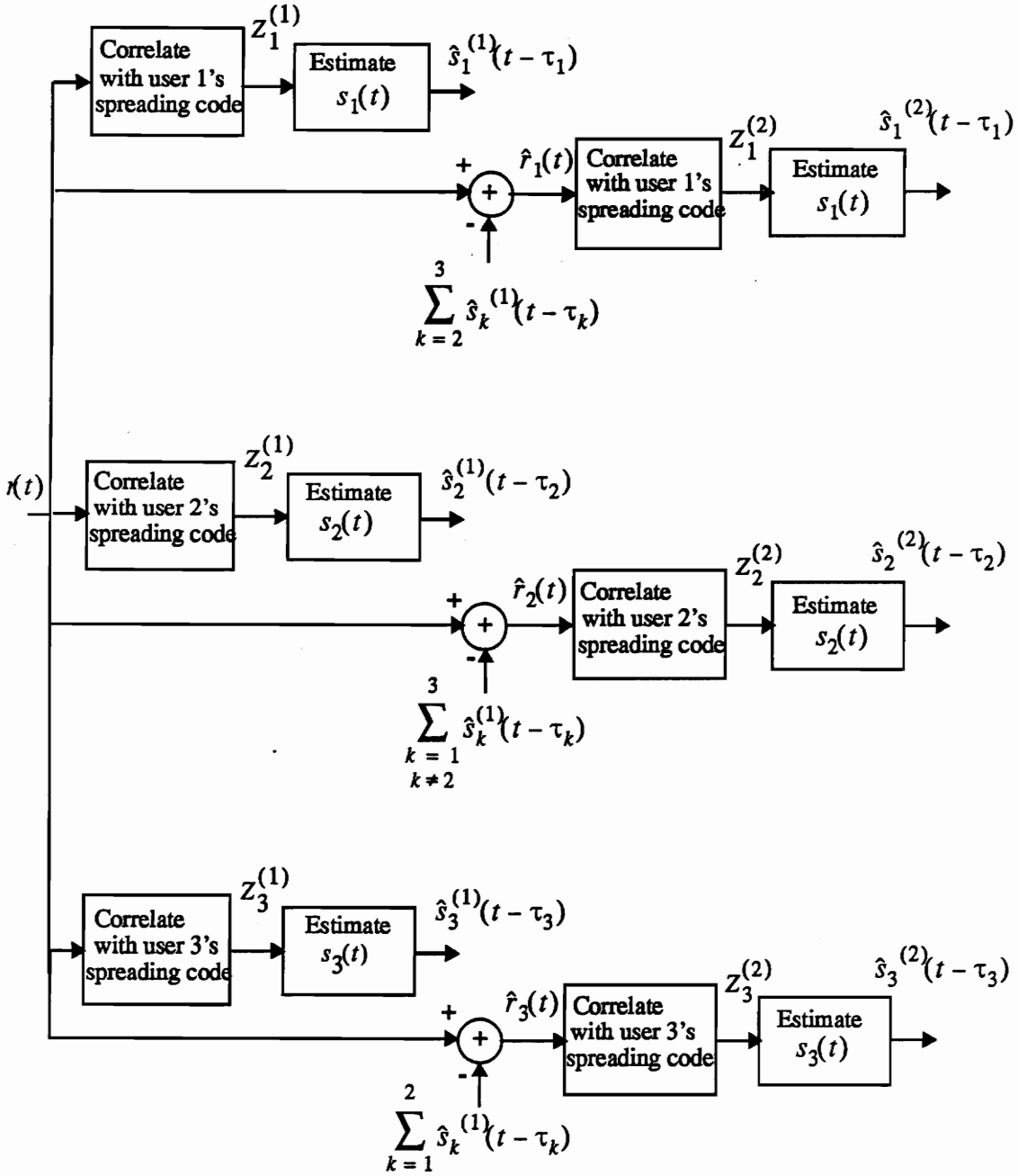

Figure 3.1: Block Diagram of a two stage interference cancellation receiver for three users

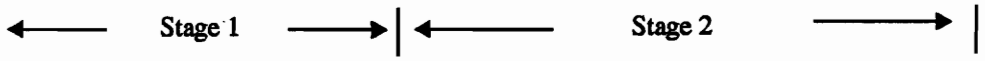

Figure 1: Block diagram of a two stage interference cancellation receiver for three users.

statistic for the ith bit of the kth user at stage s. Then the decision statistic for user k for stage 1 (i. e., before any interference cancellation) is given by

$$Z_{k,i}^{(1)} = \int_{iT+\tau_k}^{(i+1)T+\tau_k} r(t)a_k(t-\tau_k)cos(\omega_c t + \phi_k)dt. \tag{3.3}$$

This standard CDMA model is now extended to include adaptive multistage interference cancellation as illustrated in Figure 3.1. The decision statistic $Z_{k,i}^{(s)}$ can be used to form an estimate $\hat{s}_k^{(s)}(t)$ of user k's signal after stage s:

$$\hat{s}_k^{(s)}(t) = \frac{2}{T}a_k(t)\cos(\omega_c t + \phi_k)\sum_{i=-\infty}^{\infty} Z_{k,i}^{(s)} p_T(t-iT). \tag{3.4}$$

Interference cancellation is performed by subtracting the estimated signals of the interfering users from the received signal $r(t)$ to form a new received signal $\hat{r_k^{(s)}}(t)$ for the kth user after stage s, given by

$$\hat{r_k^{(s)}}(t) = r(t) - \sum_{\kappa=1,\kappa\neq k}^{K} \hat{s}_\kappa^{(s)}(t-\tau_k)$$

$$= n(t) + \sqrt{2P_k}b_k(t-\tau_k)a_k(t-\tau_k)\cos(\omega_c t + \phi_k) + \sum_{\kappa=1,\kappa\neq k}^{K}\left[s_\kappa(t-\tau_\kappa) - \hat{s}_\kappa^{(s)}(t-\tau_\kappa)\right] \tag{3.5}$$

The decision statistic $Z_{k,i}^{(s+1)}$ for the ith bit of the kth user at stage $s+1$ (i. e., after s stages of interference cancellation) is formed by correlating $r_k^{(s)}(t)$ with the kth user's spreading signal:

$$Z_{k,i}^{(s+1)} = \int_{iT+\tau_k}^{(i+1)T+\tau_k} r_k^{(s)}(t)a_k(t-\tau_k)\cos(\omega_c t + \phi_k)dt \tag{3.6}$$

Using this procedure, an arbitrary number of stages of interference cancellation may be performed to form successive estimates of the data transmitted by each user.

3.1.2 Assumptions

We make the following assumptions in analyzing the model presented above:

1. The multistage receiver is located at the base station, and transmissions are along the reverse channel from the mobile to the base station.

2. MAI is modeled as a Gaussian random variable.

3. We have modeled a single cell environment. At this stage, no adjacent cell interference is considered. We will analyze the multicellular environment later in the thesis.

4. We assume coherent demodulation.

5. Phase and delays of all users are accurately tracked by the receiver.

3.2 Analysis of Receiver Performance

In this section, we use the simple Gaussian approximation to analyze the performance of the receiver [12]. The decision statistic for user k at stage 1 may be expressed as the sum of three components.

$$Z_{k,i}^{(1)} = \xi + A_k + \sum_{\kappa=1,\kappa\neq k}^{K} I_{\kappa}^{(1)}, \tag{3.7}$$

where ξ is the contribution of the AWGN, A_k is the contribution of the desired user's signal, and $I_{\kappa}^{(1)}$ is the MAI from the κth user at stage 1. The noise term ξ is given as

$$\xi = \int_{iT+\tau_k}^{(i+1)T+\tau_k} n(t)a_k(t-\tau_k)\cos(\omega_c t + \phi_k)dt\cdot \tag{3.8}$$

Since $n(t)$ is a zero mean Gaussian random process and integration is a linear operation, ξ is a Gaussian random variable with mean 0 and variance $\frac{N_0 T}{4}$. The desired user's contribution is given by

$$A_k = \int_{iT+\tau_k}^{(i+1)T+\tau_k} \sqrt{2P_k}b_k(t-\tau_k)a_k^2(t-\tau_k)\cos^2(\omega_c t+\phi_k)dt = b_{k,i}T\sqrt{\frac{P_k}{2}}\cdot \tag{3.9}$$

The MAI is a Gaussian random variable with mean 0 and

$$Var\left[\sum_{\kappa=1,\kappa\neq k}^{K} I_{\kappa}^{(1)}\right] = \frac{NT_c^2}{6}\sum_{\kappa=1,\kappa\neq k}^{K} P_{\kappa}\cdot \tag{3.10}$$

Thus, using the Gaussian approximation for the MAI, we can model $Z_{k,i}^{(1)}$ as a Gaussian random variable with its mean and variance given by

$$E[Z_{k,i}^{(1)}] = A_k = b_{k,i}T\sqrt{\frac{P_k}{2}}, \tag{3.11}$$

and

$$Var[Z_{k,i}^{(1)}] = \frac{N_0 T}{4} + \frac{NT_c^2}{6} \sum_{\kappa=1,\kappa\neq k}^{K} P_\kappa. \tag{3.12}$$

For an equiprobable data source ($P[b_{k,i} = 0] = P[b_{k,i} = 1] = \frac{1}{2}$), the probability of bit error $P_{b_k}^{(1)}$ can be defined as

$$P_{b_k}^{(1)} = P\left[\left(\xi + \sum_{\kappa=1,\kappa\neq k}^{K} I_\kappa^{(1)}\right) > |A_k|\right] = Q\left\{\frac{|A_k|}{\sqrt{Var[Z_{k,i}^{(1)}]}}\right\}. \tag{3.13}$$

Substituting Eqns. 3.11 and 3.12 into Eqn. 3.13, we can write

$$P_{b_k}^{(1)} = Q\left\{\left[\frac{P_k T^2}{2Var[Z_{k,i}^{(1)}]}\right]^{1/2}\right\}. \tag{3.14}$$

Now, we can substitute Eqn. 3.12 into Eqn. 3.14 to express the probability of bit error at stage 1 as

$$P_{b_k}^{(1)} = Q\left\{\left[\frac{P_k T^2/2}{\frac{N_0 T}{4} + \frac{NT_c^2}{6}\sum_{\kappa=1,\kappa\neq k}^{K} P_\kappa}\right]^{1/2}\right\}. \tag{3.15}$$

Thus, for stage 1, we get the probability of bit error as

$$P_{b_k}^{(1)} = Q\left\{\left[\frac{1}{2(E_{b_k}/N_0)} + \frac{1}{3N}\frac{\sum_{\kappa=1,\kappa\neq k}^{K} P_\kappa}{P_k}\right]^{-\frac{1}{2}}\right\}, \tag{3.16}$$

where $E_{b_k} = P_k T$.

3.3 BER Analysis for Interference Cancellation

The closed form expression for BER as presented in this section was presented in [10], and rigorously developed in [8][9]. Since the estimates $\hat{s}_k^{(s)}(t)$ of the interfering signals in Eqn. (3.4) are formed using the decision statistic from the previous stage, it is possible to estimate the power of each interfering signal from Eqn. (3.3). Those estimates will be subject to both noise and MAI. The decision statistic for user k at stage $s+1$ can be expressed as the sum of three components.

$$Z_{k,i}^{(s+1)} = \xi + A_k + \sum_{\kappa=1,\kappa\neq k}^{K} I_\kappa^{(s+1)}, \tag{3.17}$$

where ξ is the contribution of the noise, A_k is the contribution of the desired user's signal, and $I_\kappa^{(s+1)}$ is the MAI from the κth user at stage $s+1$ remaining after interference cancellation at stage s, and is given by

$$I_\kappa^{(s+1)} = I_\kappa^{(s)} - \hat{I}_\kappa^{(s)} \tag{3.18}$$

where $\hat{I}_\kappa^{(s)}$ is the estimate of the MAI from the κth user formed at stage s. Assuming the power P_k to be constant over the operation of the receiver (i. e. considering the variance of $I_\kappa^{(1)}$ to be constant over the operating of the receiver), the variance of the MAI at stage $s+1$ will be equal to the variance of the estimate of the MAI at stage s.

$$Var\left[\sum_{\kappa=1,\kappa\neq k}^{K} I_\kappa^{(s+1)}\right] = Var\left[\sum_{\kappa=1,\kappa\neq k}^{K} \hat{I}_\kappa^{(s)}\right] \tag{3.19}$$

Kaul and Woerner [8]ashish derived a recursive expression for the variance of the decision statistic at each stage of interference cancellation:

$$Var\left[\sum_{\kappa=1,\kappa\neq k}^{K} I_\kappa^{(s+1)}\right] = \frac{1}{3N} \cdot Var\left[\sum_{\kappa=1,\kappa\neq k}^{K} Z_{\kappa,i}^{(s)}\right] \tag{3.20}$$

$$Var[Z_{k,i}^{(s+1)}] = \frac{N_0 T}{4} + \frac{1}{3N} \cdot Var\left[\sum_{\kappa=1,\kappa\neq k}^{K} I_\kappa^{(s+1)}\right] \tag{3.21}$$

Eqns. 3.20 and 3.21 can be used recursively to compute the variance of $Z_{k,i}^{(s)}$ at any stage s, and hence the probability of bit error $P_{b_k}^{(s)}$ at that stage. In [8][9] it is shown by mathematical induction that the variance of the decision statistic at stage s is given by

$$Var[Z_k^{(s+1)}] = \frac{N_0 T}{4}\left[\frac{1-\left(\frac{K-1}{3N}\right)^{s+1}}{1-\frac{K-1}{3N}}\right] + \frac{T^2}{2.(3N)^{s+1}}\left[\frac{(K-1)^{s+1}-(-1)^{s+1}}{K}\left(\sum_{\kappa=1}^{K} P_\kappa\right) + (-1)^{s+1}.P_k\right]. \tag{3.22}$$

Since $E[Z_{k,i}^{(s)}] = \sqrt{\frac{P_k}{2}} T b_{k,i}$ due to the desired signal component, a signal to noise ratio may be formed, and the average probability of error for this adaptive multistage CDMA receiver may be approximated by the formula:

$$P_{b_k}^{(s)} = Q\left\{\left[\frac{1}{2(E_{b_k}/N_0)}\left(\frac{1-(\frac{K-1}{3N})^s}{1-\frac{K-1}{3N}}\right) +\right.\right.$$

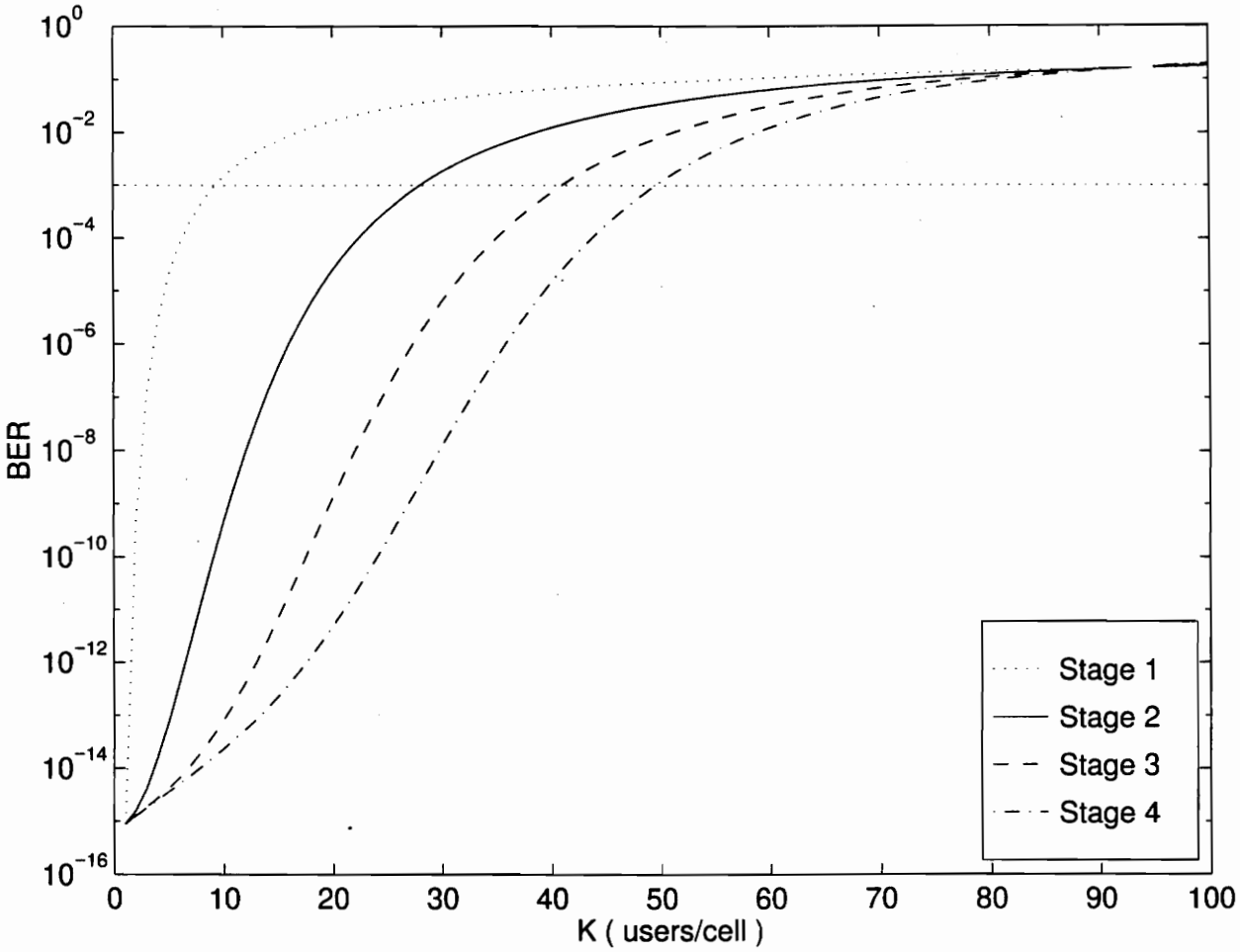

Figure 3.2: Performance of Interference Cancellation in a Single Cell, ($N = 31$, $\frac{E_b}{N_0} =$ 15 dB)

$$\frac{1}{(3N)^s}\left(\frac{(K-1)^s-(-1)^s}{K}\left(\frac{\sum_{\kappa=1}^{K} P_\kappa}{P_k}\right)+(-1)^s\right)\Bigg]^{-\frac{1}{2}}\Bigg\} \tag{3.23}$$

where K is the number of simultaneous users sharing the channel, N is the number of chips per bit, $P_{b_k}^{(s)}$ is the probability of bit error at stage s for the kth user, N_0 is the one sided power spectral density of the Gaussian noise, s is the number of stages in the receiver, and P_k is the power of the kth user. Figure 3.2 plots the BER as a function of the number of users per cell K for a multistage interference cancellation receiver according to Eqn. 3.23. An $\frac{E_b}{N_0}$ value of 15 dB and a processing gain $N = 31$ are assumed for this figure. Perfect power control is assumed. BER curves are shown for

$s = 1...4$, where $s = 1$ corresponds to the conventional receiver, and $s = 4$ corresponds to three stages of interference cancellation. For convenience, a line showing a desired BER of 10^{-3} is displayed. This figure shows the impressive capacity gains that can be obtained by adaptive interference cancellation in a single cell environment. At a desired BER of 10^{-3}, a two stage ($s = 2$) receiver can provide almost three times the capacity of a conventional receiver, and a receiver with three stages leads to about five times increase in capacity as compared to a conventional single stage receiver. As the number of interference cancellation stages is increased, further improvements diminish and performance tends towards an asymptotic limit. Figure 3.3 plots the BER versus the $\frac{E_b}{N_0}$ for a system with $K = 20$ users, and a processing gain of $N = 31$. This figure has been plotted assuming perfect power control. Here again, we see that a two stage interference cancellation receiver can provide substantial performance improvement over a conventional receiver with no interference cancellation. Further stages provide some additional performance improvement, and performance tends towards an asymptotic limit. Thus, most of the performance improvement that can be obtained from a multistage interference cancellation receiver is achieved in the first few stages of the receiver. In Chapter 4, we will use the result in Eqn. 3.23 to explore the use of interference cancellation in a multicellular environment. In [8][9][10] this result has been verified against simulations and has shown to yield good results for BER$\geq 10^{-4}$. Recall from Section 3.1.2 that these results were obtained assuming that the delays τ_k and phase ϕ_k are known by the receiver. Performance in the presence of phase and timing errors is an important practical consideration, since imperfect cancellation could potentially add interference into the signal. The effect of phase and timing errors has been investigated in [30] and [31]. It is shown in [30] that interference cancellation is fairly robust to significant tracking errors. However, the sensitivity to timing errors can increase when pulse shaping is employed.

3.4 Extensions

In this section, we describe some important and insightful extensions [8][9][10] of the result presented in Eqn. 3.23.

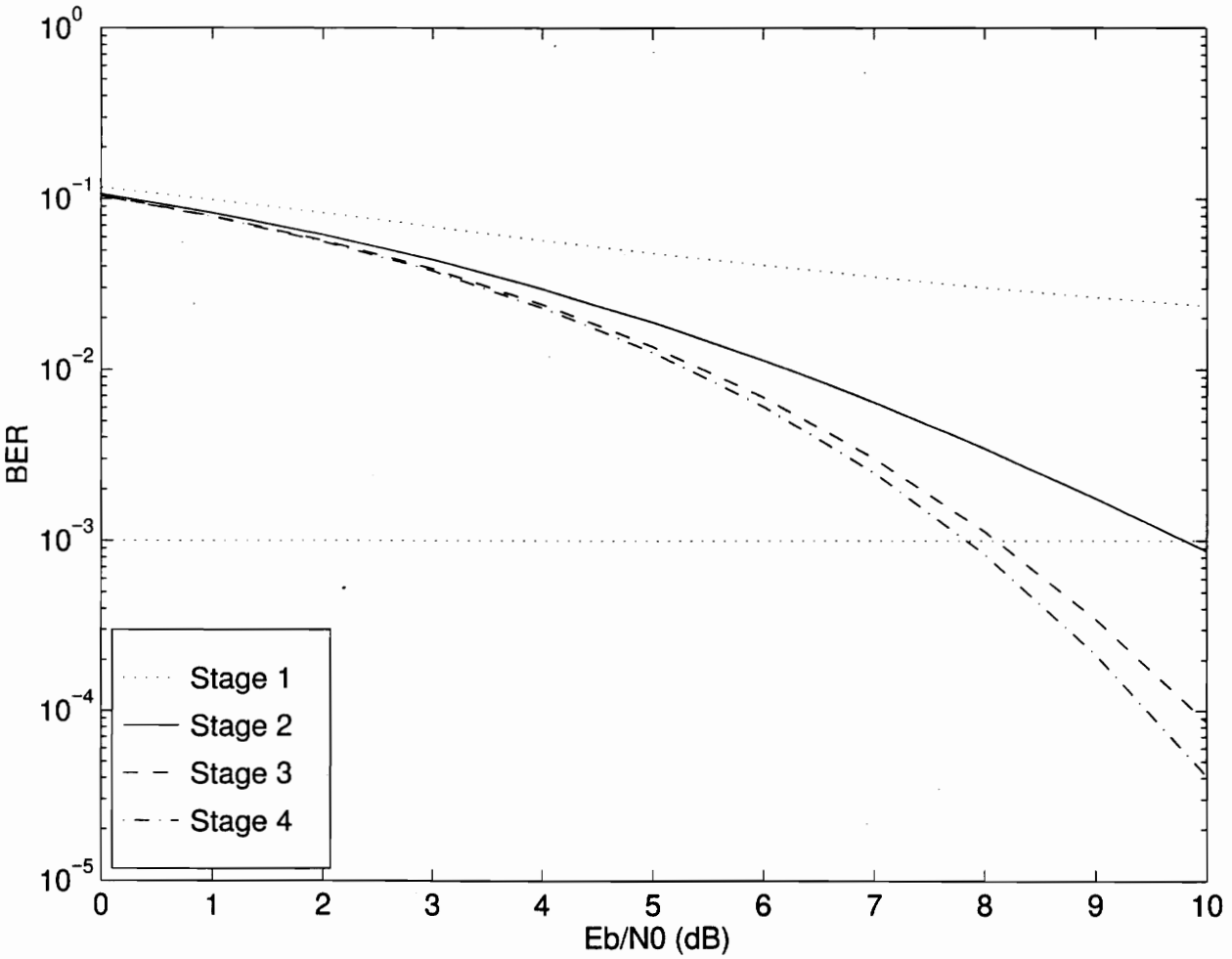

Figure 3.3: BER vs. Eb/N0 for Interference Cancellation in a Single Cell, ($N = 31, K = 20$)

1. **Single stage** For a single stage receiver (no interference cancellation), we would substitute $s = 1$ in Eqn. 3.23, which reduces it to Eqn. 3.16, the BER expression for a standard correlation receiver.

2. **Ideal Power Control** In the case of ideal power control, $P_1 = P_2 = P_3 = ... = P_k = P$. This simplifies Eqn. 3.23 to

$$P_{b_k}^{(s)} = Q\left\{\left[\frac{1}{2(E_b/N_0)}\left(\frac{1-\left(\frac{K-1}{3N}\right)^s}{1-\left(\frac{K-1}{3N}\right)}\right)+\left(\frac{K-1}{3N}\right)^s\right]^{-1/2}\right\}, \tag{3.24}$$

where $E_b = PT$ is the energy per bit for any of the equal power users.

3. **Limitation of adaptive multistage interference cancellation (for ideal power control)** Eqn. 3.24 can be used to determine a set of conditions under which interference cancellation actually degrades performance, implying $P_{b_k}^{(s+1)} > P_{b_k}^{(s)}$. Comparing the argument of the Q-function at stages s and $s+1$ in Eqn. 3.24, we can write

$$P_{b_k}^{(s+1)} > P_{b_k}^{(s)} \Leftrightarrow \left(\frac{K-1}{3N} > 1\right) or \left(\frac{E_b}{N_0} < \frac{1}{2\left(1-\frac{K-1}{3N}\right)}\right). \tag{3.25}$$

Eqn. 3.25 indicates that for the case of equal signal powers, interference cancellation degrades performance if either the level of interference is too large or the signal to noise ratio is too small. In either case, the variance of the decision statistics will be so large, that using the decision statistics to form estimates of signal amplitudes for cancellation will actually introduce more interference into the system.

4. **Best possible performance** Provided that the condition of Eqn. 3.25 does not hold, then we can predict the best possible performance for the multistage receiver by letting the number of stages approach infinity.

$$\lim_{s\to\infty} P_{b_k}^{(s)} = Q\left\{\left[\frac{1}{2(E_{b_k}/N_0}\left(\frac{1}{1-\frac{K-1}{3N}}\right)\right]^{-1/2}\right\}. \tag{3.26}$$

Thus, even when the number of interference cancellation stages approaches infinity, the MAI is never completely cancelled. There exists an error floor, such that the performance of the multistage receiver is still worse than that of a single user ($K = 1$) CDMA system.

5. **Limitation of adaptive multistage interference cancellation (for unequal signal powers)** Eqn. 3.25 presented the limitation of interference cancellation in case of ideal power control. In the case of unequal signal powers we can derive a similar condition

$$P_{b_k}^{(2)} > P_{b_k}^{(1)} \Leftrightarrow Var[Z_{k,i}^{(2)}] > Var[Z_{k,i}^{(1)}] \Leftrightarrow P_\kappa < \frac{N_0}{2T} + \frac{1}{3N}\left(\sum_{u=1,u\neq\kappa}^{K} P_u\right). \quad (3.27)$$

Eqn. 3.27 says that if the power received from the κ th interferer is below a certain threshold, then we cannot get a good decision statistic from the signal of that user, and performing interference cancellation will only add noise to the system, resulting in a degradation in performance. Thus, attempting to cancel MAI from such an user will not only prove ineffective, but could harm performance. This result suggests the use of selective interference cancellation, and we will use it in the analysis of interference cancellation in a multicellular system. Note that Eqn. 3.27 is strictly true only at the first stage of interference cancellation, and does not apply to cancellation at all stages

3.5 Improved Gaussian Approximation

In the analysis to this point, we modeled each interference term as an independent Gaussian random variable. However, since bit errors are not necessarily independent of each other, it may not be appropriate to model the MAI as AWGN. It is shown in [32] that in general, MAI cannot be accurately modeled as a Gaussian random variable unless the number of simultaneous users is large. Morrow [32] presents a more accurate improved Gaussian approximation by averaging the BER due to all possible combinations of desired signature sequences, and interfering signal delays and phases. Holtzman [33] derived a new simpler expression for the BER:

$$P_{b_k}^{(1)} \approx \frac{2}{3}Q\left(\sqrt{\frac{P_k T^2}{2(\mu_\psi + \frac{N_0 T}{4})}}\right) + \frac{1}{6}Q\left(\sqrt{\frac{P_k T^2}{2(\mu_\psi + \sqrt{3}\sigma_\psi + \frac{N_0 T}{4})}}\right) + \frac{1}{6}Q\left(\sqrt{\frac{P_k T^2}{2(\mu_\psi - \sqrt{3}\sigma_\psi + \frac{N_0 T}{4})}}\right), \quad (3.28)$$

where the random variable ψ is the conditional variance of the total MAI, and μ_ψ and σ_ψ^2 are the mean and the variance respectively of ψ. The values of μ_ψ and σ_ψ^2 have been evaluated for the case of equal signal powers [34] and for imperfect power control [35]. By letting the received signal power P_κ from the interfering user κ be a random variable with mean μ_{P_κ} and variance $\sigma_{P_\kappa}^2$, the mean and variance can be expressed as [35]:

$$\mu_\psi = \frac{NT_c^2}{6} \sum_{\kappa=1,\kappa\neq k}^{K} \mu_{P_\kappa} \tag{3.29}$$

and

$$\sigma_\psi^2 = \frac{T_c^2}{4}\left[\frac{23N^2+18N-18}{360}\sum_{\kappa=1,\kappa\neq k}^{K}\mu_{P_k}^2 + \frac{7N^2+2N-2}{40}\sum_{\kappa=1,\kappa\neq k}^{K}\sigma_{P_\kappa}^2 + \frac{N-1}{36}\sum_{\kappa=1,\kappa\neq k}^{K}\sum_{j=1,j\neq k,\kappa}^{K}\mu_{P_\kappa}\mu_{P_j}\right]. \tag{3.30}$$

Buehrer and Woerner [11] have used the improved Gaussian approximation in Eqns. 3.28, 3.29 and 3.30 to analyze the performance of a multistage receiver using the improved Gaussian approximation. By recursively computing the statistics of signal powers at each stage of interference cancellation, and taking into account the second order effects of the MAI, the mean received power from an interferer at any stage of interference cancellation can be expressed as [11]:

$$\mu_{P_\kappa}^{(s+1)} = \frac{N_0}{2T}\left[\frac{1-(\frac{K-1}{3N})^s}{1-\frac{K-1}{3N}}\right] + \frac{1}{(3N)^s}\left[\frac{(K-1)^s-(-1)^s}{K}(\sum_{\kappa=1}^{K}\mu_{P_\kappa}^{(1)}) + (-1)^s\mu_{P_k}^{(1)}\right] \tag{3.31}$$

where $\mu_{P_\kappa}^{(1)} = E[P_\kappa]$, and the variance of the MAI at stage $s+1$ can expressed in terms of the mean and the variance at stage s as [11]:

$$(\sigma_{P_\kappa}^{(s+1)})^2 = \frac{N_0^2}{2T^2} + \frac{4N_0}{T^3}\mu_{\psi(s)} - \frac{4}{T^4}(\mu_{\psi(s)})^2 + \frac{9(4N^2-3N)}{40N^4}\sum_{\kappa\neq k}[(\sigma_{P_k}^{(s)})^2 + (\mu_{P_k})^2] + \frac{4N^2-9N+13}{12N^4}\sum_{\kappa\neq k}\sum_{i\neq k,l\neq\kappa}\mu_{P_\kappa}^{(s)}\mu_{P_l}^{(s)}. \tag{3.32}$$

We can apply this analysis to model both in-cell and out-of-cell interference using the improved Gaussian approximation with the goal of obtaining more accurate results, although we will find that for our problem of interest, the improved Gaussian approximation does not significantly change the results.

3.6 Conclusion

In this chapter, we have presented a simple model for multistage interference cancellation which we shall use in the remainder of this thesis. We have summarized previously known analytical results for this model. The contribution of this thesis is a thorough exploration of the selective cancellation criterion presented in Eqn. 3.27. In Chapters 4 and 5 we apply this criterion to multicell and multipath environments respectively.

Chapter 4

Selective Cancellation of Multicell Interference

4.1 Motivation

Most research to date has focussed on the use of interference cancellation within a single cell environment. However, it is known that in cellular systems up to 40% of the total MAI can originate from users outside the cell of interest [3]. Ironically, if interference cancellation is successful within the cell of interest, CDMA performance may be limited by the interference from out-of-cell users. It was suggested in [33] that out-of-cell interference could limit the potential capacity improvements from interference cancellation. In this chapter, we undertake an analysis of the performance of CDMA interference cancellation techniques in a multicellular environment [36][37]. We consider three specific cases: the case where interference cancellation is performed only on users within the cell of interest, the case where interference cancellation is performed on all out-of-cell as well as in-cell users, and the case in which interference cancellation is performed on all in-cell but only on selected out-of-cell interferers. The criteria for selecting out-of-cell interferers for cancellation was suggested in [9].

The remainder of this chapter is organized as follows. Section 4.2 presents the models for both hexagonal and circular cell geometries. A circular geometry similar to that which was proposed in [38][39] is employed. The model yields tractable analytical results which closely match those obtained for the familiar hexagonal cell geometry.

The interference cancellation model follows the model presented in Chapter 3. This model was used in [8][9][10], in which a closed form analytical expression for BER was derived for the single cell case. This closed form result, Eqn. 3.23, has been shown to compare well with results from simulations [9]. Section 4.3 shows how the single cell results of [8][9][10][38] may be extended to examine performance of interference cancellation in a multicellular environment in the three cases of interest. Numerical results corresponding to a microcellular environment are presented in Section 4.4. Results for a microcellular environment obtained by using the improved Gaussian approximation outlined in Section 3.5 are presented in Section 4.4.3.

4.2 Cell Layout

In this section, we present a model for the cell geometries examined. Two cell geometries are considered: the conventional hexagonal grid, and a new circular geometry which yields closed form results.

4.2.1 Hexagonal Layout

One frequently used cell geometry in the analysis of cellular systems is the standard hexagonal grid [40]. In this model, each cell is assumed to be hexagonal in shape, and the cells form a hexagonal mosaic. In this case, the central cell is surrounded by six cells having the same area. The base stations are assumed to be located at the center of each hexagon. Thus, if the base station of the central cell has rectangular coordinates $(0, 0)$, then the base station of the cell above it will be located at $(0, \sqrt{3}R)$, where R is the major radius of the hexagon. This will be true if the cells are laid out as shown in Figure 4.1. We assume a uniform spatial distribution of users within each cell. We also assume that each user within a cell is under perfect power control from its base station. For a user at any location in one of the surrounding cells, the power that is transmitted by the user to maintain unit received power at its base station is calculated using the path loss exponent law. The power received at the central base station due to this interferer then is found using the same path loss rule over the distance from the interferer to the central base station. The average received power from an interferer in a neighboring cell may be found by numerical integration. We

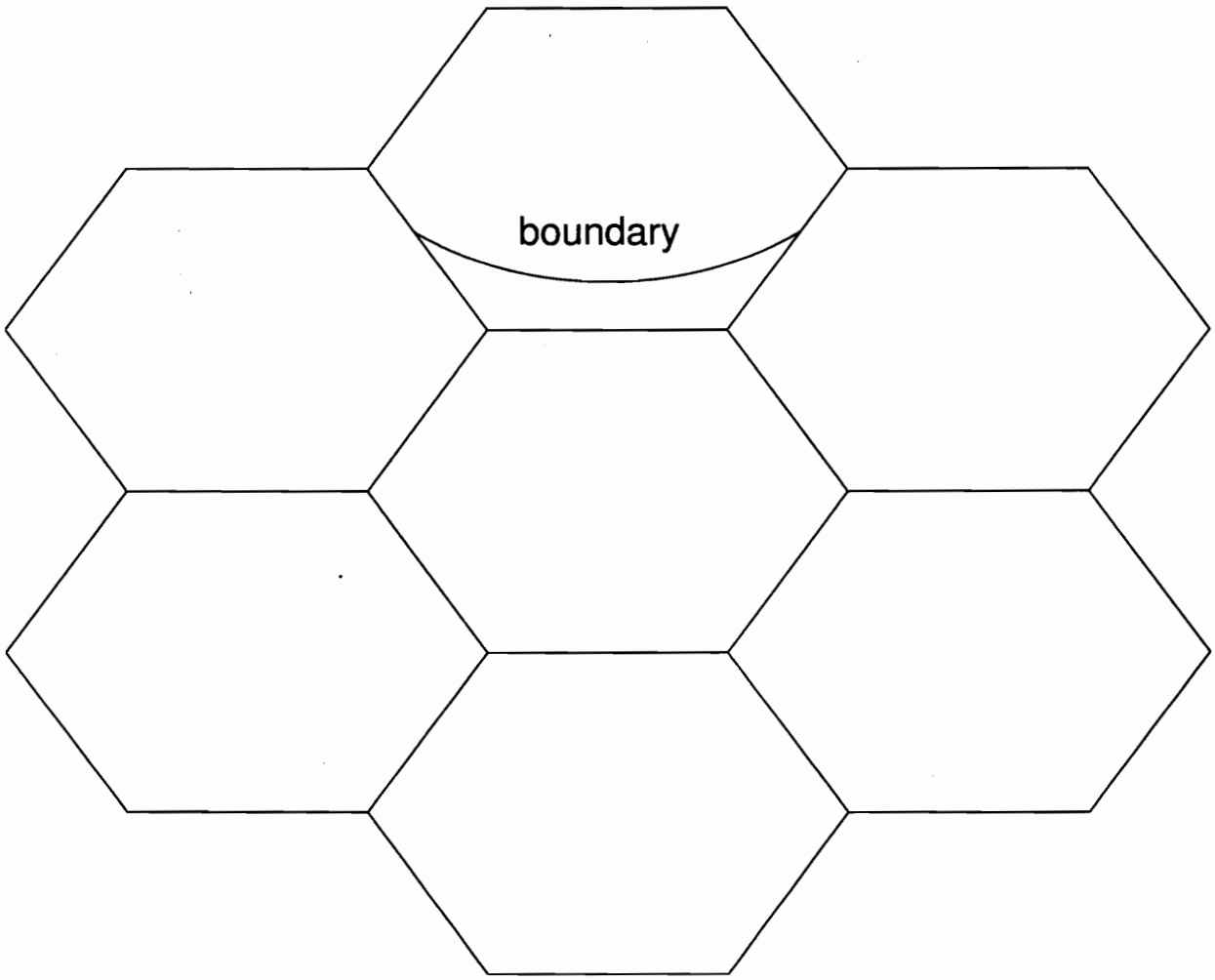

Figure 4.1: Hexagonal Model for Cell Layout

exploit the symmetry of the cell layout by performing the calculations over only one of the adjoining cells.

4.2.2 Circular Layout

Although the hexagonal cellular geometry is frequently employed in the analysis of co-channel interference effects in cellular systems, analytical results quickly become intractable for this model because integration must be performed over the hexagonal region. Since the hexagonal cell shape is only an idealization of the irregular cell shapes found in real microcell systems, it is reasonable to employ an alternative model to aid in analysis. We employ a variation of the circular geometry which was introduced in [38] and shown to yield results nearly identical to those obtained by using the hexagonal geometry [39]. The circular geometry that we will use is shown in Figure 4.2 We assume that the cell of interest is circular, and the adjacent cells are of the shape of wedges surrounding the central cell. We could consider any number of rings (layers) of cells around the cell of interest, but we focus on the first ring of adjacent cells. We also assume each cell to have equal area and an equal number of users. As shown in Figure 4.2, the central cell has a radius d. The cells in the surrounding layers extend from d to $3d$. For each cell to have equal area, the angle of the wedge will have to be $\frac{\pi}{4}$ radians, so there will be eight adjacent cells in the first ring of surrounding cells. We also assume that the base station of the cell of interest is at its center, while the base stations of the surrounding cells lie along arcs of a circle of radius $2d$. We represent the base stations as arcs of a circle, rather than points, to create a tractable mathematical model. This distributed location for the base station is an extension of the model of [38][39], and we will verify its accuracy by comparison with the hexagonal cell geometry. The circle with radius R_{th} represents a boundary for selective cancellation, and will be defined later in in Section 4.3.3. We will assume a uniform spatial distribution of users within each cell. Since the area of the inner sector of any adjacent cell will be less than that of the outer sector, we need to weight the number of users in (or the interference power received from) each sector, such that both inner and outer sectors have an equal number of users, and their sum equals the number of users in each cell. For the first ring of cells, these weighting factors are calculated as follows [38]. Since both sectors have an equal number of

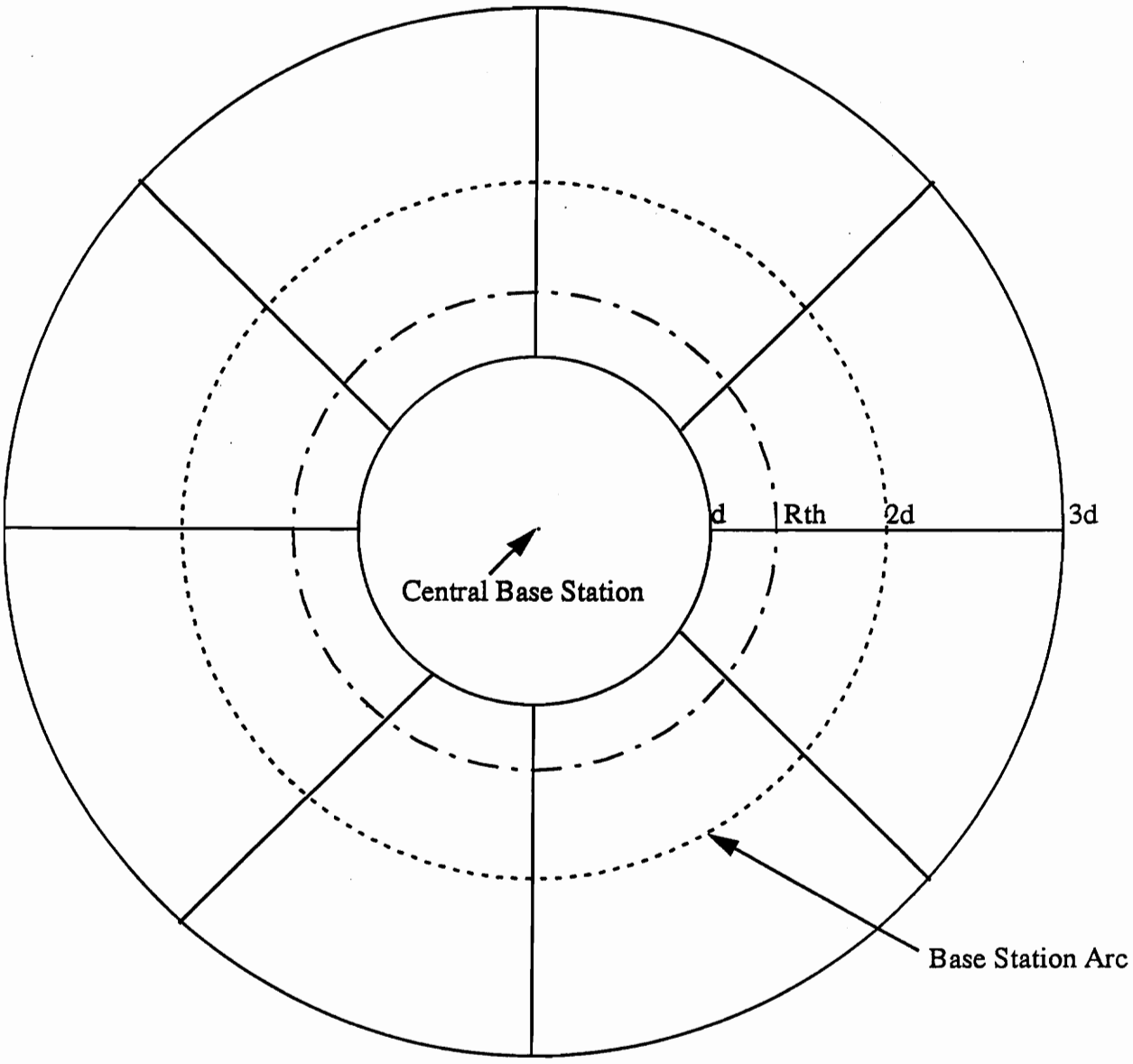

Figure 4.2: Circular Model for Cell Layout

users, we can write

$$W_i \times \pi(4d^2 - d^2) = W_o \times \pi(9d^2 - 4d^2)$$

i. e.

$$3W_i = 5W_o, \tag{4.1}$$

and since their sum equals the number of users in each cell,

$$W_o \times \pi(9d^2 - 4d^2) + W_i \times \pi(4d^2 - d^2) = \pi(9d^2 - d^2)$$

i. e.

$$5W_o + 3W_i = 8, \tag{4.2}$$

where W_i is the weighting factor for the inner sector and W_o is the weighting factor for the outer sector. Solving Eqns. 4.1 and 4.2 simultaneously, yields weighting factors of 4/3 for the inner sector and 4/5 for the outer sector. Using this model instead of the usual hexagonal geometry leads to simple closed form expressions for the BER. In order to determine the power received at the central base station due to out-of-cell interferers, the following assumptions are made:

1. A subscriber in any cell is assumed to be under perfect power control from its base station.

2. The power received at a base station from any in-cell subscriber is unity.

3. If $P(r, \theta)$ is the location of an out-of-cell subscriber, the location of its base station is at $B(2d, \theta)$.

Since the power received at a base station from an in-cell subscriber is unity, the subscriber must transmit power $(\frac{r'}{d_0})^n$, where $r' = |2d - r|$ is the distance between the subscriber and its base station, d_0 is a close in reference distance in the far field of the base station antenna, and n is the path loss exponent, which typically lies in the range $2 \leq n \leq 4$. Assuming the path loss exponent to be independent of r and d_0, the power received at the central base station due to an out-of-cell interferer will be $(\frac{r'}{r})^n$.

4.3 Multicell Analysis of Interference Cancellation

In order to explore the effect of out-of-cell interference on the performance of interference cancellation, we will divide out-of-cell-interferers into two sets. Interferers which are sufficiently far away from the central base station result in only weak interference to the central base station. As suggested in [33], it will introduce needless complexity with little benefit to cancel interference from these weak interferers. It is shown in Section 3.4 that cancellation of sufficiently weak users can actually degrade performance[8][9][10]. The weak out-of-cell interferers which are not cancelled will contribute to the background noise, and we denote the total power of these interferers an $P_{n,out}$. Interference cancellation is performed on the remaining strong out-of-cell interferers, and we denote their total power as $P_{res,out}$.

The unresolvable components will degrade the value of $\frac{E_b}{N_0}$ in the system. This effect may be modeled by the standard Gaussian approximation. Since each of the unresolvable out-of-cell interferers is relatively weak, the Gaussian approximation should be effective.

We write Eqn. 1.10 in the form:

$$r(t) = n(t) + \sum_{k \in S_{res}} s_k(t - \tau_k) + \sum_{k \in S_{noise}} s_k(t - \tau_k) \tag{4.3}$$

where S_{res} is the set of all resolvable users in the central cell or adjacent cells upon which interference cancellation is performed, and S_{noise} is the set of all unresolvable users in adjoining cells. The sum of the powers from resolvable users, $\sum_{k \in S_{res}} P_k$, may be substituted for $\sum_{\kappa=1}^{K} P_\kappa$ in Eqn. (3.23) to account for interference cancellation in the multicell case.

We now account for the interference from uncanceled users. Using the notation of [12][41] we may write the decision statistic at stage s as

$$Z_{k,i}^{(s)} = \sqrt{\frac{P_k}{2}} T b_{k,i} + \eta + \sum_{k \in S_{res}} I_{k,i}^{(s)} + \sum_{k \in S_{noise}} I_k \tag{4.4}$$

where $\sqrt{\frac{P_k}{2}} T b_{k,i}$ is the contribution of the desired signal, η represents the effect of noise $n(t)$ and is a Gaussian random variable with mean zero and variance $\frac{N_0 T}{4}$,

$\sum_{k\in S_{res}} I_{k,i}^{(s)}$ represents the MAI from the resolvable users and may be modeled as discussed above, and $\sum_{k\in S_{noise}} I_k$ represents the effect of the uncanceled users. The Central Limit Theorem implies that the contribution of a large number of identically distributed chips of interference from each uncanceled interferer will tend towards a Gaussian distribution. Applying the standard Gaussian Approximation [12] to the kth uncanceled user, we find that the uncanceled interference has mean $E[\sum_{k\in S_{noise}} I_k] = 0$ and variance given by

$$Var[\sum_{k\in S_{noise}} I_k] = \frac{\sum_{k\in S_{noise}} P_k}{6N}. \tag{4.5}$$

The factor N arises due to the fact that the interferer's power is reduced in proportion to the processing gain, while the factor of 6 is present because the MAI is not aligned in phase or time with the desired user. As a result, the combined contribution from the noise and uncanceled interference can be lumped together into a single noise process $n'(t)$ with two-sided power spectral density $\left(\frac{N_0'}{2}\right)$ given by

$$\frac{N_0'}{2} = \frac{N_0}{2} + \frac{T}{3N}\sum_{k\in S_{noise}} P_k. \tag{4.6}$$

As a result, we may now generalize Eqn. (3.23) to the case in which cancellation is performed in a multicell environment on all, none, or part of the out-of-cell interference.

$$P_{b_k}^{(s)} = Q\left\{\left[\frac{1}{2(E_{b_k}/N_0')}\left(\frac{1-(\frac{K_r-1}{3N})^s}{1-\frac{K_r-1}{3N}}\right) + \frac{1}{(3N)^s}\left(\frac{(K_r-1)^s-(-1)^s}{K_r}(K+P_{res,out})+(-1)^s\right)\right]^{-\frac{1}{2}}\right\} \tag{4.7}$$

where K_r is the total number of resolvable users which equals the number of users in the central cell plus the total number of resolvable users in all adjoining cells, whereas K is the number of users per cell. We now apply this approach to the three cases of interest.

4.3.1 Interference Cancellation on In-Cell Users Only

If interference cancellation is performed only on in-cell interferers, then the total resolvable power will be K, and the total out-of-cell noise power $P_{n,out}$ can be obtained

by integrating over the ring from radius d to $3d$.

$$P_{n,out} = (\frac{4}{3})\frac{1}{\pi(4d^2 - d^2)}\frac{K3\pi d^2}{\pi d^2}\int_0^{2\pi}\int_d^{2d}\left(\frac{2d-r}{r}\right)^n rdrd\theta + (\frac{4}{5})\frac{1}{\pi(9d^2 - 4d^2)}\frac{K5\pi d^2}{\pi d^2}\int_0^{2\pi}\int_{2d}^{3d}\left(\frac{r-2d}{r}\right)^n rdrd\theta \quad (4.8)$$

As discussed in Section 4.2.2, $\frac{4}{3}$ and $\frac{4}{5}$ are the weighting factors for the inner and outer sector respectively of the wedge[38]. Eqn. 4.8 simplifies to

$$P_{n,out} = 2\pi\frac{4K}{3\pi d^2}\int_d^{2d}\left(\frac{2d-r}{r}\right)^n rdr + 2\pi\frac{4K}{5\pi d^2}\int_{2d}^{3d}\left(\frac{r-2d}{r}\right)^n rdr. \quad (4.9)$$

For a path loss exponent $n = 4$, this further simplifies to

$$P_{n,out} = \frac{8K}{3d^2}\left[\frac{-3d^2(11 + 16\ln[d])}{2} + 24d^2\ln[2d]\right] + \frac{8K}{5d^2}\left[-24d^2\ln[2d] + \frac{d^2(-175 + 432\ln[3d])}{18}\right]. \quad (4.10)$$

Since none of the out-of-cell interferers is being resolved by the center base station, $P_{res,out} = 0$, and $K_r = K$.

4.3.2 Complete Interference Cancellation

If interference cancellation is performed on all out-of-cell-users as well as in-cell users, the total resolvable power from out-of-cell interferers can be written as

$$P_{res,out} = (\frac{4}{3})\frac{1}{\pi(4d^2 - d^2)}\frac{K3\pi d^2}{\pi d^2}\int_0^{2\pi}\int_d^{2d}\left(\frac{2d-r}{r}\right)^n rdrd\theta + (\frac{4}{5})\frac{1}{\pi(9d^2 - 4d^2)}\frac{K5\pi d^2}{\pi d^2}\int_0^{2\pi}\int_{2d}^{3d}\left(\frac{r-2d}{r}\right)^n rdrd\theta \quad (4.11)$$

For a path loss exponent $n = 4$, this simplifies to

$$P_{res,out} = \frac{8K}{3d^2}\left[\frac{-3d^2(11 + 16\ln[d])}{2} + 24d^2\ln[2d]\right] + \frac{8K}{5d^2}\left[-24d^2\ln[2d] + \frac{d^2(-175 + 432\ln[3d])}{18}\right] \quad (4.12)$$

and in this case, $P_{n,out} = 0$. Note that $P_{res,out}$ for the case of complete cancellation is the same as $P_{n,out}$ for the case of cancellation on in-cell-users only. Here, $K_r = 9K$.

4.3.3 Selective Interference Cancellation

As discussed in Section 3.4, if the power received at the central base station from any user k is less than a certain threshold, then performing interference cancellation will increase the variance of the power from that user, resulting in a higher BER. It is shown in [8][9] that the BER will increase after interference cancellation if the power of that user is sufficiently small. This happens because the estimate of that low power user's signal is so imprecise that cancellation will actually introduce additional noise. In order to obtain the maximum capacity, users are classified into two groups. The two groups comprise of users who will degrade the BER when interference cancellation is performed on them, and those who will improve the BER. We can then perform interference cancellation only on the favorable users. The threshold power, P_{th}, below which interference cancellation will degrade performance is given by Eqn. 3.27[8][9]:

$$P_{th} = \frac{N_0}{2T} + \frac{1}{3N} \sum_{\kappa=1,\kappa\neq k}^{K_{all}} P_\kappa \tag{4.13}$$

where $K_{all} = 9K$ is the total number of users for this model.

Assuming that the power received from each in-cell user is unity after power control is applied, we can perform interference cancellation on all in-cell interferers. However, we would like to cancel only those out-of-cell interferers whose power at the central base station is higher than the threshold. We choose not to use the rest of the users for interference cancellation, so the power from such users must be added to the unresolvable noise. The radius R_{th}, corresponding to P_{th} will be given by $P_{th} = \frac{|2d-R_{th}|^n}{(R_{th})^n}$ and is illustrated in Figure 4.2. Thus, we will perform interference cancellation on all interferers within a radius of R_{th} from the center base station.

The total interfering power from the resolvable out-of cell interferers in all adjoining cells is given by the expression (assuming $R_{th} \leq 2d$)

$$P_{res,out} = 2\pi \frac{4K}{3\pi d^2} \int_d^{R_{th}} \frac{|2d-r|^n}{r^n} r dr \tag{4.14}$$

For a path loss exponent $n = 4$, this simplifies to

$$P_{res,out} = 2\pi \frac{4K}{3\pi d^2} \left[-\frac{8d^4}{R_{th}^2} + \frac{32d^3}{R_{th}} - 8dR_{th} + \frac{R_{th}^2}{2} - \frac{3d^2(11+16\ln[d])}{2} + 24d^2 \ln[R_{th}] \right] \tag{4.15}$$

The total unresolvable interfering power from all adjacent cell can be written as

$$P_{n,out} = 2\pi \frac{4K}{3\pi d^2} \int_{R_{th}}^{2d} \left(\frac{(2d-r)}{r} \right)^n r dr + 2\pi \frac{4K}{5\pi d^2} \int_{2d}^{3d} \left(\frac{r-2d}{r} \right)^n r dr \quad (4.16)$$

For a path loss exponent $n = 4$, this simplifies to

$$P_{n,out} = 2\pi \frac{4K}{3\pi d^2} \left[\frac{8d^4}{R_{th}^2} - \frac{32d^3}{R_{th}} + 8dR_{th} - \frac{R_{th}^2}{2} + 24d^2 \ln[2d] - 24d^2 \ln[R_{th}] \right] + 2\pi \frac{4K}{5\pi d^2} \left[-24d^2 \ln[2d] + \frac{d^2(-175 + 432 \ln[3d])}{18} \right]. \quad (4.17)$$

The total number of resolvable users, K_r, equals the number of users in the central cell plus the total number of resolvable users in all adjoining cells, and may be approximated by $K_r = K + \frac{4}{3}K \left[\frac{\pi(R_{th}^2 - d^2)}{\pi d^2} \right]$.

In order to analyze the hexagonal layout in Figure 4.1, we plot the boundary within which all interferers are strong enough to justify interference cancellation [36]. The rest of the users are added to the unresolvable noise and a similar numerical analysis as presented for the circular model is carried out. The values of $\left(\frac{E_{b_k}}{N_0} \right)$ and $\sum_{k \in S_{res}} P_k$ thus obtained may be substituted in Eqn. (3.23) to compute the BER. The shape of the boundary obtained for the hexagonal layout may be found numerically, and is shown in Figure 4.1.

4.4 Numerical Results

Although this work focuses primarily on analytical results which explore the potential value of selective interference cancellation for a multicell environment in a qualitative sense, the individual analytical techniques which are combined here have been verified for numerical accuracy against simulation results. Simulation results presented in [8][9][10] have shown that the analytical expression for BER of adaptive multistage interference cancellation used in Eqn. 3.23 shows reasonably good agreement for BER above 10^{-4}. Simulation results presented in [38] show that capacity results for the circular cell geometry agree closely with those obtained from a hexagonal cell geometry when K is reasonably large.

4.4.1 Circular Layout

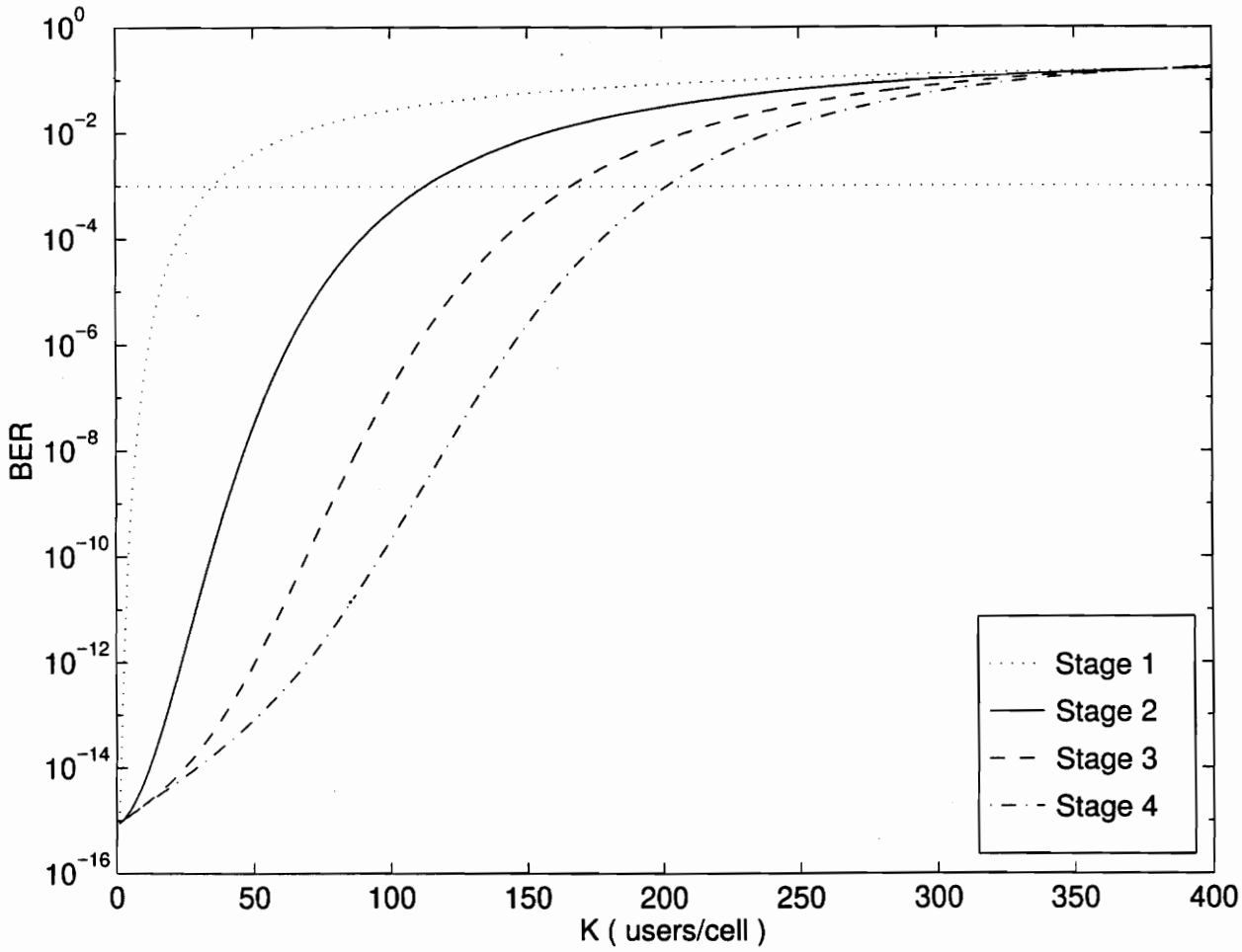

Figure 4.3: Interference Cancellation for a Single Cell Environment ($N = 128$, $\frac{E_b}{N_0} =$ 15 dB, Perfect Power Control).

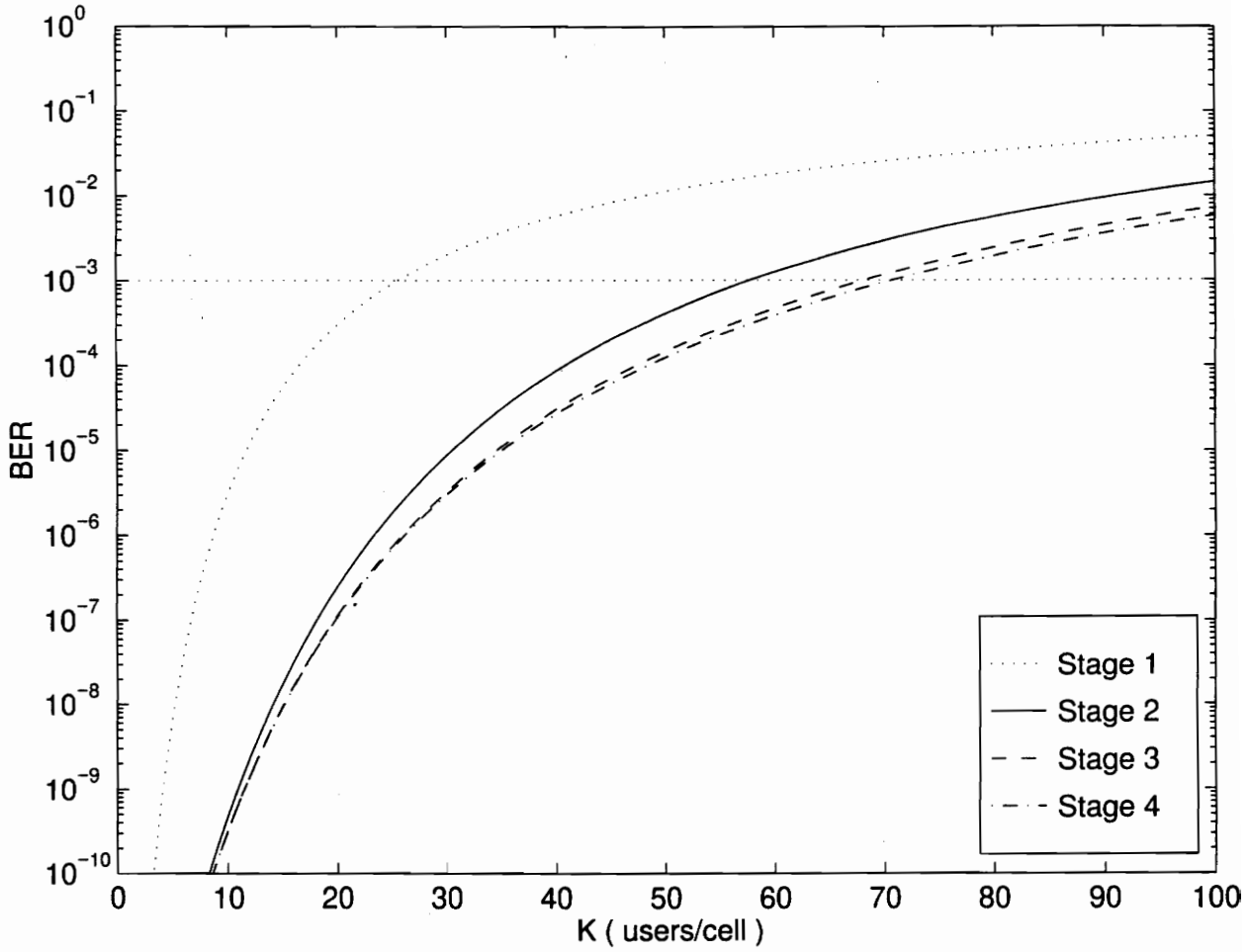

Figure 4.4: Performance of Interference Cancellation for Multicellular Environment, No Interference Cancellation on Out-of-Cell Interferers ($N = 128$, $\frac{E_b}{N_0} = 15$dB, $d = 1000$ m, $n = 4$)

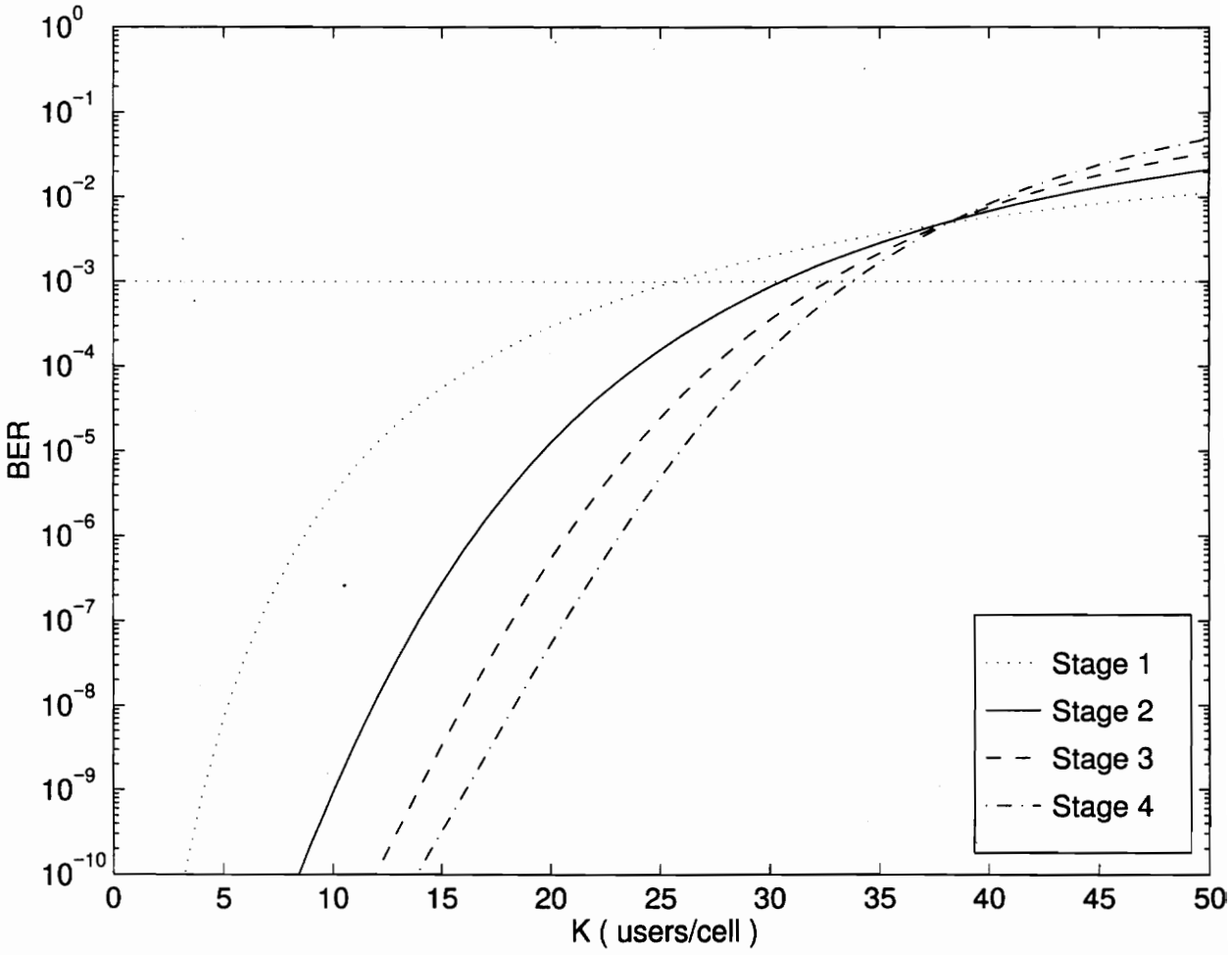

Figure 4.5: Performance of Interference Cancellation for Multicellular Environment, Complete Interference Cancellation ($N = 128$, $\frac{E_b}{N_0} = 15$dB, $d = 1000$ m, $n = 4$)

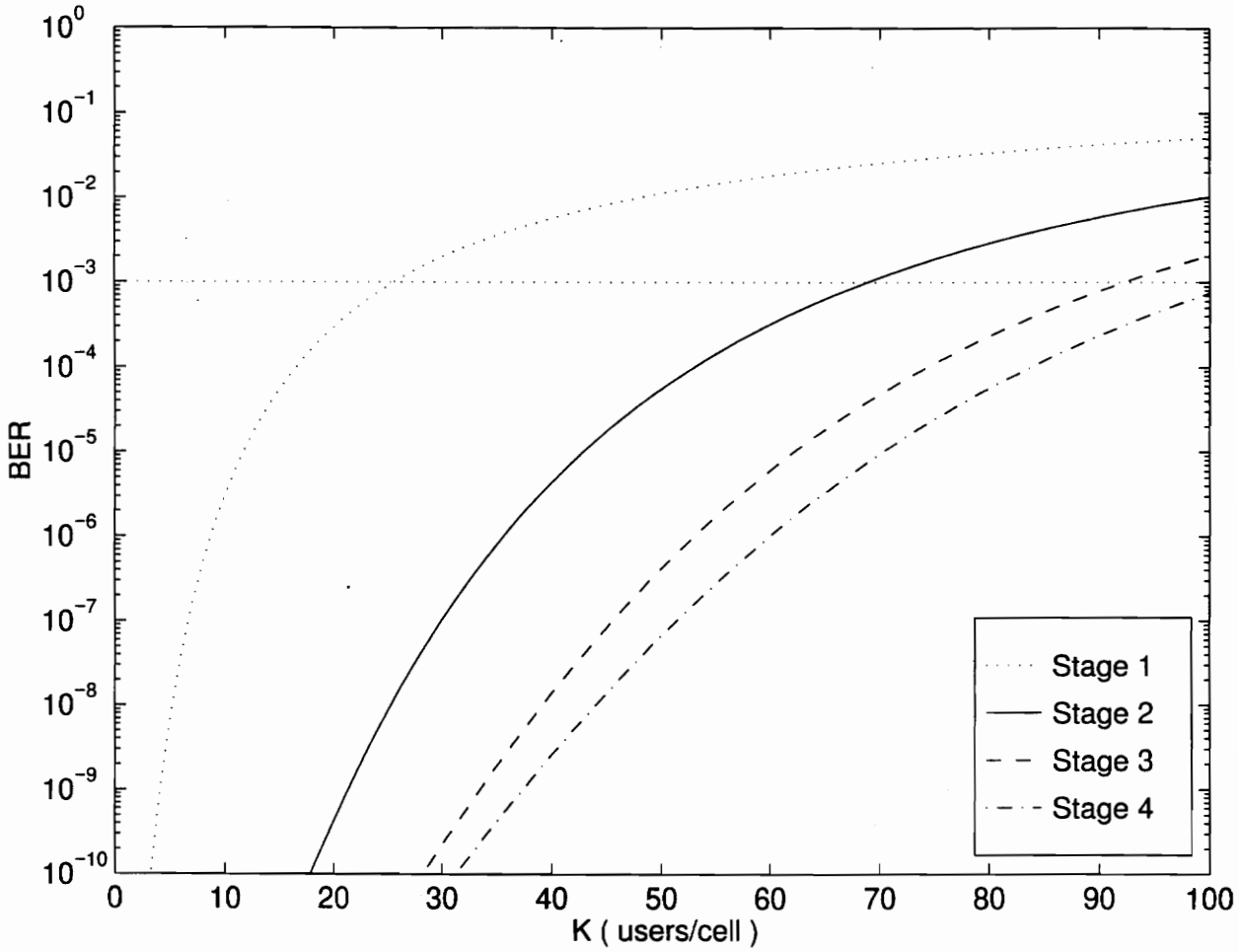

Figure 4.6: Performance of Interference Cancellation for Multicellular Environment, Selective Interference Cancellation ($N = 128$, $\frac{E_b}{N_0} = 15$dB, $d = 1000$ m, $n = 4$)

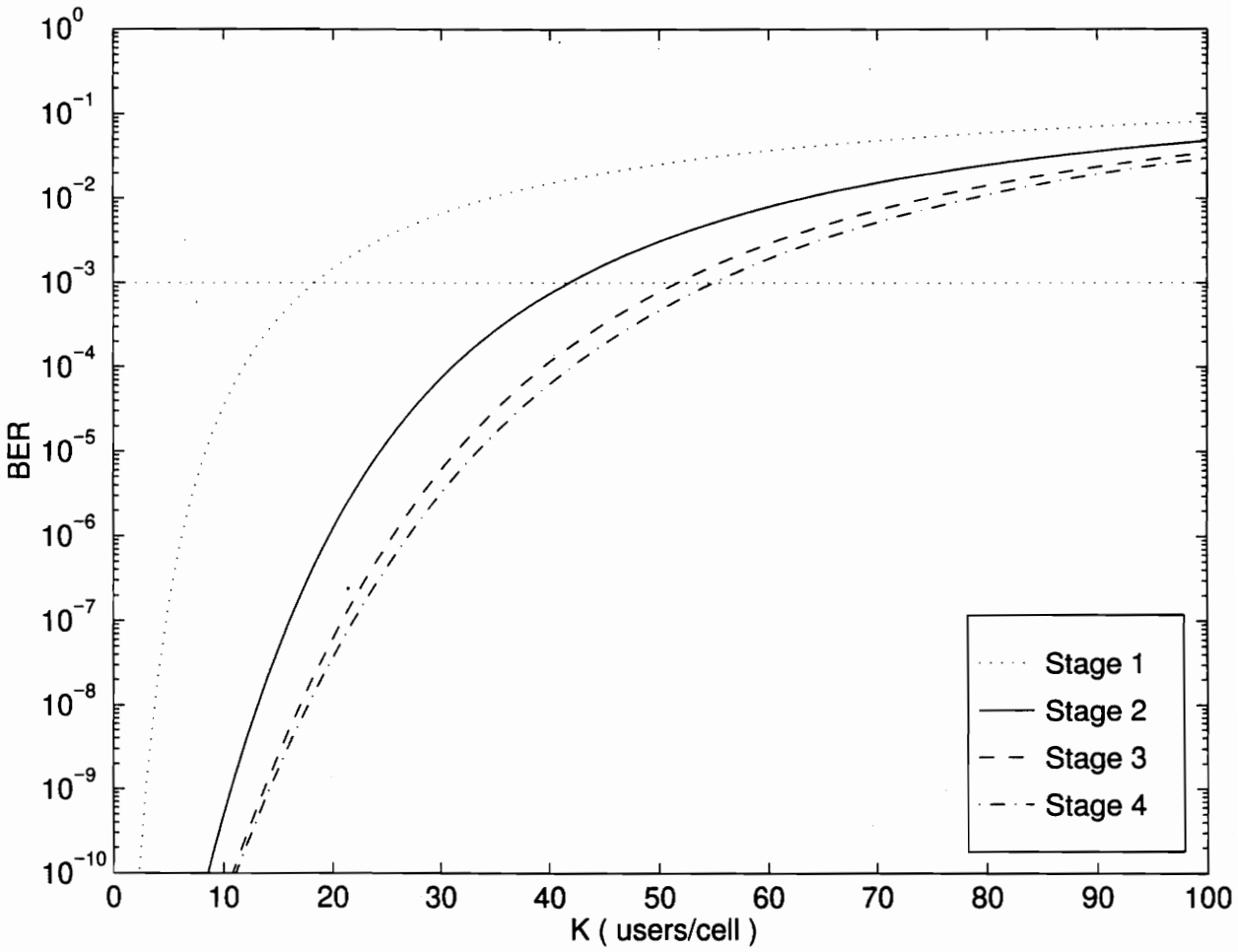

Figure 4.7: Performance of Interference Cancellation for Multicellular Environment, Selective Interference Cancellation ($N = 128$, $\frac{E_b}{N_0} = 15$dB, $d = 1000$ m, $n = 2$)

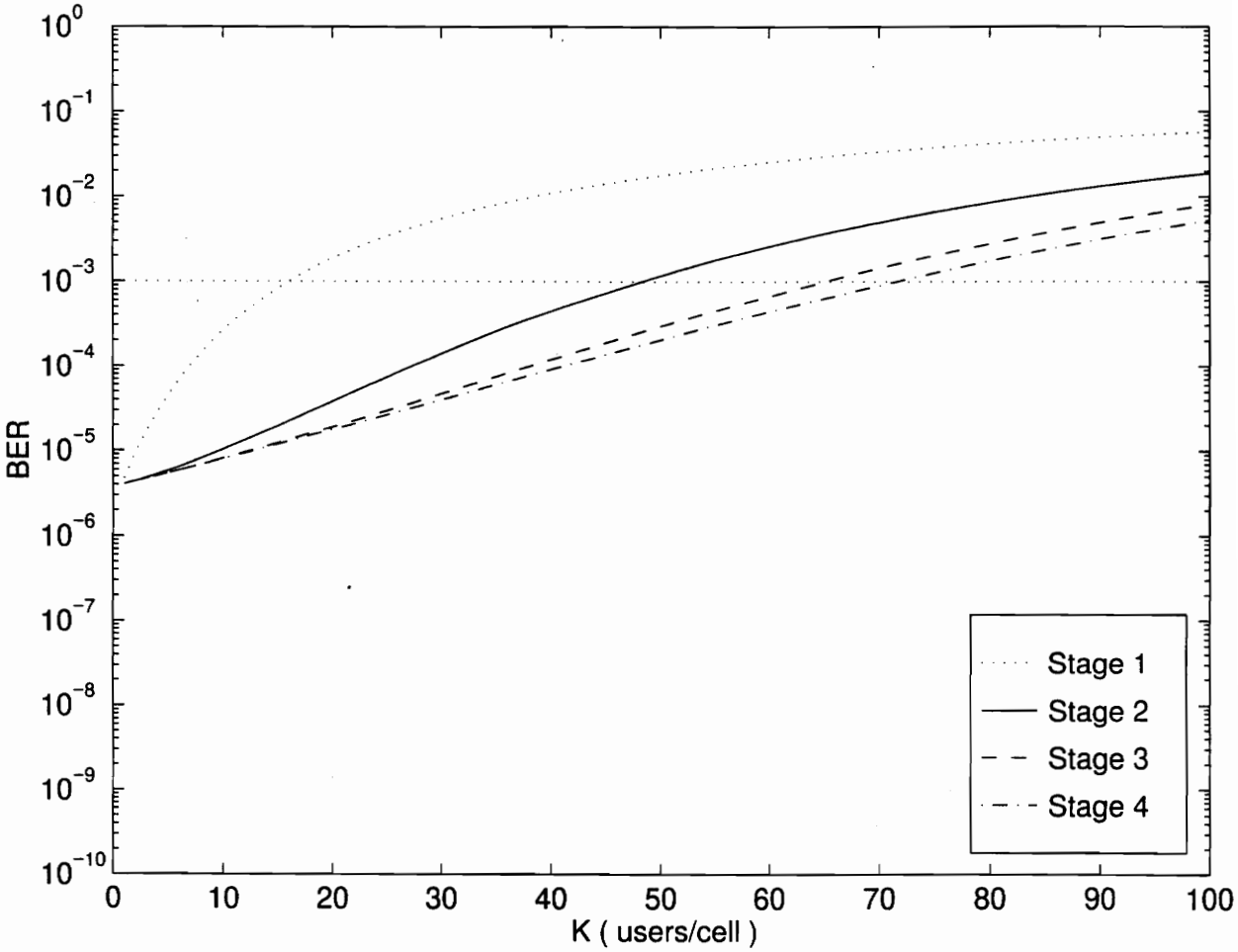

Figure 4.8: Performance of Interference Cancellation for Multicellular Environment, Selective Interference Cancellation ($N = 128$, $\frac{E_b}{N_0} = 10$dB, $d = 1000$ m, $n = 4$)

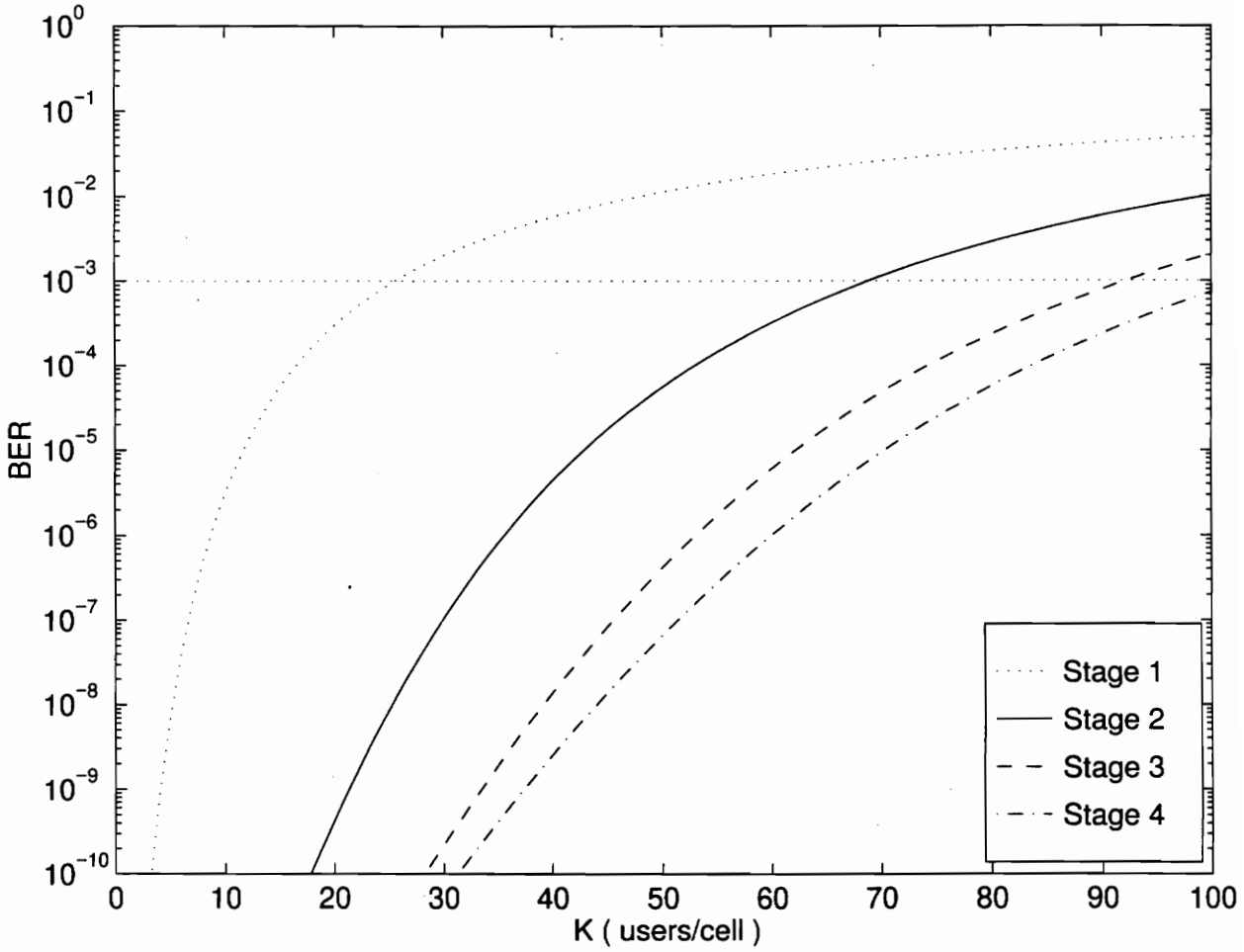

Figure 4.9: Performance of Interference Cancellation for Multicellular Environment, Selective Interference Cancellation ($N = 128$, $\frac{E_b}{N_0} = 15$dB, $d = 5000$ m, $n = 4$)

Figure 4.3 plots BER as a function of the number of users per cell K for a single cell environment according to Eqn. 3.23 [8][9]. For this figure, $\frac{E_b}{N_0} = 15$ dB for the desired user, and a processing gain of $N = 128$ is considered. Perfect power control is assumed. BER curves are shown for $s = 1, ..., 4$, where $s = 1$ corresponds to the conventional receiver and $s = 4$ corresponds to three stages of adaptive interference cancellation. For convenience, a line showing a desired BER of 10^{-3} is also displayed. Interference cancellation is shown to provide a significant increase in capacity for a single cell environment. As the number of interference cancellation stages is increased, further improvements diminish and performance tends towards an asymptotic limit.

Figure 4.4 through Figure 4.6 explore the effect of implementing interference cancellation in a multicellular environment using the circular cell geometry. For the remainder of the results in this section, we will assume $\frac{E_b}{N_0} = 15$ dB, a path loss exponent of $n = 4$, a cell-radius of $d = 1000$ m, and a processing gain of $N = 128$ corresponding to typical values for a microcellular environment, except as specifically noted. Figure 4.4 shows BER as a function of K for a multicellular environment in which interference cancellation is performed only on interferers in the central cell, according to Eqn. 4.10. The number of users K, which can be supported at a BER of 10^{-3} is severely decreased from Figure 4.3, and only the first stage of interference cancellation yields any significant improvement. This illustrates how the out-of-cell interference dominates the system performance after interference cancellation mitigates the in-cell interference.

Figure 4.5 illustrates the result of applying interference cancellation indiscriminately to all users within the first ring of cells surrounding a base station, using the results of Eqn. 4.3.2. Interference cancellation provides almost no improvement over the standard receiver and performance is significantly worse than the performance shown in Figure 4.4 in which no attempt was made to cancel any out-of-cell interference. The crossing of curves in Figure 4.5 shows that interference cancellation can actually hurt performance if we attempt to cancel many low power out-of-cell interferers in violation of the condition in Eqn. 4.13. Clearly, indiscriminate cancellation of out-of-cell interference is undesirable.

Figure 4.6 plots BER as a function of K for the case of selective interference cancellation, according to Eqns. 4.15 and 4.17. Interference cancellation is performed

only on those interferers which satisfy the condition in Eqn. 4.13. For the idealized model considered here, those interferers lie within the circular region about the central cell which is illustrated in Figure 4.2. For a practical situation, the region will have an irregular shape, but it is reasonable to postulate that a small number of users in the surrounding cells contribute significant interference power to the central cell. It should be possible to identify those users by their received powers. CDMA base stations already monitor nearby users in neighboring cells to implement soft hand-off. Comparison of the curves corresponding to multistage receivers with $s = 1$ and $s = 4$ in Figure 4.6 shows that selective interference cancellation can result in a more than fourfold increase in capacity over a standard receiver. Moreover, comparison with Figure 4.4 shows that selective interference cancellation on out-of-cell interferers can potentially provide a 20 - 40% improvement in capacity over the cancellation of only in-cell interference.

Figure 4.7 through Figure 4.9 explore the sensitivity of selective interference cancellation to system parameters. In Figure 4.7, the path loss exponent is reduced to the free space value of $n = 2$. Not surprisingly, the system capacity is reduced significantly because of the increased importance of out-of-cell interference. However, the use of selective interference cancellation still provides a potential threefold capacity increase over a conventional receiver. Figure 4.8 illustrates the case in which the signal to background noise ratio has been reduced to $\frac{E_b}{N_0} = 10$ dB. Once again, performance of all receivers is reduced but selective interference cancellation still provides a significant improvement in capacity. Figure 4.9 presents results for a cell radius of 5000 m. The results are virtually identical to the microcell example in Figure 4.6, indicating that the basic principle of selective cancellation should be scalable.

4.4.2 Hexagonal Layout

Figure 4.10 through 4.12 present plots of the BER against the number of users per cell using the hexagonal layout for typical microcell parameters ($\frac{E_b}{N_0} = 15$ dB, major radius $r = 1000$m, and path loss exponent $n = 4$), repeating the results of Figure 4.4 through 4.6 for the hexagonal geometry. For these figures, Eqn. 4.7 is used but the closed form expressions derived in Section 4.3 are no longer applicable. Instead, numerical integration over the hexagonal region is used to find average interference

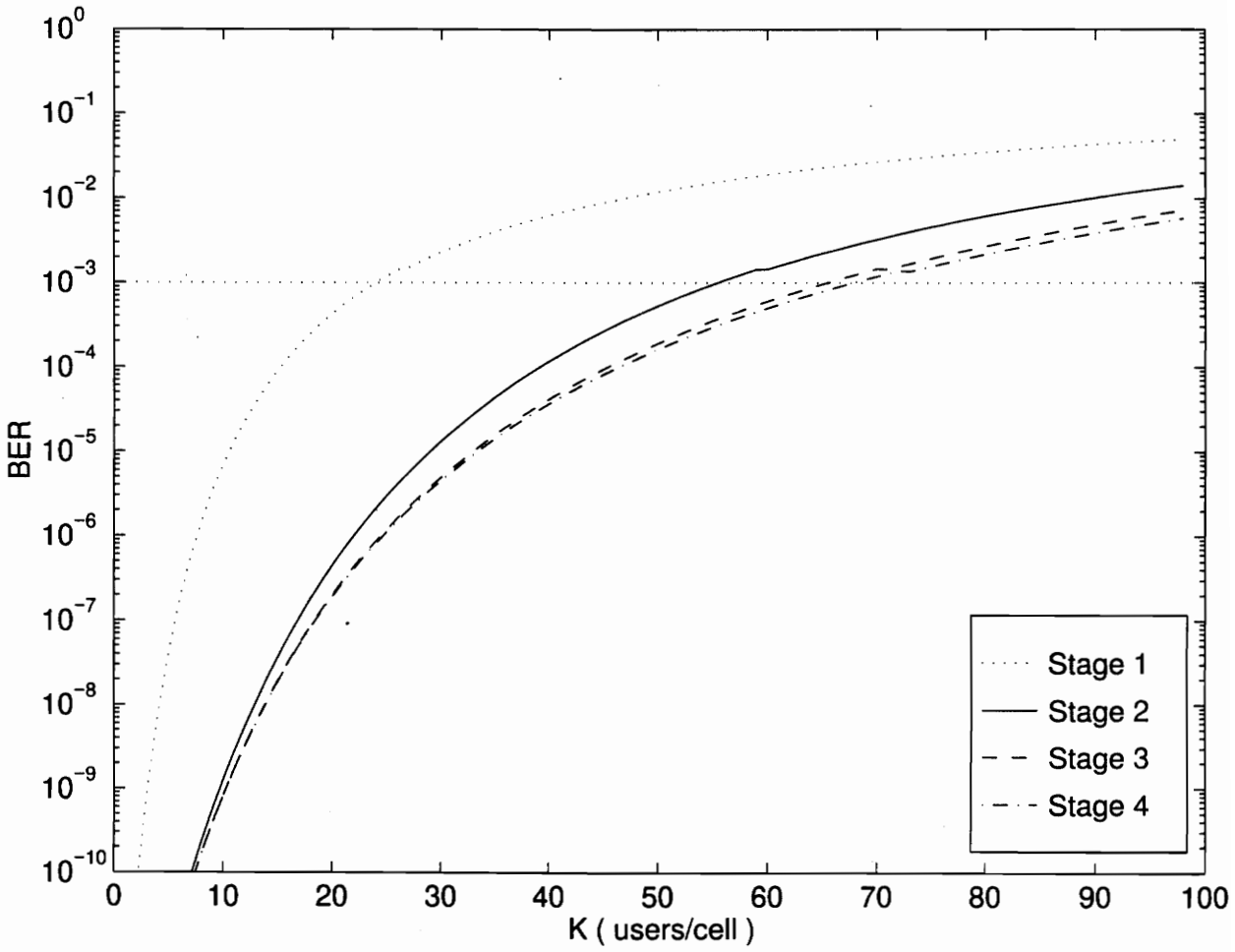

Figure 4.10: Performance of Interference Cancellation for Multicellular Environment using Hexagonal Geometry, No Interference Cancellation on Out-of-Cell Interferers ($N = 128$, $\frac{E_b}{N_0} = 15$ dB, $r = 1000$ m, $n = 4$)

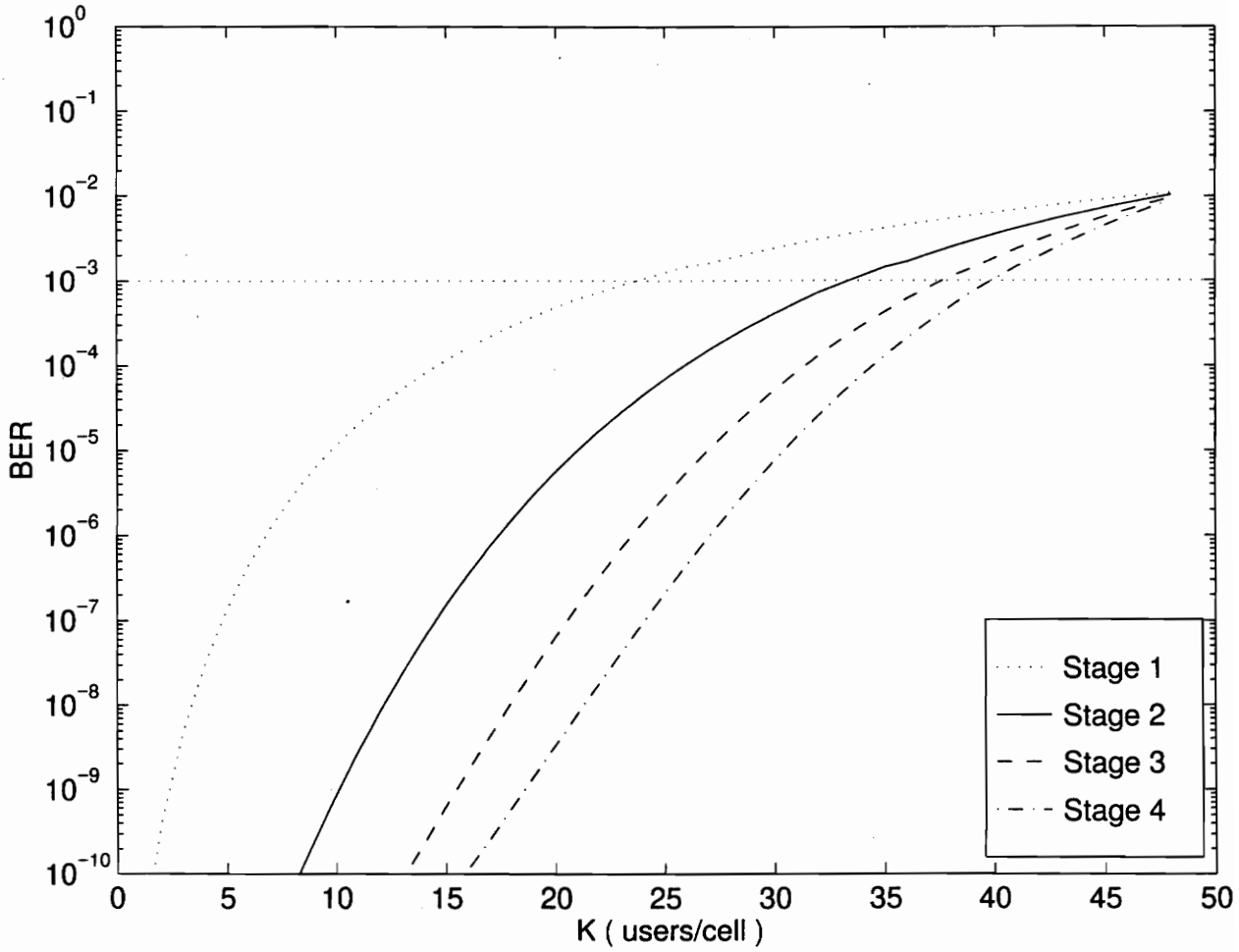

Figure 4.11: Performance of Interference Cancellation for Multicellular Environment using Hexagonal Geometry, Complete Interference Cancellation ($N = 128$, $\frac{E_b}{N_0} = 15$ dB, $r = 1000$ m, $n = 4$)

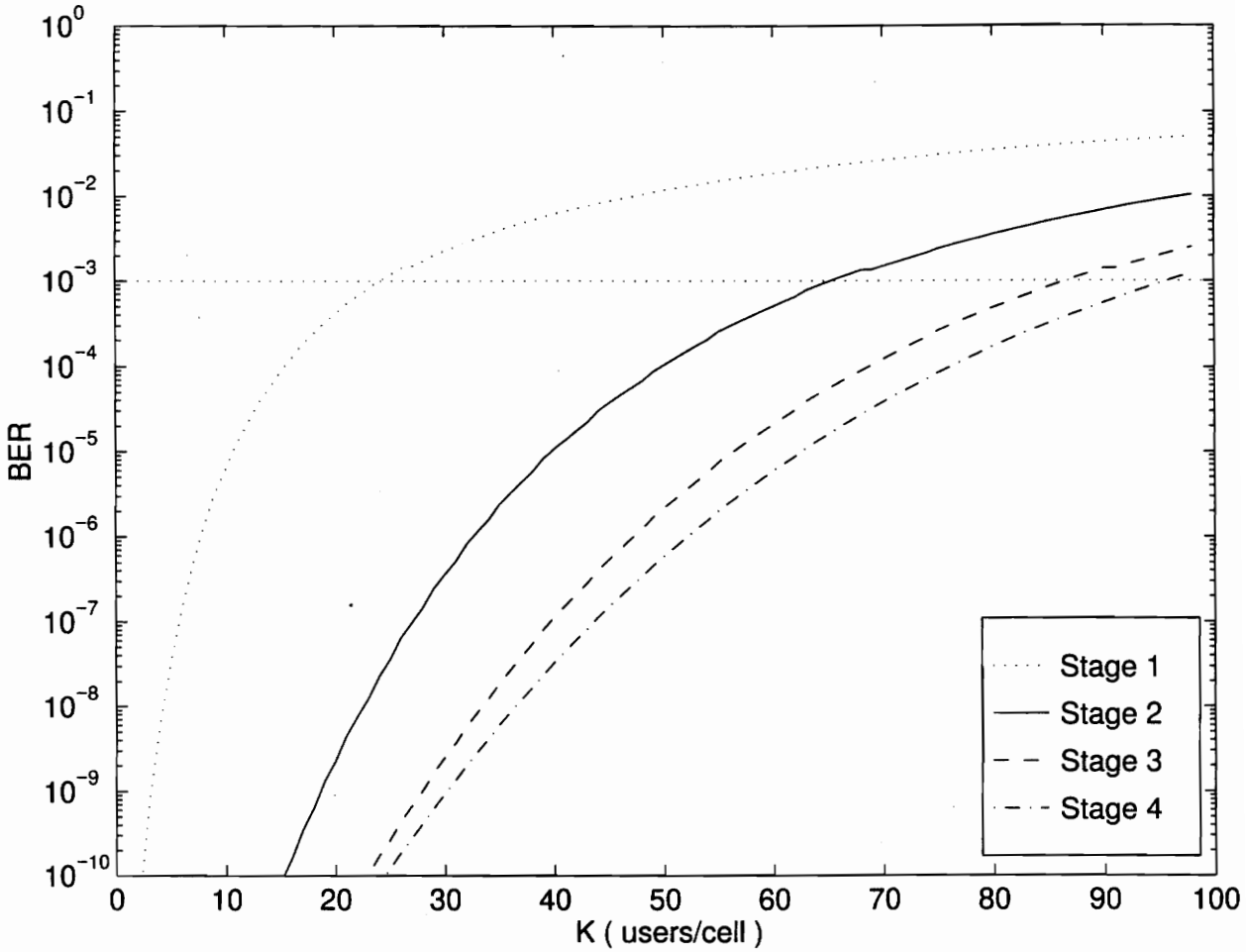

Figure 4.12: Performance of Interference Cancellation for Multicellular Environment using Hexagonal Geometry, Selective Interference Cancellation ($N = 128$, $\frac{E_b}{N_0} = 15$ dB, $r = 1000$ m, $n = 4$)

powers. Figures 4.4 and 4.10 for the case of interference cancellation on in cell interference only yield virtually identical results, perhaps because out of cell interference is a second order effect in this case. Comparing Figure 4.5 with Figure 4.11, and Figure 4.6 with Figure 4.12 for the cases of complete and selective cancellation respectively indicates that the circular geometry yields slightly optimistic results for the case of selective cancellation, and slightly pessimistic for complete interference cancellation. However, the resulting capacities still usually agree within 10 - 15% as was found in [39]. Thus, the circular layout yields results comparable to those from the hexagonal layout, while making the problem more tractable mathematically.

4.4.3 The Improved Gaussian Approximation

Figures 4.13 through 4.15 present results obtained by modeling the interference with the improved Gaussian approximation outlined in Section 3.5. These results were obtained using the hexagonal geometry. Figure 4.13 is a plot of the BER against the number of users per cell for the case when no interference cancellation is performed on out of cell interferers. We see that this result is virtually identical to that in Figure 4.10, where the simple Gaussian approximation was used to model the interference. Figure 4.14 presents the results for the case of complete interference cancellation. Here too, we see that complete interference cancellation actually hurts performance, and the capacities predicted by these results are much worse than for the case of interference cancellation on in-cell users only. Moreover, the results in Figure 4.14 are same as those in Figure 4.11 which showed the result for complete interference cancellation using the simple Gaussian approximation for the hexagonal geometry. Figure 4.15 is a plot of the BER versus number of users per cell for selective cancellation in the hexagonal layout. The improved Gaussian approximation is used. Again, we see the huge capacity gains that could be obtained by selective cancellation of a small number of strong out-of-cell interferers. Also, the results in this figure are identical to those in Figure 4.12 which was plotted using the simple Gaussian approximation. In all the three cases of interest, the results from the improved Gaussian approximation are nearly identical to those obtained using the simple Gaussian approximation. While this increases our confidence in the results presented, it also points out that under the assumptions made for this analysis, the improved Gaussian approximation

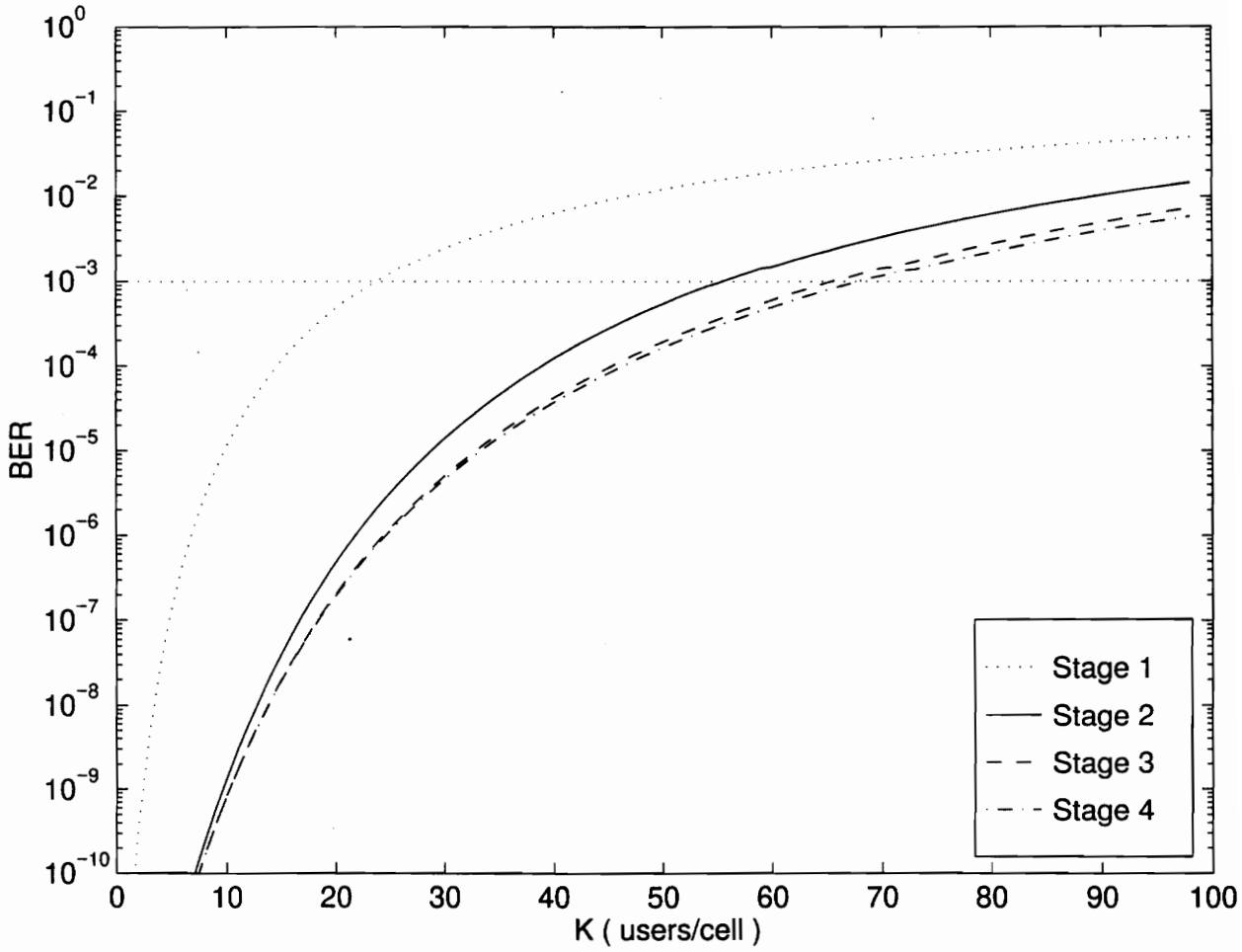

Figure 4.13: Performance of Interference Cancellation for Multicellular Environment using Hexagonal Geometry and the Improved Gaussian Approximation, No Interference Cancellation on out-of-cell interferers ($N = 128$, $\frac{E_b}{N_0} = 15$ dB, $r = 1000$ m, $n = 4$)

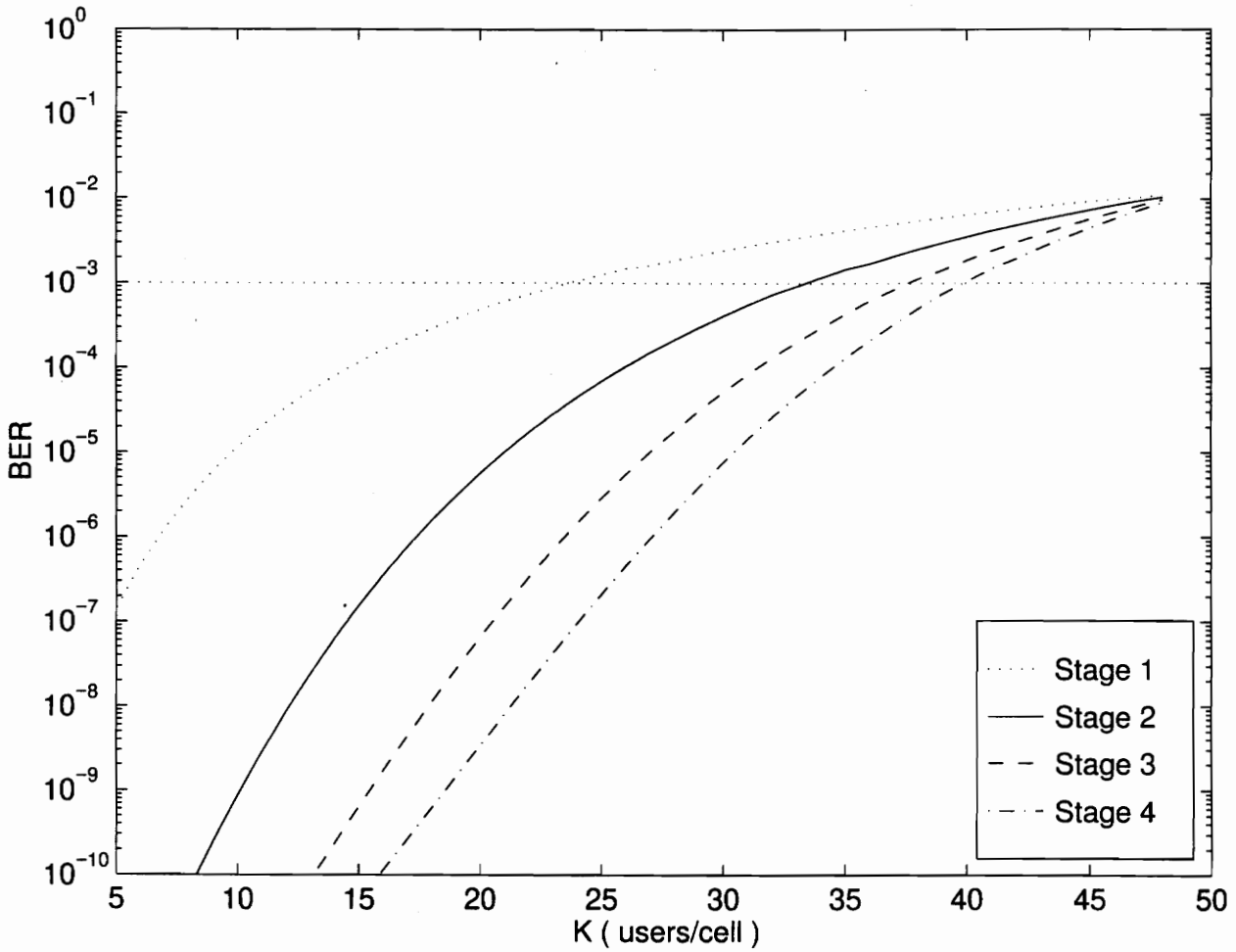

Figure 4.14: Performance of Interference Cancellation for Multicellular Environment using Hexagonal Geometry and the Improved Gaussian Approximation, Complete Interference Cancellation ($N = 128$, $\frac{E_b}{N_0} = 15$ dB, $r = 1000$ m, $n = 4$)

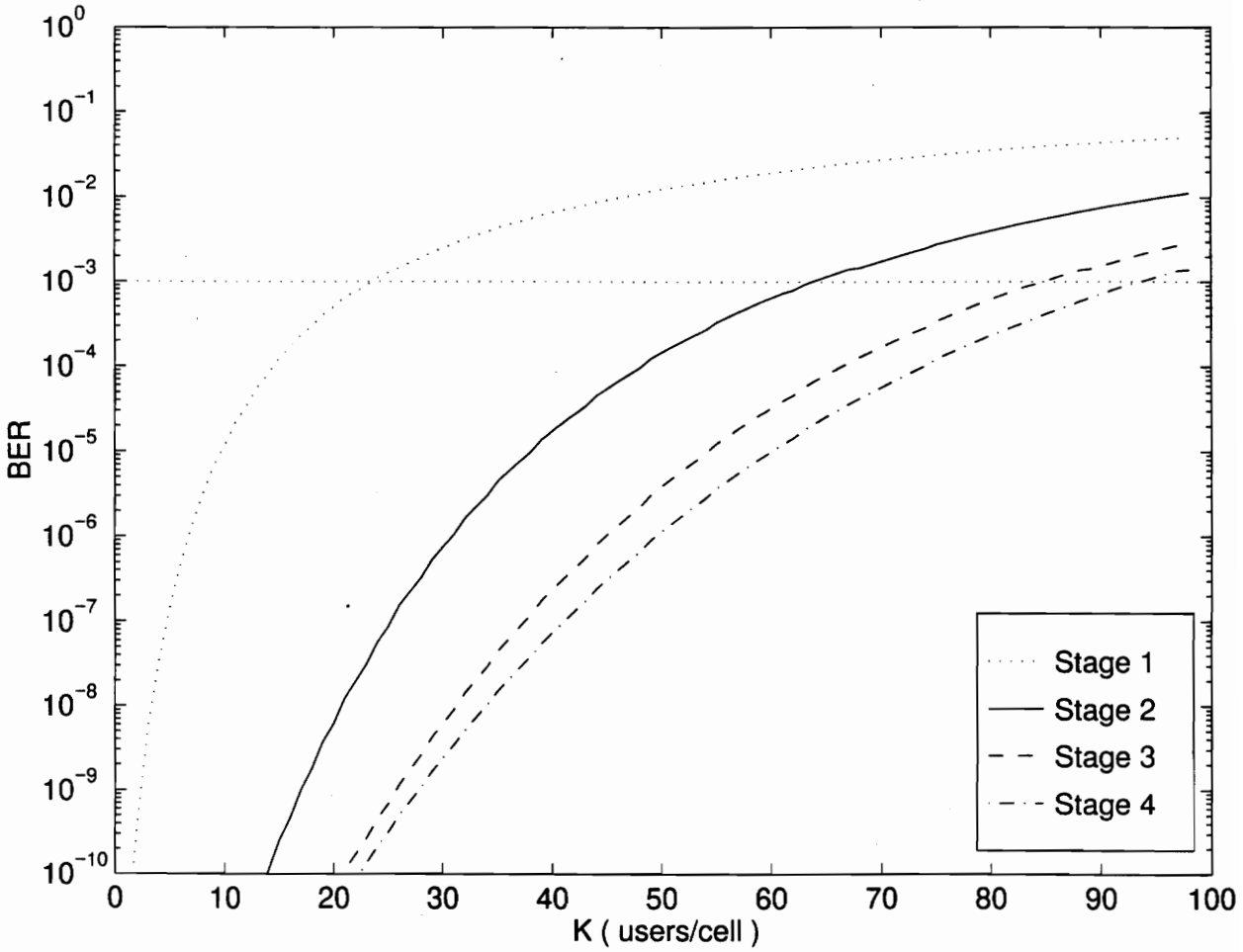

Figure 4.15: Performance of Interference Cancellation for Multicellular Environment using Hexagonal Geometry and the Improved Gaussian Approximation, Selective Interference Cancellation ($N = 128$, $\frac{E_b}{N_0} = 15$ dB, $r = 1000$ m, $n = 4$)

does not seem to make a noticeable difference. The simple Gaussian approximation serves our purpose equally well. The improved Gaussian approximation could however produce a significant improvement in the accuracy of the results in situations where the channel is much worse, and especially under conditions where there are a small number of users per cell, K [11].

Chapter 5

Selective Cancellation Using Bit Averaging

5.1 Motivation

This chapter explores the use of averaging power estimates over several previous bits to improve the selective cancellation criteria. More accurate power estimates can improve the selective cancellation process in several ways. The following considerations motivate us to explore ways of improving selective cancellation criteria.

1. The wireless channel is characterized by multipath propagation as signals reflect and scatter off objects in the transmission path. In [42][25], a multistage RAKE receiver was proposed. The motivation behind these works was to combine the benefits of the RAKE and multistage receivers into one integrated receiver design. The RAKE receiver takes advantage of multipath propagation, and the multistage receiver gives successively better estimates of the desired signal by subtracting the interference from the received signal. It was shown that a two stage RAKE receiver provides better performance than a single stage RAKE, even in harsh Rayleigh channels. Since interference cancellation performed on selected out-of-cell interferers yields significant capacity improvements as shown in Chapter 4, it is reasonable to believe that selective cancellation of resolvable multipath components should lead to an improvement on the results reported

in [42][25], especially under severe fading conditions. To perform selective cancellation on multipath components under severe fading conditions, a good criterion to select multipath components for interference cancellation is required. It should be possible to select multipath components for cancellation by comparing their received powers to the threshold of Eqn. 3.27. However, in order to apply this criterion, it is necessary to have a good estimate of the power in the multipath component, to ensure that we do not cancel weak components and hurt performance in the process.

2. An improvement in the power estimate will also lead to a better selection of out-of-cell interferers for cancellation.

3. Moreover, the better the amplitude estimate, the more complete is the interference cancellation process at any stage.

4. As mentioned in Section 2.2, with a fairly mild set of assumptions, maximal ratio combining of decision statistics from different fingers of a RAKE receiver is equivalent to weighting the decision statistics from the RAKE fingers in proportion to their magnitude. Thus, even in RAKE receivers which do not employ interference cancellation, a better amplitude estimate is always welcome, since it would lead to maximizing the signal to noise ratio of the overall decision statistic because of near optimum combining of the decision statistics from individual fingers.

In the model used in [8][9][10], information from only one bit is used to form an estimate of the bit transmitted by an interferer, as well as the power of the interferer. At any stage s of the receiver, the decision statistic $Z_{k,i}^{(s)}$ is used to form an unbiased estimate of the product $b_{k,i}\sqrt{P_k}$, where $\hat{b}_{k,i} = Z_{k,i}^{(s)}/|Z_{k,i}^{(s)}|$ is an estimate of the kth user's data bit, and $\hat{P}_k = 2[Z_{k,i}^{(s)}/T]^2$ is an estimate of the kth user's power. In other words, $\hat{A}_k^{(s)} = 2|Z_{k,i}^{(s)}|/T$ is an estimate of the kth user's amplitude. We could potentially improve the accuracy of the amplitude estimate by averaging amplitude estimates over several consecutive symbols, to give

$$\hat{A_k^{(s)}} = \frac{1}{p}\sum_{i=1}^{p} 2\frac{|Z_{k,i}^{(s)}|}{T}, \tag{5.1}$$

where p is the number of bits that we average over to produce the improved amplitude estimate. We know that $2\frac{Z_{k,i}^{(s)}}{T}$ is an unbiased estimator for $A_k \times b_{k,i}$ [8][9]. However, $2\frac{|Z_{k,i}^{(s)}|}{T}$ is a biased estimator for A_k. Hence, $\hat{A_k}^s$ is a slightly biased estimator for A_k. We will however assume that $\hat{A_k^{(s)}}$ is an unbiased and consistent estimator for A_k, i. e.

$$E[\hat{A_k^{(s)}}] = E\left[\frac{1}{p}\sum_{i=1}^{p} 2\frac{|Z_{k,i}^{(s)}|}{T}\right] \approx A_k. \tag{5.2}$$

and

$$\begin{aligned}\lim_{p\to\infty} Var[\hat{A_k^{(s)}}] &= \lim_{p\to\infty} Var\left[\frac{1}{p}\sum_{i=1}^{p} 2\frac{|Z_{k,i}^{(s)}|}{T}\right] \\ &= \lim_{p\to\infty}\frac{1}{p}\left\{\frac{4}{T^2}Var\left[|Z_{k,i}^{(s)}|\right]\right\} = 0.\end{aligned} \tag{5.3}$$

Thus,

5.2 Hard Decisions

Although the bit estimate and the power estimate could have been formed separately, Kaul and Woerner [8][9] were interested in the product $b_{k,i}\sqrt{P_k}$. So, $Z_{k,i}^{(s)}$ was used directly to provide "soft decisions", which simplified the analysis. If we use power estimates averaged over several bits, we would have to form the bit estimate and the power estimate separately. In other words, we would have to make hard decisions on the bits transmitted by the users at every stage of interference cancellation, and then multiply this hard estimate by the power estimate, which could depend on amplitude information from several previous bits.

Since the first stage of the receiver is still a simple correlation detector, the BER for the first stage will remain the same as in the case of soft decisions, and is given by Eqn. 3.15 which can be written as

$$P_{b_k}^{(1)} = Q\left\{\left[\frac{P_k T^2}{2Var[Z_{k,i}^{(1)}]}\right]^{1/2}\right\} = Q\left\{\left[\frac{P_k T^2/2}{\frac{N_0 T}{4} + \frac{NT_c^2}{6}\sum_{\kappa=1,\kappa\neq k}^{K} P_\kappa^{(1)}}\right]^{1/2}\right\}. \tag{5.4}$$

Consider any stage s of the interference cancellation receiver. Let $\hat{A}_\kappa^{(s)}$ be the amplitude estimate for user κ at stage s. By multiplying the amplitude estimate and

the data estimate for any interferer κ, an estimate for the signal transmitted by an interferer is obtained. The estimate of that user's signal at stage s can be expressed as

$$\hat{s_\kappa^{(s)}} = \hat{A}_\kappa^{(s)} a_\kappa(t-\tau_\kappa)\hat{b}_\kappa(t-\tau_\kappa)\cos(\omega_c t+\phi_\kappa), \tag{5.5}$$

where $\hat{b}_\kappa(t)$ is an estimate for the data signal transmitted by the user. To perform interference cancellation, subtract the signal estimate, $\hat{s}_\kappa^{(s)}$, from the received signal. Let $P_\kappa^{(s+1)}$ be the residual power due to user κ into stage $s+1$ after interference cancellation at stage s. Now look at stage $s+1$ as the first stage, but with the powers of all users replaced by the residual powers remaining after stage s. The variance of the decision statistic for user k at stage $s+1$ can be calculated as

$$Var[Z_{k,i}^{(s+1)}] = \frac{N_0 T}{4} + \frac{NT_c^2}{6}\sum_{\kappa=1,\kappa\neq k}^{K} P_\kappa^{(s+1)}. \tag{5.6}$$

Thus, the BER for user k at stage $s+1$ is given by

$$P_{b_k}^{(s+1)} = Q\left\{\left[\frac{P_k T^2}{2Var[Z_{k,i}^{(s+1)}]}\right]^{1/2}\right\} = Q\left\{\left[\frac{P_k T^2/2}{\frac{N_0 T}{4}+\frac{NT_c^2}{6}\sum_{\kappa=1,\kappa\neq k}^{K} P_\kappa^{(s+1)}}\right]^{1/2}\right\}. \tag{5.7}$$

Now consider two possibilities:

1. The data estimate is correct.

2. The data estimate is wrong.

If we have a correct bit estimate, the residual interference from this interferer carried over to the next stage $s+1$ is

$$\nu_\kappa^{(s+1)}|correct = s_\kappa(t-\tau_\kappa) - \hat{s}_\kappa(t-\tau_\kappa) = [A_\kappa - \hat{A}_\kappa^{(s)}]a_\kappa(t-\tau_\kappa)\cos(\omega_c t+\phi_\kappa). \tag{5.8}$$

In this case, the uncanceled interference power $P_\kappa^{(s+1)}|correct$ of the remaining interference into the next stage $s+1$ will depend on how close $\hat{A}_\kappa^{(s)}$ is to A_κ. In more formal terms, $P_\kappa^{(s+1)}$ will be proportional to the variance in the amplitude estimate $\hat{A}_\kappa^{(s)}$. If, however, we make a wrong data bit estimate, we will add the amplitude estimate instead of subtracting it, and the residual interference in that case will be

$$\nu_\kappa^{(s+1)}|(wrong) = s_\kappa(t-\tau_\kappa) - \hat{s}_\kappa(t-\tau_\kappa) = [A_\kappa + \hat{A}_\kappa^{(s)}]a_\kappa(t-\tau_\kappa)\cos(\omega_c t+\phi_\kappa). \tag{5.9}$$

Given that we have made a wrong bit estimate, we denote the residual interference power from user κ fed into stage $s+1$ as $P_\kappa^{(s+1)}|incorrect$.

Assume that we average amplitude estimates over p bits to generate an improved amplitude estimate. This would reduce the variance of the amplitude estimate by a factor of $\frac{1}{p}$. Out of these p bits, suppose we have wrong data bit estimates on i bits, and correct data bit estimates on the remaining $p-i$ bit. The probability of making incorrect data estimates on given i bits out of p bits can be expressed as $(P_{b_\kappa}^{(s)})^i(1-P_{b_\kappa}^{(s)})^{(p-i)}$. Moreover, we can choose C_i^p combinations of i bits out of p bits, where C_i^p is defined as $C_i^p = \frac{p!}{i!(p-i)!}$. Thus, the residual interference power from user κ carried into the next stage will be

$$P_\kappa^{(s+1)} = \sum_{i=0}^{p} C_i^p (P_{b_\kappa}^{(s)})^i (1-P_{b_\kappa}^{(s)})^{(p-i)} \left[\frac{i}{p}\cdot P_\kappa^{(s+1)}|incorrect + \frac{(p-i)}{p}\cdot P_\kappa^{(s+1)}|correct\right]. \tag{5.10}$$

If we can find $P_\kappa^{(s+1)}|correct$ and $P_\kappa^{(s+1)}|incorrect$ for all users, $P_\kappa^{(s+1)}$ can be obtained for all users. When substituted into Eqn. 5.7, this will allow us to calculate the BER at stage $s+1$. We will direct our attention to obtaining expressions for the residual powers into stage $s+1$ given the condition that we make a correct or incorrect bit estimate (i. e. $P_\kappa^{(s+1)}|correct$ and $P_\kappa^{(s+1)}|incorrect$).

5.3 Perfect Power Estimates

5.3.1 Analysis

Let us assume for the moment that we have perfect estimates for the interfering powers, i. e. $\hat{A}_\kappa^{(s)} = A_\kappa$. If we also make the correct data bit estimate, we are able to cancel out the interference from a bit perfectly (i. e. $\nu_\kappa^{(s+1)} = 0$), and the residual interference power carried into the next stage is

$$P_\kappa^{(s+1)}|correct = 0 \tag{5.11}$$

On the other hand, if we make the wrong bit estimate, the amplitude of $\nu_\kappa^{(s+1)}$ is $2A_\kappa$, and the interference power carried into the next stage is

$$P_\kappa^{(s+1)}|incorrect = (2A_\kappa)^2/2T = 4P_\kappa^{(1)}, \tag{5.12}$$

since $P_\kappa^{(s+1)} = [A_\kappa \pm \hat{A}_\kappa^{(s)}]^2/2T$. The plus sign holds in case of an incorrect bit estimate, and the minus sign in case of a correct bit estimate. Substituting these values of residual interfering powers in Eqn. 5.10, the residual power from interferer κ fed into stage $s+1$ is obtained when averaging is performed over p bits.

$$P_\kappa^{(s+1)} = \sum_{i=0}^{p} C_i^p (P_{b_\kappa}^{(s)})^i (1 - P_{b_\kappa}^{(s)})^{(p-i)} \left[\frac{i}{p} \cdot 0 + \frac{(p-i)}{p} \cdot 4P_\kappa^{(1)} \right]. \tag{5.13}$$

Thus, we can find the residual interfering power for each user and substitute it into Eqn. 5.6 to get the variance of the decision statistic at stage $s+1$. Eqn. 5.7 will then yield the bit error probability.

5.3.2 Results

For all figures presented in this section, we assume an E_b/N_0 value of 15 dB, and a processing gain of $N = 31$ unless otherwise stated. Figure 5.1 is a plot of the BER versus the number of users for the hard decision receiver, assuming perfect amplitude estimates. This graph has been plotted with amplitude estimates from only one bit. BER curves are presented for the first four stages of the interference cancellation receiver. Note that interference cancellation provides huge benefits in capacity, and three stages of interference cancellation provide almost a seven times increase in capacity at an acceptable BER level of 10^{-3}. Figure 5.2 shows results for a similar case where the amplitude estimates are averaged over 100 bits. These results are exactly the same as those obtained in Figure 5.1 when no bit averaging was used. This is true, since in both cases perfect amplitude estimates are assumed. If the amplitude estimate is perfect, it does not matter how many bits are averaged over. Thus, averaging over more than one bit will not provide any further benefit, and the BER should be independent of p, which it is. In other words, we have excluded the effect of bad amplitude estimates, and the results depicted in the two figures examine the effect of wrong bit estimates only. When imperfect power estimates are considered, Figure 5.1 will serve as a limiting case which should be approached as our power estimates become more and more accurate. As mentioned, these figures are plotted using the analysis for hard decisions at each stage.

Figure 5.3 is a plot of the BER against the E_b/N_0 for the case of perfect amplitude estimation and no bit averaging. This figure has been plotted for $K = 20$ users, and

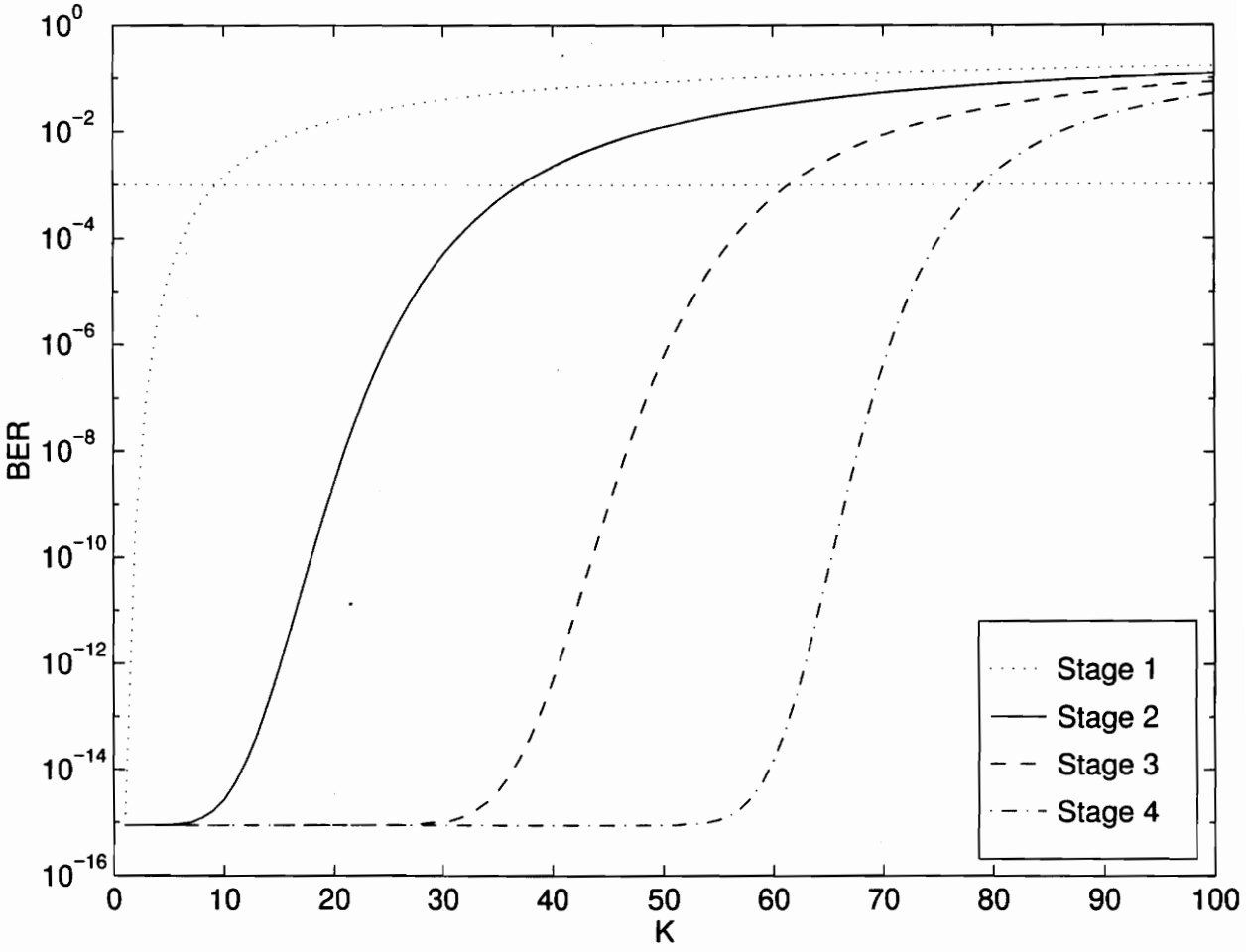

Figure 5.1: Performance of Interference Cancellation with hard decisions, assuming Perfect Amplitude Estimates, No Bit Averaging ($N = 31$, $\frac{E_b}{N_0} = 15$ dB)

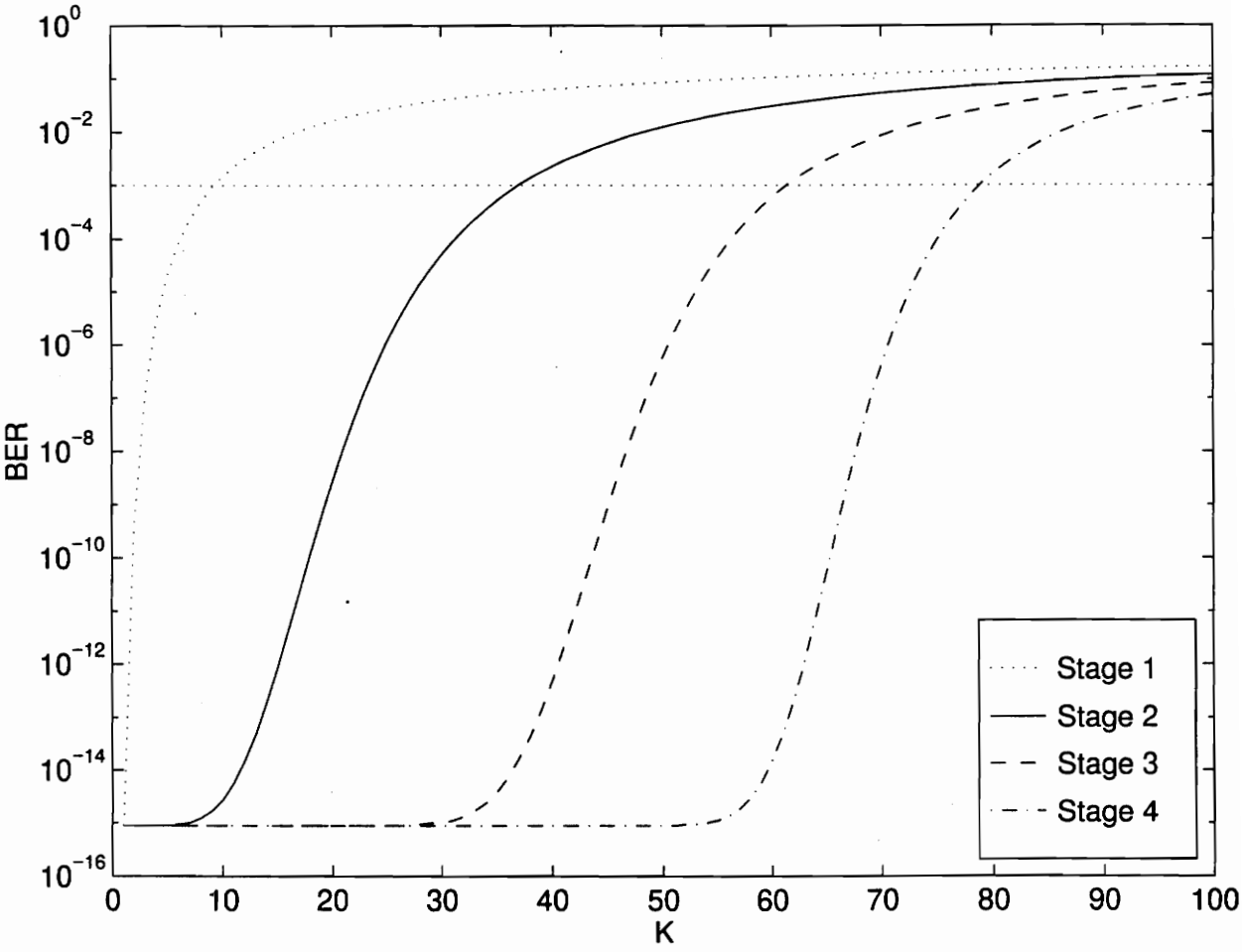

Figure 5.2: Performance of Interference Cancellation with hard decisions, assuming Perfect Amplitude Estimates, Averaging Estimates over 100 bits ($N = 31$, $\frac{E_b}{N_0} = 15$ dB)

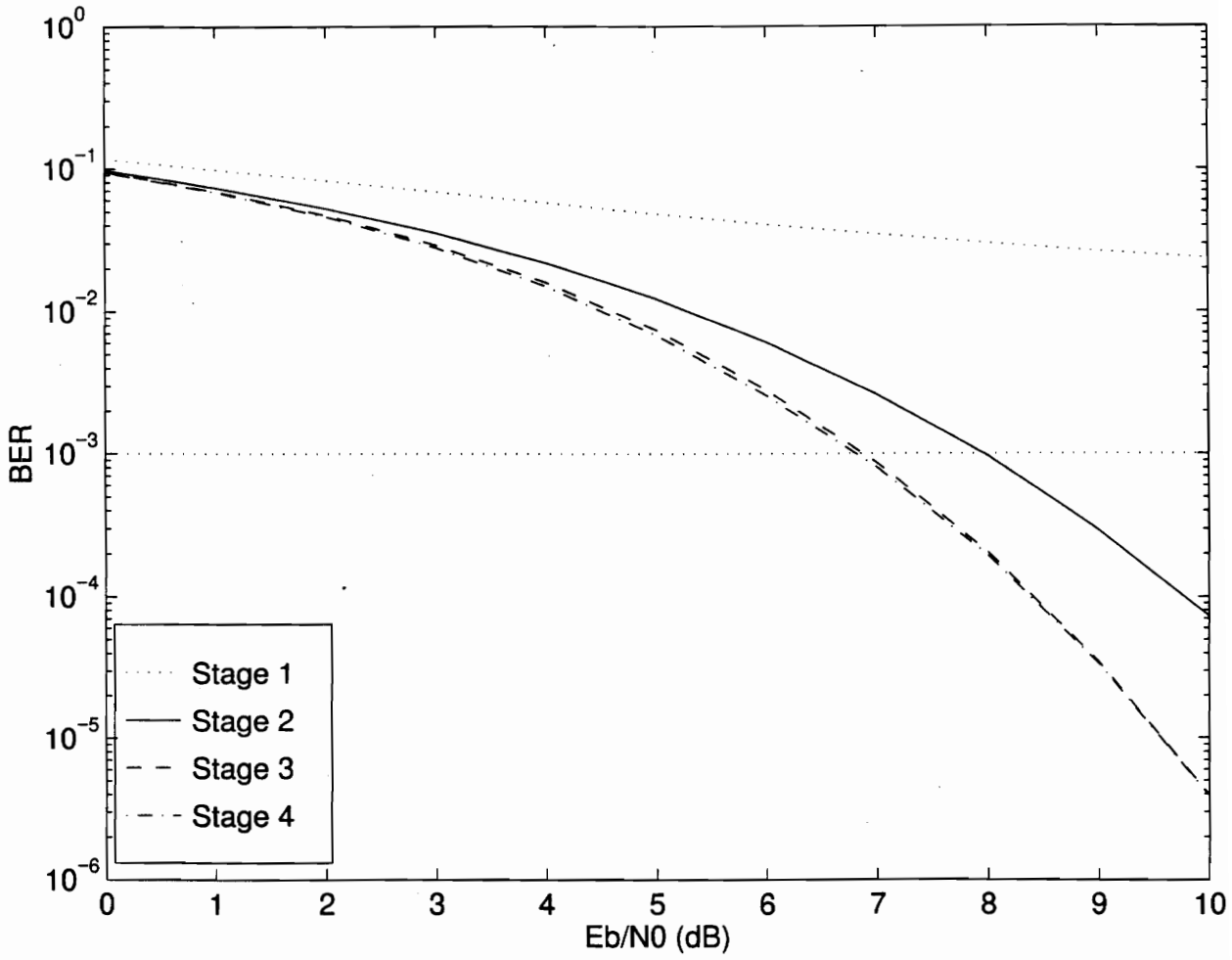

Figure 5.3: BER vs. E_b/N_0 for Interference Cancellation with hard decisions, assuming Perfect Amplitude Estimates, No bit Averaging($N = 31, K = 20$)

$N = 31$. The first stage of interference cancellation provides a huge performance improvement over the conventional CDMA receiver. The fourth stage of the receiver provides almost no improvement over the third stage. The fourth stage will however begin to provide noticeable improvement over the third stage when the number of users increases, as is seen from Figure 5.1. Varanasi and Aazhang [22] proposed a multistage multiuser detector for asynchronous CDMA. This receiver assumes a priori knowledge of received signal amplitudes and performs hard decisions at each stage. [22] presents the probability of error for a two stage receiver. Kaul and Woerner [43] have simulated the performance of such a receiver for multiple stages of interference cancellation. Figure 5.4 presents the analytical BER (from Figure 5.3) and the simulated BER on the same plot as a function of the $\frac{E_b}{N_0}$ value for $K = 20$ users [43]. Note that the results analytical and simulation results in Figure 5.4 should approach each other. Comparison of the analytical and simulation results shows that they match well at stage 1 and stage 4 of the receiver. However, for the stages 2 and 3, the simulation results are somewhat pessimistic as compared to the results obtained using the analytical treatment outlined in Section 5.3.1.

5.4 Imperfect Power Estimates

5.4.1 Analysis

Now let us consider the more realistic case of imperfect power estimates. Let $\hat{A}_\kappa^{(s)}$ be the estimate of the amplitude of user κ at stage s. We examine the case of an incorrect bit estimate first. For an incorrect bit estimate, the amplitude of the interfering signal for user κ fed into the next stage of the receiver is $A_\kappa + \hat{A}_\kappa^{(s)}$. As mentioned in Section 5.3, if $\hat{A}_\kappa^{(s)} = A_\kappa$, then $P_\kappa^{(s+1)}|incorrect = 4P_\kappa^{(1)}$. If $\hat{A}_\kappa^{(s)} > A_\kappa$, then $P_\kappa^{(s+1)}|incorrect > 4P_\kappa^{(1)}$, and the performance will be hurt further, since more interfering power will be injected into the next stage. On the other hand, if $\hat{A}_\kappa^{(s)} < A_\kappa$, then $P_\kappa^{(s+1)}|incorrect < 4P_\kappa^{(1)}$, and having made a smaller (although inaccurate) amplitude estimate will actually help us, and will, to a certain extent, compensate for the damage done by the wrong bit estimate. Assuming that amplitude estimates are equally likely to be smaller as they are to be larger than the real amplitude, the average interfering power into the next stage will still be $4P_\kappa$, which is the same as

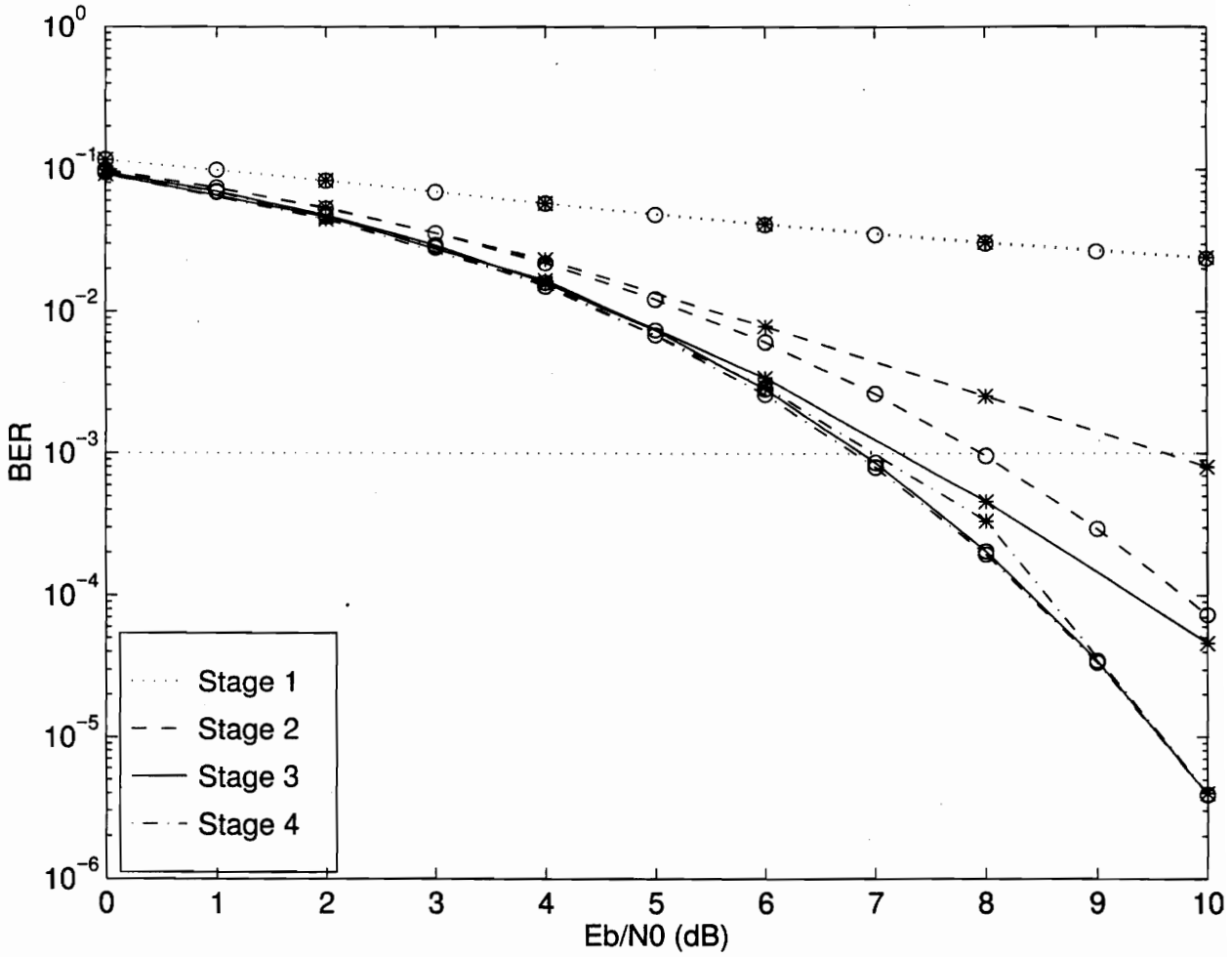

Figure 5.4: Simulated and Analytical BER vs. E_b/N_0 for Interference Cancellation with hard decisions, assuming Perfect Amplitude Estimates ($N = 31, K = 20$) o : Analytical Results, * : Simulated Results

that in case of perfect amplitude estimates. Hence,

$$E\left[P_\kappa^{(s+1)}|incorrect\right] = 4P_\kappa^{(1)}. \tag{5.14}$$

Now let us consider the case of correct bit estimates. In this case, if an imperfect amplitude estimate is made, then interference cancellation will not be complete, and there will always be some residual power introduced into the next stage. Thus, imperfect amplitude estimates always hurt performance in the case of correct bit estimates, as compared to the case of incorrect bit estimates, where imperfect amplitude estimates actually helped us half of the time. The amplitude of the interference from user κ at stage $s+1$ is $|A_\kappa - \hat{A}_\kappa^{(s)}|$. Hence, the interference power due to user κ at stage $s+1$ is $(A_\kappa - \hat{A}_\kappa^{(s)})^2/2$. Note that $E[\hat{A}_\kappa^{(s)}] = A_\kappa$, and $Var[\hat{A}_\kappa^{(s)}] = E[(A_\kappa - \hat{A}_\kappa^{(s)})^2]$. Thus, the interference power due to user κ at stage $s+1$ given a correct bit estimate can be expressed as

$$P_\kappa^{(s+1)}|correct = Var[\hat{A}_\kappa^{(s)}]/2. \tag{5.15}$$

Recall that $\hat{A}_\kappa^{(s)} = (1/p)\sum_{i=1}^{p} 2|Z_{k,i}^{(s)}|/T$. Therefore $Var[\hat{A}_\kappa^{(s)}] = 4Var[|Z_{k,i}^{(s)}|]/(pT^2)$. Since we have a correct bit estimate, it would be reasonable to assume that $Var[|Z_{k,i}^{(s)}|] \approx Var[Z_{k,i}^{(s)}]$. This leads to

$$P_\kappa^{(s+1)}|correct \approx \frac{2}{p}\frac{Var[Z_{k,i}^{(s)}]}{T^2}. \tag{5.16}$$

Substituting these values for the interference power for each user into Eqn. 5.10 will yield the total interference power at stage $s+1$, enabling the calculation of the BER at stage $s+1$. Note that Kaul and Woerner have developed a closed form expression for the BER in [10]. Here, we have not developed a closed form expression, but have a set of recursive expressions, although it might be possible to develop a closed form expression for this case too.

5.4.2 Results

Figure 5.5 presents the BER as a function of the number of users K when no bit averaging is used. We have assumed an E_b/N_0 of 15 dB, and a processing gain of $N = 31$. We will use the same parameters for all results presented in this section unless otherwise mentioned. We see that three stages of selective interference cancellation provide approximately four times increase in capacity. What is striking is

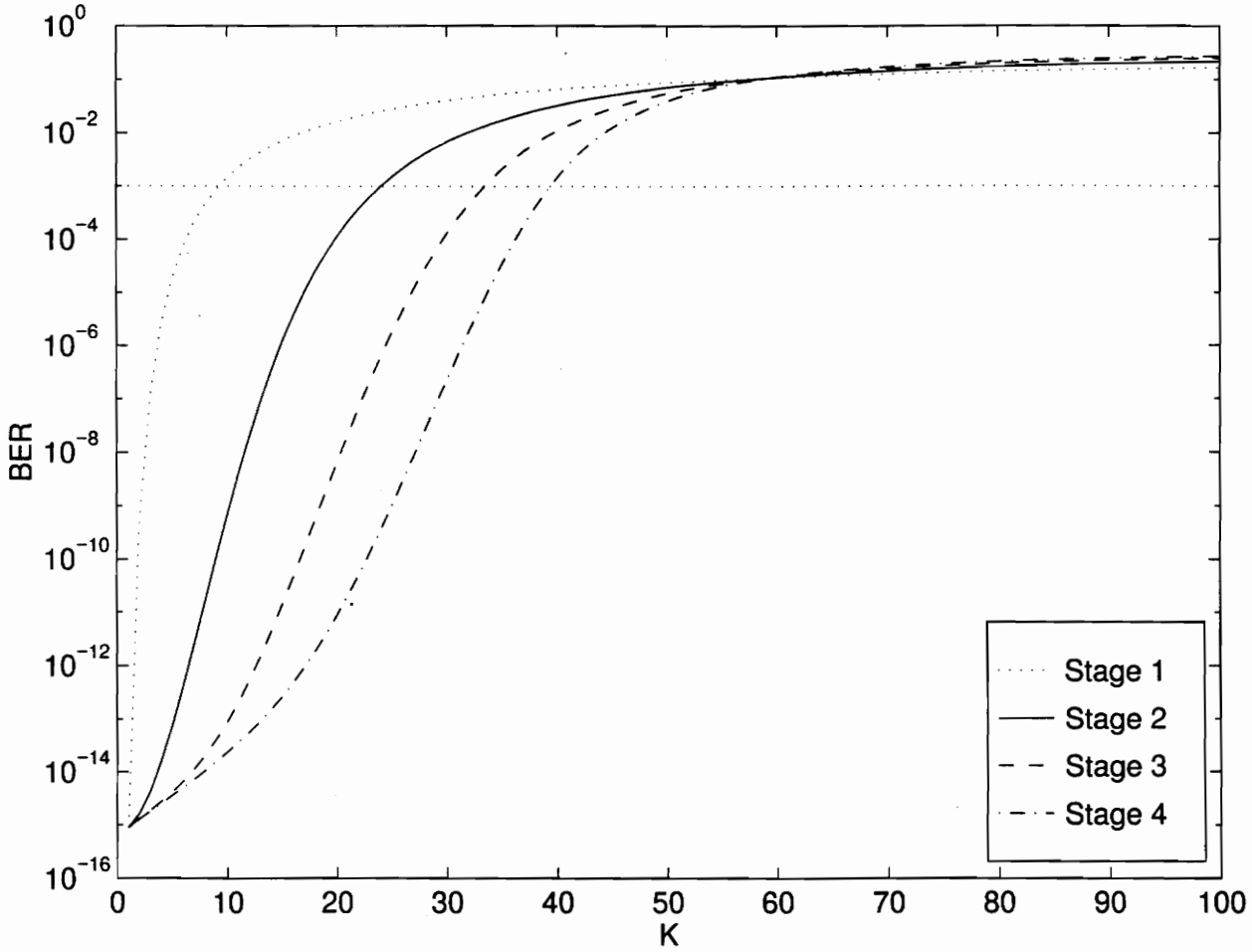

Figure 5.5: Performance of Interference Cancellation with hard decisions, No Bit Averaging ($N = 31, \frac{E_b}{N_0} = 15$ dB)

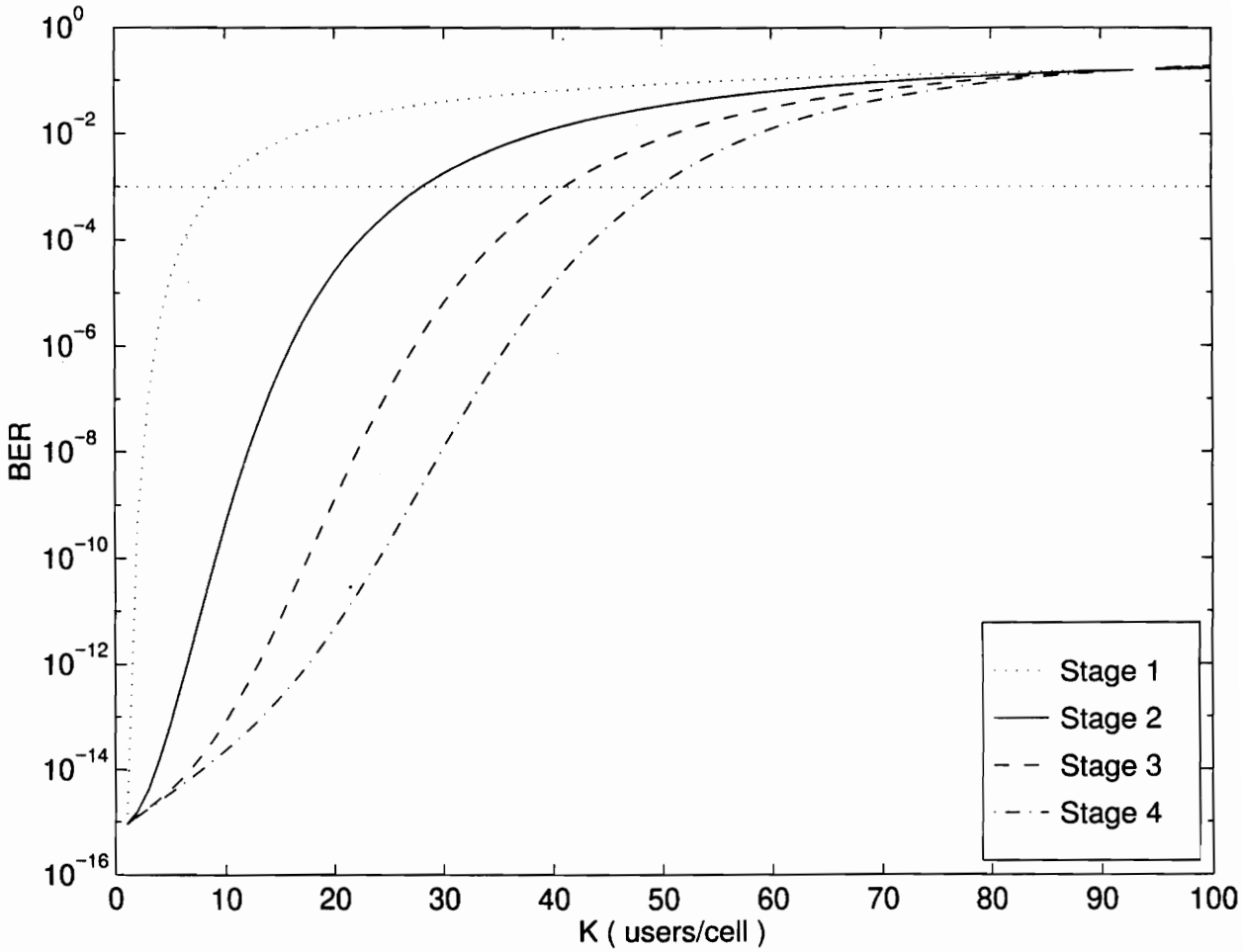

Figure 5.6: Performance of Interference Cancellation with soft decisions, ($N = 31$, $\frac{E_b}{N_0} = 15$ dB)

the difference in the capacities predicted by this figure, and by Figure 5.1, in which perfect amplitude estimates are assumed. The case of imperfect amplitude estimated reduces the capacity to almost half. This points out the importance of having accurate amplitude estimates. Comparison between Figures 5.5 and 5.1 brings to light the potential improvement in performance obtainable if better amplitude estimates are used. Since Figure 5.5 presents the results for the case of no bit averaging for hard estimates, it is in order to see how these results compare with the soft estimate case. In either situation, the only source of information for the amplitude estimate is the decision statistic $Z_{k,i}^{(s)}$. Therefore, in the case of no bit averaging, hard decisions are essentially the same as soft decisions, since the amplitude estimate is obtained from the decision statistic of just one bit in both cases. Moreover, this also points out that soft estimates can be viewed as a special case of hard estimates, when no extra information about the amplitude is available. The analysis for hard estimates thus presents a more generalized view for the performance of the interference cancellation receiver. Figure 5.6 plots equivalent results ($E_b/N_0 = 15$ dB, $N = 31$) for the case of soft estimates discussed in Chapter 3. We find that Figure 5.6 shows slightly better performance than Figure 5.5. Simulation results presented in [8][10] show that the analysis for soft cancellation produces somewhat optimistic results as compared to the simulations. For instance, under perfect power control with a processing gain of $N = 64$ and $K = 30$ users, analytical results predict a BER of approximately 10^{-4}, whereas simulations yield a BER of about 2×10^{-4} [8]. We may thus have found a way to get rid of some of the optimism in the analytical results presented in [10]. Figure 5.7 is a plot of the BER against the E_b/N_0 for the case of hard decisions and no bit averaging. It is plotted for a spreading gain of $N = 31$ and for $K = 20$ users.

Figures 5.8, 5.9, and 5.10 plot the BER against the number of users when the amplitude estimates are averaged over 2, 10 and 100 bits respectively. Comparing these results to those for no bit averaging (Figure 5.5), we see that even averaging amplitude estimates over just 2 bits produces a noticeable improvement in performance over no bit averaging. Averaging over 10 bits provides almost 1.5 times capacity increase over the no bit averaging case. Recall that no bit averaging provided about half the capacity predicted with perfect amplitude estimates. Thus, averaging over 10 bits gains back about half the capacity lost because of imperfect power estimates. As we

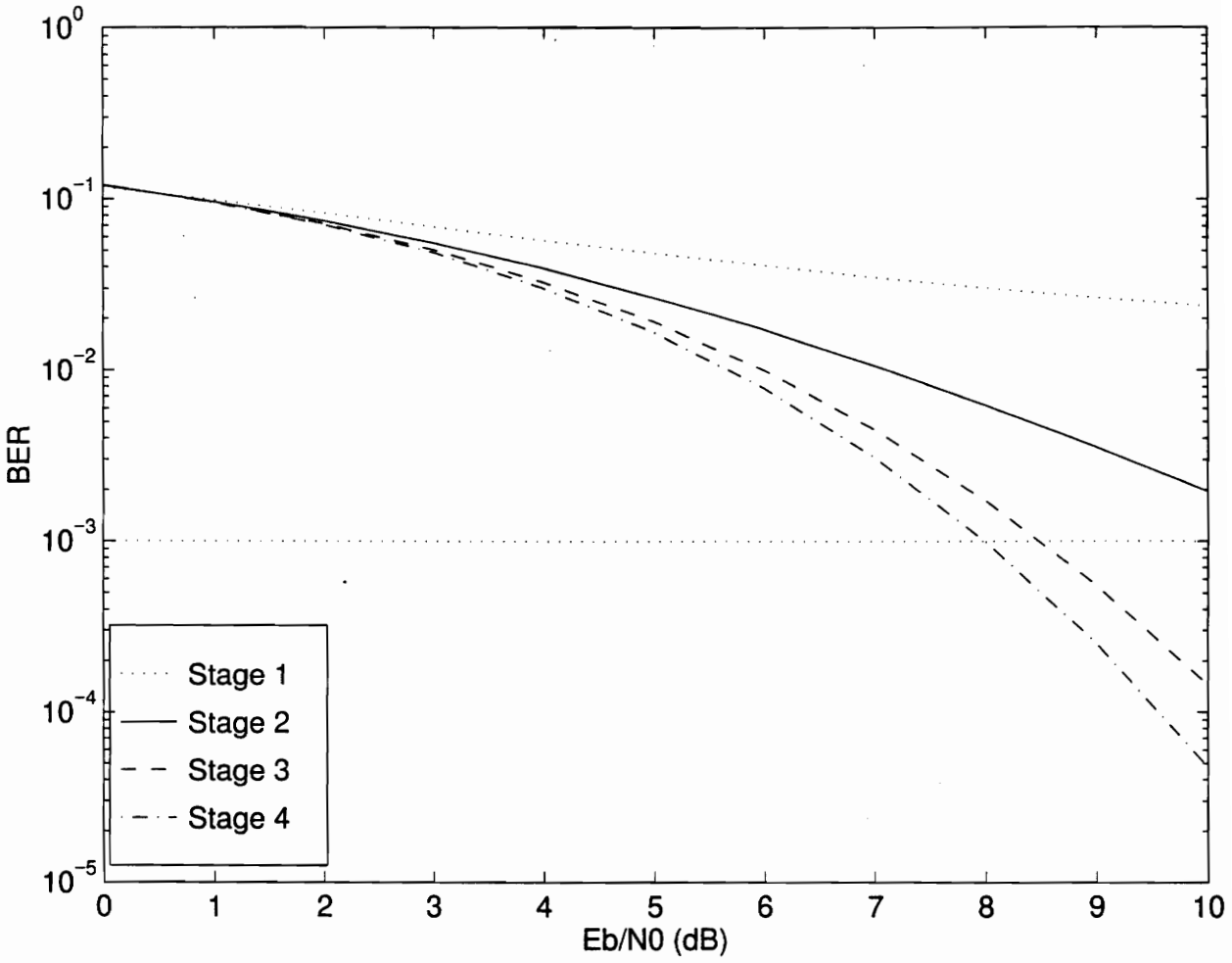

Figure 5.7: BER vs. E_b/N_0 for Interference Cancellation with hard decisions, No Bit Averaging, ($N = 31, K = 20$)

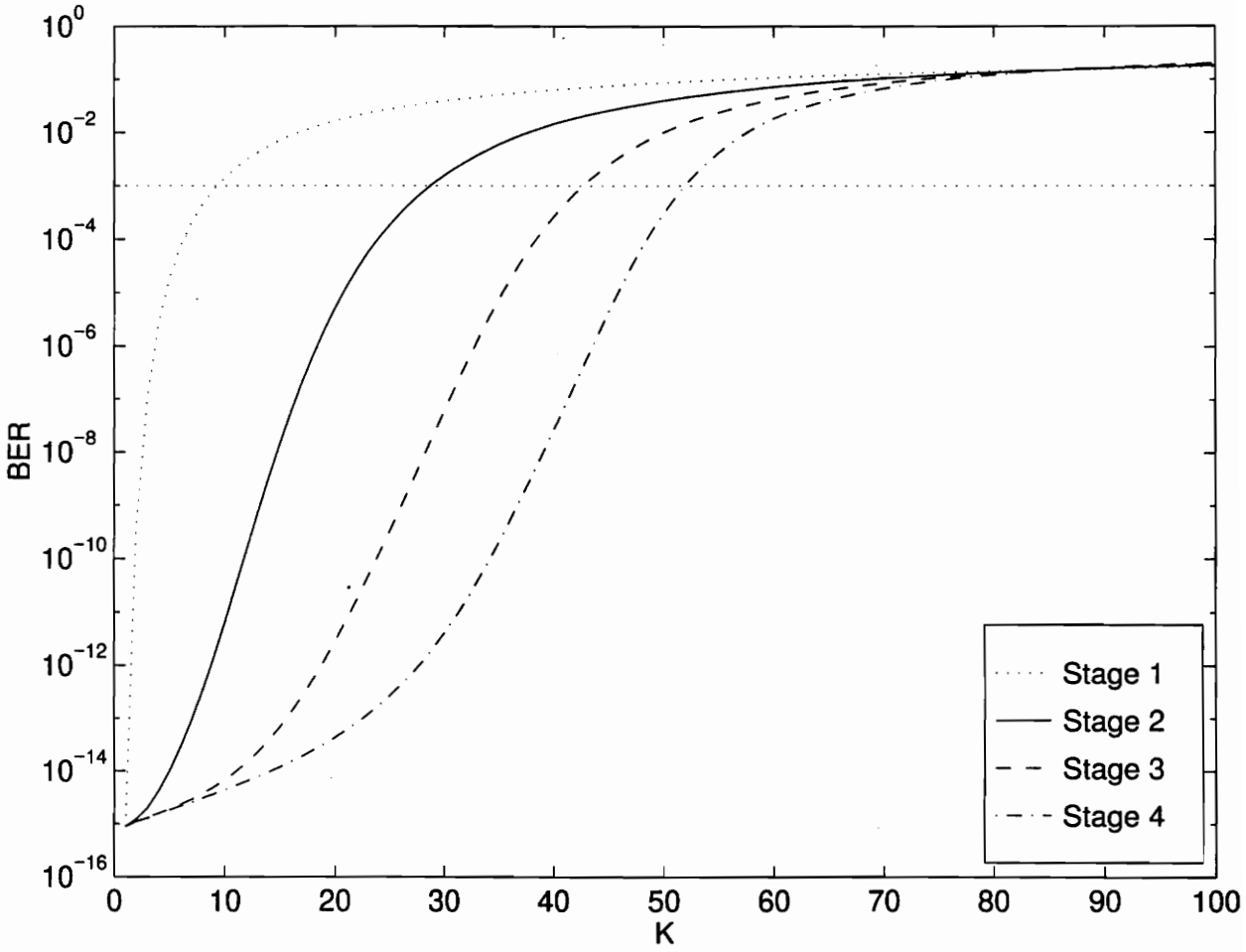

Figure 5.8: Performance of Interference Cancellation with hard decisions, Averaging Amplitude Estimates over 2 bits($N = 31, \frac{E_b}{N_0} = 15$ dB)

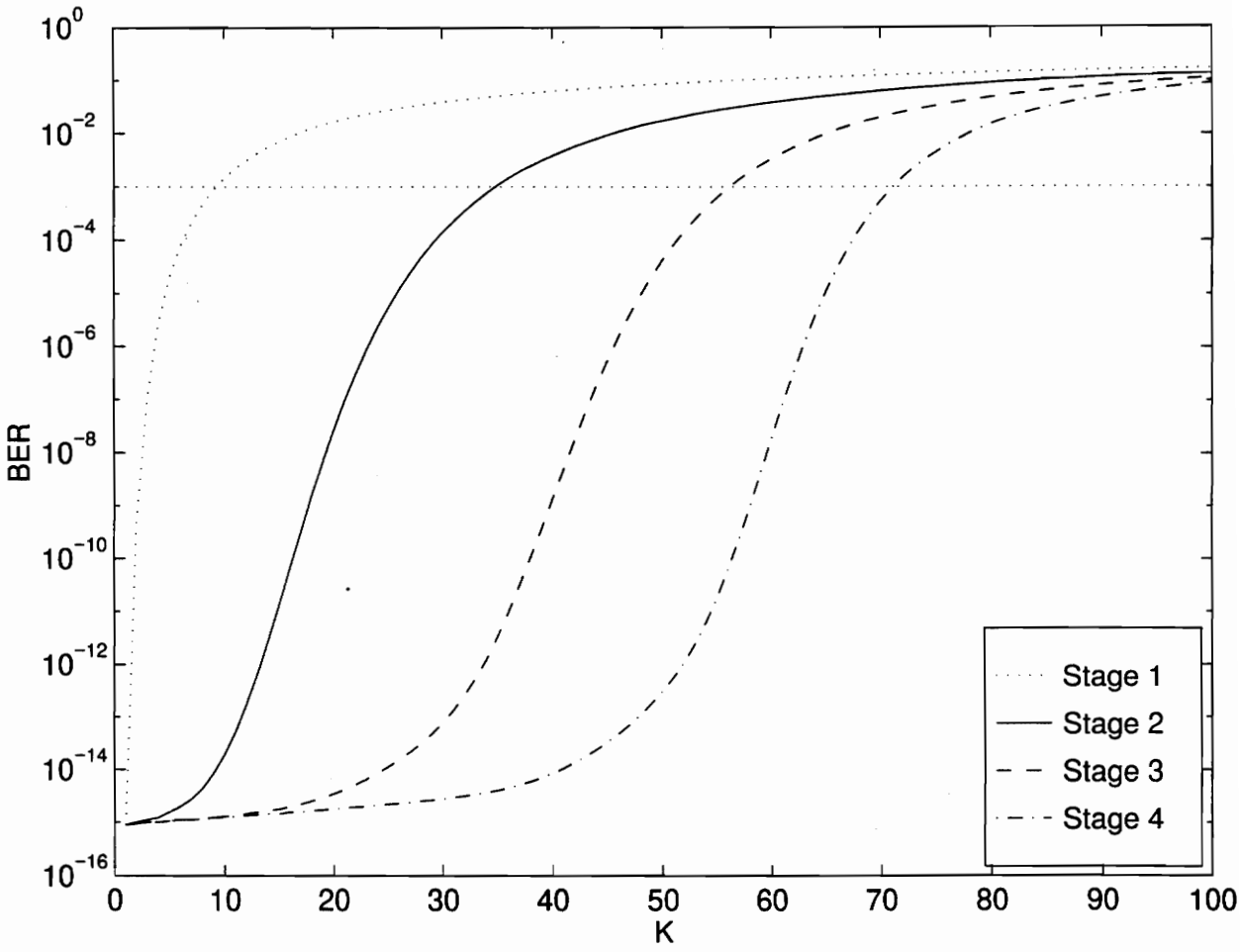

Figure 5.9: Performance of Interference Cancellation with hard decisions, Averaging Amplitude Estimates over 10 bits($N = 31$, $\frac{E_b}{N_0} = 15$ dB)

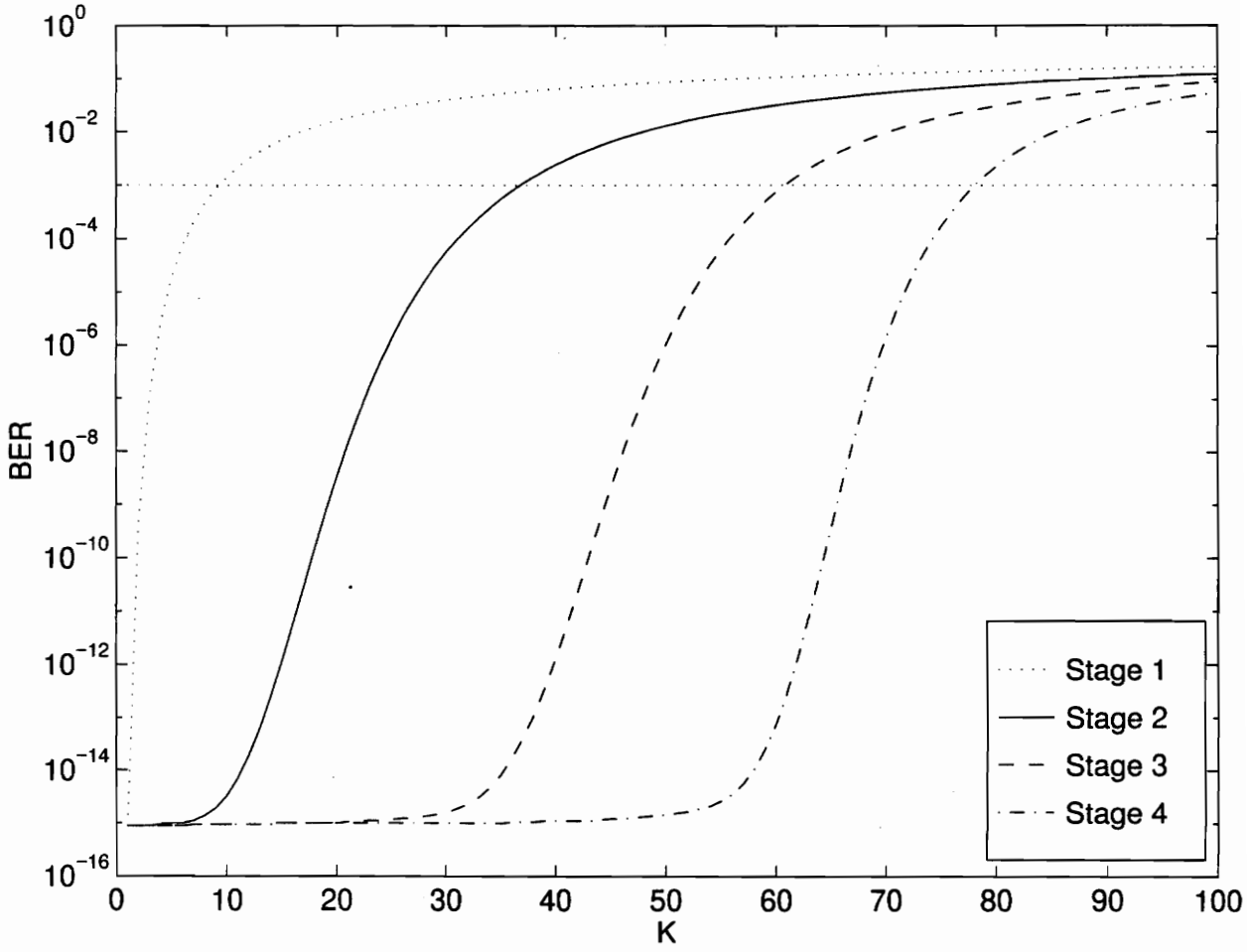

Figure 5.10: Performance of Interference Cancellation with hard decisions, Averaging Amplitude Estimates over 100 bits($N = 31$, $\frac{E_b}{N_0} = 15$ dB)

average amplitude estimates over more and more bits, the results get closer to those presented in the perfect amplitude case in Figure 5.1. In fact, the results in Figure 5.10, where amplitude estimates are averaged over 100 bits, are very close to those in the perfect amplitude estimate case. Thus, averaging amplitude estimates over several bits can result in considerable increase in capacity. If averaging is performed over 1000 bits the resulting performance is closer to the perfect power estimate case, but the improvement over the $p = 100$ bits case is not as dramatic as the improvement from the $p = 100$ case over $p = 10$ case. Moreover, time varying fading might change the channel characteristics during that time. Thus, the improvement obtained from averaging starts diminishing, and the performance tends towards the asymptotic limit set by the perfect estimate case. One common assumption in all results presented above is perfect power control. Because of the perfect power control, averaging over more and more bits leads to improving performance, although with diminishing improvements. In a more practical environment, however, this would not be the case. Under a fading channel, for instance, it is reasonable to expect that there is an optimum number of bits to average over to extract the best possible performance from the receiver. The optimum number of bits is proportional to the ratio of the coherence time of the channel to the bit period. In other words, in a slowly fading channel, we would average estimates over a larger number of bits than in fast fading, where the received power is changing at a faster rate. The slower the signal power varies, the greater the optimum number of bits to average over. Perfect power control is an extreme case, where the received power does not change at all. This explains why increasing p always improves performance in the case of perfect power control.

Figure 5.11 is a plot of the BER against the E_b/N_0 when amplitude estimates are averaged over 2 bits. Comparison of Figure 5.8 with Figure 5.5 shows that averaging over two bits provides a considerable improvement in performance over no bit averaging, especially at the first stage of interference cancellation. Figures 5.9 and 5.10 present similar results when amplitude estimates are averaged over 10 and 100 bits respectively. Notice that as the number of bits averaged over, p, goes on increasing, the improvement obtained diminishes. Figure 5.10 where estimates are averaged over 100 bits is very similar to Figure 5.3, where perfect amplitude estimates are assumed.

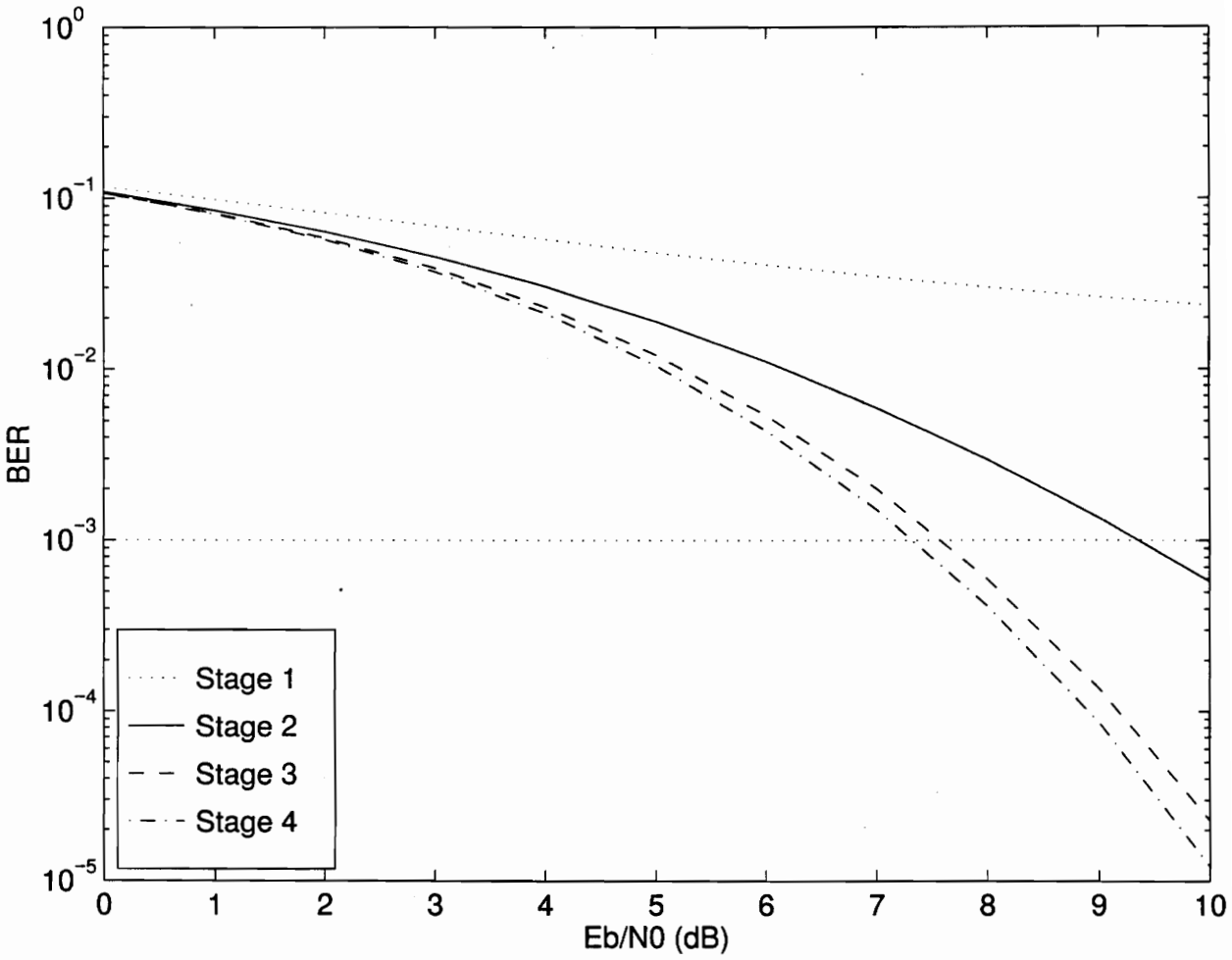

Figure 5.11: BER vs. E_b/N_0 for Interference Cancellation with hard decisions, Averaging Amplitude Estimates over 2 bits($N = 31, K = 20$)

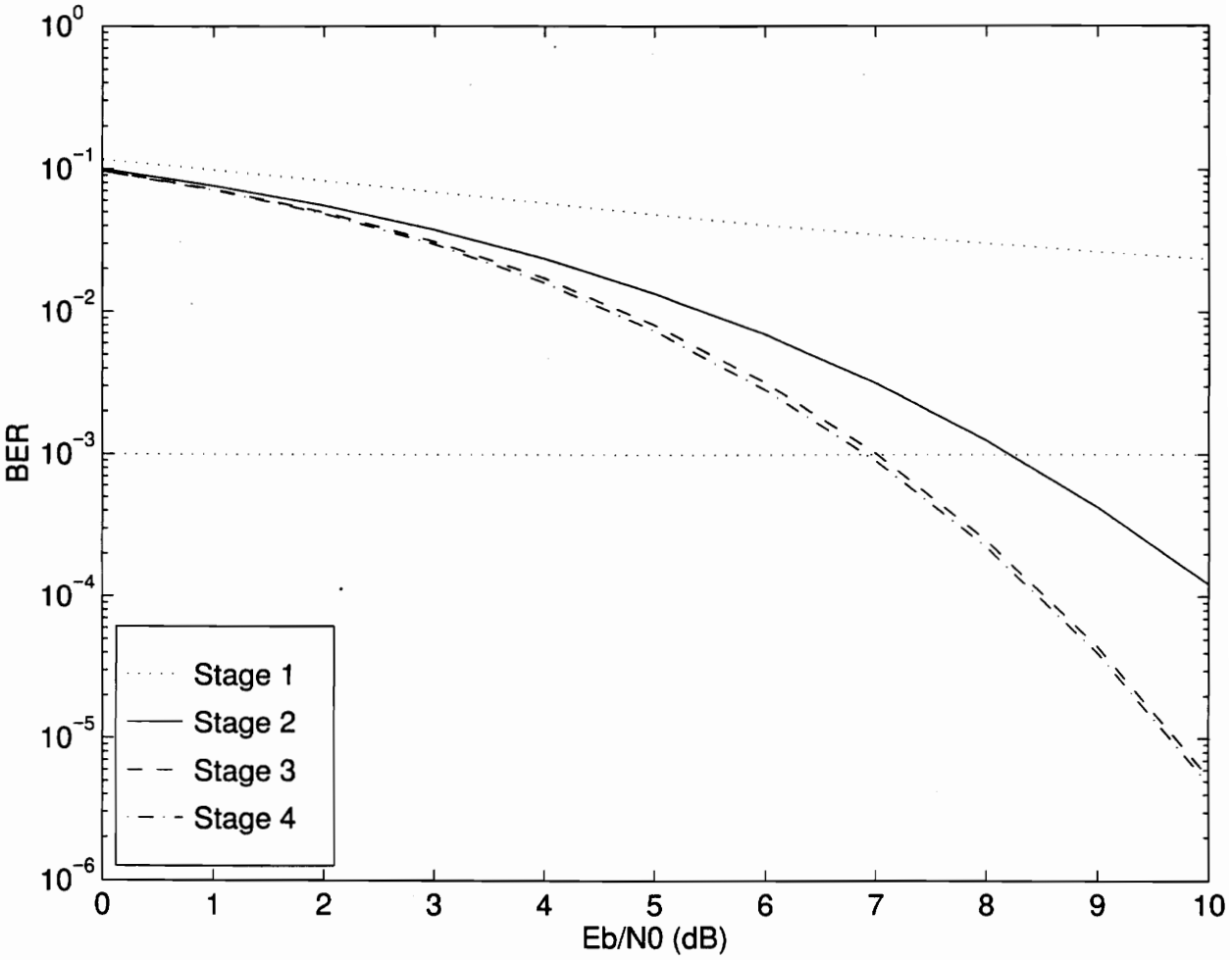

Figure 5.12: BER vs. E_b/N_0 for Interference Cancellation with hard decisions, Averaging Amplitude Estimates over 10 bits($N = 31, K = 20$)

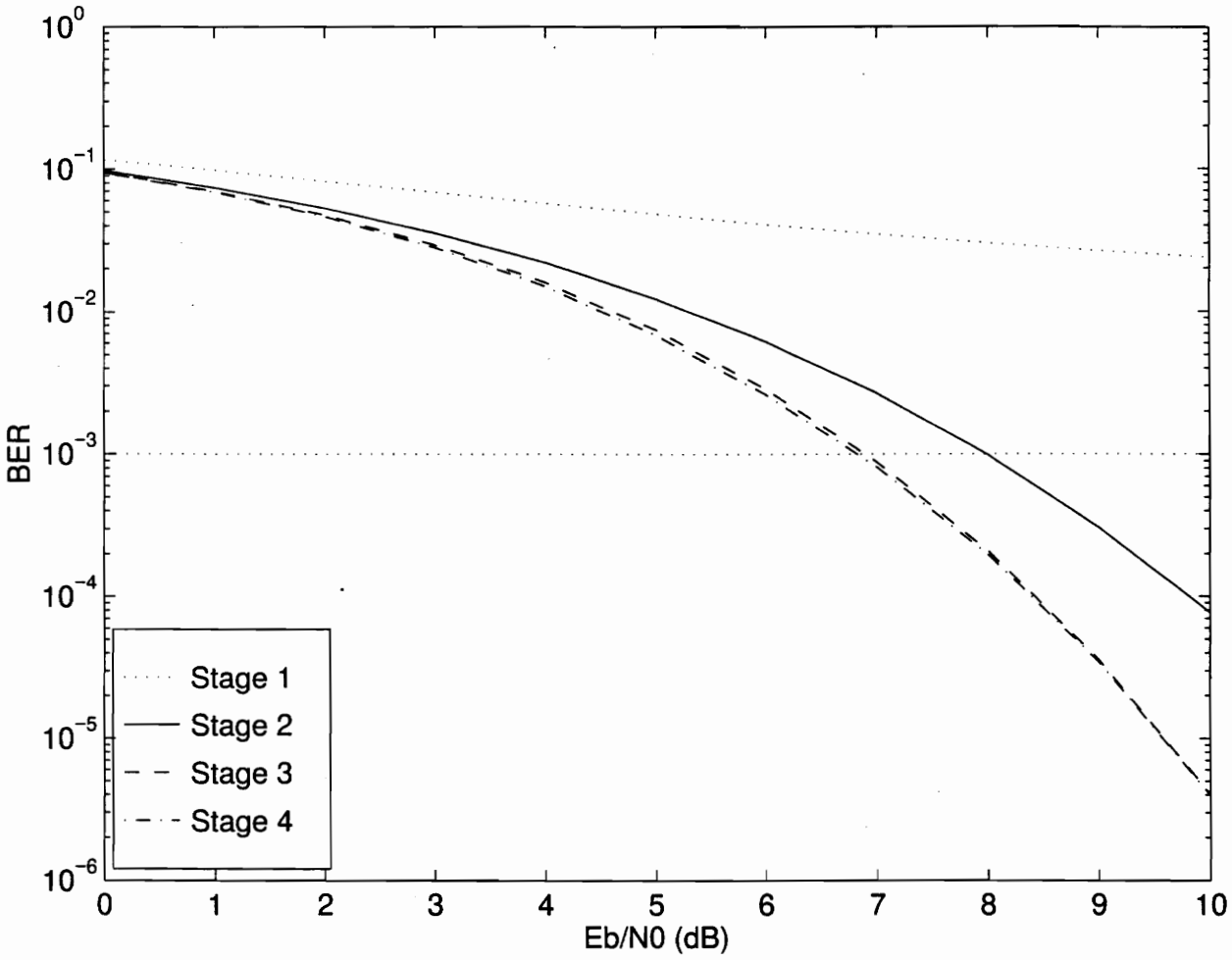

Figure 5.13: BER vs. E_b/N_0 for Interference Cancellation with hard decisions, Averaging Amplitude Estimates over 100 bits($N = 31, K = 20$)

5.5 Summary

In this chapter, we analyzed the issues involved in applying the interference cancellation criterion presented in Eqn. 3.27 to a multipath environment. To perform cancellation of multipath components in a fading channel, it is necessary to have a very accurate estimate of the power in the multipath component. We investigated the effect of averaging power estimates over several previous symbols with the goal of improving the accuracy of the power estimates. To do this, we had to analyze the performance of a multistage interference cancellation receiver with hard decisions. This also helped us to separate the effects of incorrect data estimates and imperfect power estimates on the performance of the interference cancellation receiver. We found that imperfect amplitude estimates contribute a major part in degradation of the performance of the receiver. This points towards the importance of having good amplitude estimates. Moreover, accurate amplitude estimates will help us select users and multipath components for cancellation accurately, thus increasing our confidence in the criterion used for selective cancellation. As mentioned above, this will be especially useful in selecting multipath components in severe fading environments. We analyzed the performance of adaptive interference cancellation with bit averaging and found that averaging amplitude estimates over a large number of bits improves the performance considerably. In a practical channel, it is reasonable to believe that there will exist an optimum number of bits over which the amplitude estimates should be averaged to extract the best possible performance from the selective cancellation receiver. This optimum number of bits should be a function of the quality of the channel, and proportional to the coherence time of the channel. The use of averaging power estimates over an optimum number of bits to perform interference cancellation on multipath components should lead to an improvement in the capacity of the CDMA system.

Chapter 6

Conclusions

6.1 Conclusions

Multistage interference cancellation holds potential to improve both capacity and near-far resistance of the reverse link of CDMA systems. In this thesis, we have extended the work of previous research by examining how selective interference cancellation could be applied to both multipath and multicellular environments.

We have analyzed the effect of out-of-cell interference on the performance of adaptive interference cancellation in a multicell environment. We have employed a circular cellular geometry and a Gaussian approximation for analyzing the performance of multistage interference cancellation. This analysis leads to the conclusion suggested in [33], that out-of-cell interference will limit the effectiveness of interference cancellation performed within a single cell. Furthermore, the indiscriminate use of interference cancellation on out-of-cell interferers could severely degrade performance (as well as greatly increase complexity). However, selective interference cancellation on a small number of out-of-cell interferers with large powers can lead to significant capacity improvements. The results obtained using the circular geometry have been verified against those obtained using the hexagonal geometry, and they agree within $10 - 15\%$. We also modeled the interference using the improved Gaussian approximation and the results were virtually identical to those obtained by using the simple Gaussian approximation. The improved Gaussian approximation might provide a noticeable improvement in accuracy in poorer channel conditions, especially for a small

number of users per cell.

We also analyzed the performance of the interference cancellation receiver with hard decisions, and the effect of averaging power estimates over several bits to improve the accuracy of the estimate. We found that averaging amplitude estimates over a large number of bits improves the performance considerably. Isolation of the effect of bit errors in the previous stage from errors in amplitude estimates on the receiver performance indicates that the imperfect amplitude estimates contribute a major part in degradation of the performance of the receiver. This points towards the importance of having good amplitude estimates. Moreover, accurate amplitude estimates will help us select users and multipath components for cancellation accurately, thus increasing our confidence in the criterion used for selective cancellation. This will be especially useful in selecting multipath components in severe fading environments. In a practical channel, it is reasonable to believe that there will exist an optimum number of bits over which the amplitude estimates should be averaged to extract the best possible performance from the selective cancellation receiver. This optimum number of bits should be a function of the quality of the channel, and proportional to the coherence time of the channel.

6.2 Future work

The idea of averaging amplitude estimates over several previous bits to obtain more accurate estimates was introduced and analyzed in Chapter 5. It was mentioned that the bit averaging technique is particularly applicable in cancellation of multipath components of the interferers. Although this thesis forms the basis for an in-depth analysis of the cancellation of multipath components using bit averaging, further analytical and simulation studies should be performed to investigate the use of bit averaging with selective cancellation under fading channels. This would lead to a more thorough understanding of the number of bits that should be averaged over to get the best possible performance from the interference cancellation receiver as a function of the channel conditions.

This thesis, as well as the work in [8],[9] and [10], applies the selective cancellation criterion at the first stage of interference cancellation, and interference cancellation

is performed at all later stages only on users which are found to be strong enough to justify cancellation at the first stage. Thus, if the condition in Eqn. 3.27 is true at the first stage of cancellation for a certain interferer, the receiver will not perform cancellation on that user at any stage. However, it might help to perform cancellation on some of such users at later stages in the receiver. This should be explored. Note that the condition in Eqn. 3.27 is strictly true only at the first stage of interference cancellation. Similar cancellation criteria could be applied at each stage of the multistage interference cancellation receiver, and the amount of performance improvement that might be obtained through such an implementation should be investigated.

The most important extension to the work presented in this thesis is to investigate the issues concerning the practical implementation of a multistage adaptive interference cancellation receiver. This would then lead to building such a receiver that can be deployed at the base station of a cellular system to achieve the significant capacity gains predicted by this and other works.

To conclude, it would suffice to say that selective cancellation of interference in a CDMA environment will lead to impressive gains in capacity. Accuracy of the selective cancellation criteria is a very important factor, and averaging over consecutive bits to increase the accuracy will further improve performance.

Bibliography

[1] T. S. Rappaport, "The wireless revolution," *IEEE Communications Magazine*, pp. 52–62, November 1991.

[2] N. J. Boucher, *The Cellular Radio Handbook.* Quantum Publishing, second ed., June 1992.

[3] K. S. Gilhousen, I. M. Jacobs, R. Padovani, A. J. Viterbi, L. A. Weaver, and C. E. Wheatley, "On the capacity of a cellular CDMA system," *IEEE Transactions on Vehicular Technology*, vol. 40, pp. 303–311, May 1991.

[4] L. W. Couch, *Digital and Analog Communication Systems.* MacMillan Publishing Company, fourth ed., 1993.

[5] R. C. Dixon, *Spread Spectrum Systems.* New York: Wiley, 1984.

[6] H. Taub and D. L. Schilling, *Principles of Communication Systems.* McGraw-Hill Book Company, second ed., 1986.

[7] R. Price and P. E. Green, "A communication technique for multipath channels," in *Proceedings of the IRE 46*, pp. 555–570, March 1958.

[8] A. Kaul and B. D. Woerner, "An adaptive multistage interference cancellation receiver for CDMA," Master's thesis, Virginia Polytechnic Institute and State University, March 1995.

[9] A. Kaul and B. D. Woerner, "An analysis of adaptive multistage interference cancellation for CDMA," *Submitted to the IEEE Transactions on Communications*, October 1994.

[10] A. Kaul and B. D. Woerner, "Analytical limits on the performance of adaptive multistage interference cancellation for CDMA," *IEE Electronic Letters*, November 1994.

[11] R. M. Buehrer and B. D. Woerner, "Analysis of adaptive multistage interference cancellation for CDMA using an improved Gaussian approximation," *Submitted to the IEEE Journal on Selected Areas in Communcations.*

[12] M. B. Pursley, "Performance evaluation for phase coded spred spectrum multiple access communications," *IEEE Transactions on Communications*, vol. COM-25, pp. 795–799, August 1977.

[13] E. Geraniotis and M. B. Pursley, "Error probabilities for direct sequence spread spectrum multiple access communicaitons - part II," *IEEE Transactions on Communications*, vol. 30, pp. 985–995, May 1982.

[14] B. D. Woerner and R. Cameron, "An analysis of CDMA with imperfect power control," in *Proceedings of the 42nd IEEE Vehicular Technology Conference*, pp. 977–980, May 1992.

[15] V. Aue and J. H. Reed, "An interference robust CDMA demodulator that uses spectral correlation properties," *IEEE Vehicular TEchnology Conference*, pp. 563–567, 1994.

[16] R. D. Holley and J. H. Reed, "Time dependent adaptive filters for interference cancellation in CDMA systems," *Workshop on Cyclostationary Signal Processing*, August 1994.

[17] N. Zecevic and J. H. Reed, "Blind adaptation algorithms for single user detection and interference rejection for Direct Sequence Spread Sprcteum CDMA systems," Master's thesis, Virginia Polytechnic Institute and State University, Expexted April 1995.

[18] S. Verdu, "Minimum probability of error for asynchronous Gaussian multiple access channels," *IEEE Transactions on Information Theory*, vol. IT-32, pp. 85–96, January 1986.

[19] R. Lupas and S. Verdu, "Linear multiuser detectors for synchronous code division multiple access channels," *IEEE Transactions on Information Theory*, vol. 35, pp. 123–136, January 1989.

[20] R. T. S. Z. Xie, C. K. Rushforth and T. K. Moon, "Joint signal detection and parameter estimation in multiuser communications," *IEEE Transactions on Communications*, vol. 41, pp. 1208–1215, August 1993.

[21] A. J. Viterbi, "Very low rate convolution codes for maximum theorotical performance of spread spectrum multiple-access channels," *IEEE Journal on Selected Areas in Communications*, vol. 8, pp. 641–649, May 1990.

[22] M. K. Varanasi and B. Aazhang, "Multistage detection in asynchronous code division multiple access communications," in *IEEE Transactions on Communications*, vol. 38, pp. 509–519, April 1990.

[23] M. K. Varanasi and B. Aazhang, "Near optimum detection in synchronous code division multiple access system," *IEEE Transactions on Communications*, vol. 39, pp. 509–519, May 1991.

[24] R. M. Buehrer and B. D. Woerner, "A survey of multiuser receivers for CDMA," *Submitted to Wireless Personal Communications- An International Journal, Special Issue on Signal Separation and Interference Cancellation*, March 1995.

[25] N. Y. S. Striglis, A. Kaul and B. D. Woerner, "A multistage RAKE receiver for improved capacity of CDMA systems," in *Proceedings of the 44th IEEE Vehicular Technology Conference*, (Stocklolm, Sweden), pp. 789–793, June 8-10 1994.

[26] D. Divsalar and M. K. Simon, "Improved CDMA performance using parallel interference cancellation," *IEEE Military Communications Conference (MILCOM '94)*, pp. 911–917, October 1994.

[27] P. Patel and J. Holtzman, "Analysis of a simple successive interference cancellation scheme in a DS/CDMA system," *IEEE Journal on Selected Areas in Communications*, vol. 12, pp. 796–807, June 1994.

[28] X. Zhang and D. Brady, "Soft decision multistage detection for asynchronous AWGN channels," *31 st Annual Allerton Conference on Communications, Control and Computing*, pp. 54–63, September 1993.

[29] D. S. Chen and S. S. Roy, "An adaptive multiuser receiver for CDMA systems," *IEEE Journal on Selected Areas in Communications*, vol. 12, pp. 808–816, June 1994.

[30] R. M. Buehrer and B. D. Woerner, "Performance of CDMA multistage interference cancellation with phase and timing errors," *1995 IEEE Universal Personal Communications Conference (UPC '95)*, November 6-10 1995.

[31] F. C. Cheng and J. M. Holtzman, "Effect of tracking errors on DS/CDMA successive interference cancellation," *GLOBECOM '94 -Communication Theory Mini Conference*, pp. 166–170, December 1994.

[32] J. Robert K. Morrow, "Bit to bit error dependence in slotted DS/CDMA packet systems with random signature sequences," *IEEE Transactions on Communications*, vol. 37, pp. 1052–1061, October 1989.

[33] J. M. Holtzman, "Successive interference cancellation for direct-sequence code division multiple access," *IEEE Military Communications Conference (MILCOM '94)*, pp. 997–1001, March 1992.

[34] J. M. Holtzman, "A simple accurate method to calculate spread-spectrum multiple-access error probabilities," *IEEE Transactions on Communications*, vol. 40, pp. 461–464, March 1992.

[35] J. C. Liberti and T. S. Rappaport, "A simplified expression for the improved Gaussian approximation to compute CDMA bit error rates in slowly fading channels with imperfect power control," *Submitted to IEEE Transactions on Communications*, 1990.

[36] P. Agashe and B. D. Woerner, "Interference cancellation for a multicellular CDMA environment," *Wireless Personal Communications- An International Journal, Special Issue on Signal Separaation and Interfernce Cancellation for PIMRC*, December 1995.

[37] P. Agashe and B. D. Woerner, "Analysis of interference cancellation for a multicellular CDMA environment," in *Proceedings of the 6th IEEE International Symposium on Personal, Indoor and Mobile Radio Communicaitons (PIMRC 95)*, vol. 2, (Toronto, Canada), pp. 747–752, September 1995.

[38] T. Rappaport and L. Milstein, "Effects of radio propagation path loss on DS-CDMA cellular frequency reuse efficiency for the reverse channel," *IEEE Transactions on Vehicular Technology*, vol. 41, pp. 231–242, August 1992.

[39] J. C. Liberti and T. S. Rappaport, "Analytical results for capacity improvements in CDMA," *IEEE Transactions on Vehicular Technology*, vol. 43, pp. 680–690, August 1994.

[40] W. C. Y. Lee, *Mobile Cellular Telecommunications- Analog and Digital Systems.* McGraw-Hill, Inc., second ed.

[41] J. Lehnert and M. B. Pursley, "Error probabilities for binary direct sequence spread spectrum communications with random signature sequences," *IEEE Transactions on Communications*, January 1987.

[42] S. Striglis and B. D. Woerner, "A multistage rake receiver for CDMA," Master's thesis, Virginia Polytechnic Institute and State University, August 1994.

[43] A. Kaul and B. D. Woerner, "An analysis of adaptive multistage interference cancellaiton for CDMA," *Accepted for IEEE Transactions on Communications*, 1995.

Vita

Parag Agashe was born in Gwalior, India on August 7, 1971. He received the Bachelor of Engineering (B.E.) degree in Electronics and Telecommunication from the Maharashtra Institute of Technology, University of Pune, India in June 1994. He worked as a Teaching Assistant at the Maharashtra Institute of Technology during the Summer of 1994. He joined the Bradley Department of Electrical Engineering at Virginia Tech, Blacksburg, Virginia in Fall 1994 to pursue his M.S. degree in Electrical Engineering. He became a member of the Mobile and Portable Radio Research Group in January 1995, where he worked as a Research Assistant investigating the use of selective cancellation of interference for CDMA. During the Summer of 1995, he worked as a Summer Research Intern at Allen-Bradley Co., Milwaukee, Wisconsin. His research interests include wireless communications with special interest in CDMA systems. In January 1996, he will join QUALCOMM Inc., San Diego, California as a Systems Engineer.